Entergy

Entergy Operations, Inc.
1448 S R 333
Russellville, AR 72801
Tel 501-858-4888

Craig Anderson
Vice President
Operations ANO

1CAN040302

April 2, 2003

U.S. Nuclear Regulatory Commission
Attn: Document Control Desk
Washington, DC 20555

SUBJECT: Arkansas Nuclear One, Unit 1 (ANO-1)
Docket No. 50-313
License Amendment Request to Modify the Fuel Assembly Enrichment, the Spent Fuel Pool (SFP) Boron Concentration Technical Specification (TS) 3 7.14, the Loading Restrictions in the SFP in TS 3.7.15, and to Modify the Fuel Storage Design Features in TS 4.3

REFERENCES:

1. Letter to the NRC dated August 8, 2002, "Use of Metamic® In Fuel Pool Applications" (0CAN080201)
2. Letter to the NRC dated March 18, 2002, "Degradation of Boraflex® in ANO-1 Spent Fuel Pool" (1CAN030203)
3. Letter to the NRC dated September 6, 2000, "License Renewal Application RAIs" (1CAN090002)
4. Letter to the NRC dated January 29, 2003, "License Amendment Request to Change the Spent Fuel Pool (SFP) Loading Restrictions (2CAN010304)

Dear Sir or Madam.

Pursuant to 10CFR50.90, Entergy Operations, Inc. (Entergy) hereby requests an amendment to the Arkansas Nuclear One, Unit 1 (ANO-1) Technical Specification (TS) 3.7.14, Spent Fuel Pool Concentration, TS 3.7.15, Spent Fuel Pool Storage, and TS 4.3, Fuel Storage The ANO-1 spent fuel pool (SFP) storage racks are divided into two Regions. The Region 1 racks contain Boraflex The Region 2 racks do not contain any poison panel inserts. A portion of the SFP storage racks in Region 2 will be modified by the insertion of Metamic® poison panels. The area with the Metamic® poison panels will be defined as Region 3. No loading restrictions will apply to the newly defined Region 3 (i.e., new and spent fuel can be stored in Region 3 without restrictions). By letter dated March 18, 2002 (Reference 2), Entergy described its plans to administratively control spent fuel loading based on the degradation of Boraflex®. Continued degradation of Boraflex® is projected and therefore the proposed change will take no credit for Boraflex® in Region 1 and will include loading restrictions for Region 1. In addition to the above

A001

modification, Entergy proposes to increase the allowable initial fuel assembly uranium-235 (U-235) enrichment from 4.1 weight percent (w/o) to a maximum enrichment of 5.0 w/o. Analyses have been performed which include the effects of the U-235 enrichment, the insertion of the Metamic® poison panels, and not crediting Boraflex® in the Region 1 racks. In addition, a criticality analysis has been performed to demonstrate that the new fuel storage racks can accommodate storage of the higher enriched fuel assemblies. The proposed change will modify the minimum SFP boron concentration requirements in TS 3.7.14, the spent fuel loading restrictions defined by TS 3.7.15, and the initial fuel enrichment and effective multiplication factor (K_{eff}) and the associated Figure in TS 4.3.

Entergy submitted by letter dated August 8, 2002, a topical report (Reference 1) prepared by Holtec International that describes the physical and chemical properties of Metamic®. The report also includes the test results for the use of Metamic® in fuel pool applications. Approval of the topical report is required to support the requested plant specific TS changes addressed in the attachments to this letter.

The proposed change has been evaluated in accordance with 10CFR50.91(a)(1) using criteria in 10CFR50.92(c) and it has been determined that this change involves no significant hazards considerations. The bases for these determinations are included in the attached submittal.

The proposed change includes new commitments that are listed in Attachment 6. The Nuclear Regulatory Commission has not approved TS changes for other facilities that allow the use of Metamic® poison panels in wet storage applications. However, by letter dated January 29, 2003 (Reference 4) Entergy submitted a similar TS change for ANO, Unit 2 (ANO-2). The proposed change to the ANO-1 TS is similar to the ANO-2 change with the following exceptions: 1) ANO-1 is requesting to increase the initial fuel assembly U-235 enrichment and change the loading pattern in the new fuel storage racks; 2) the ANO-2 SFP boron concentration is being increased to allow for various loading configurations; and 3) the concentration of Boron Carbide content in the Metamic® panel differs between the two units

Entergy requests approval of the proposed amendment by November 15, 2003, in order to support fuel re-arrangement in the ANO-1 SFP in late 2003 or early 2004. Once approved, the amendment shall be implemented within 90 days. Although this request is neither exigent nor emergency, your prompt review is requested.

If you have any questions or require additional information, please contact Dana Millar at 601-368-5445.

I declare under penalty of perjury that the foregoing is true and correct. Executed on April 2, 2003.

Sincerely,

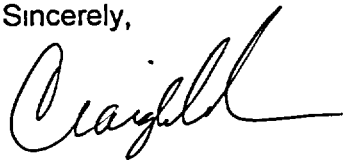

CGA/dm

Attachments:
1. Analysis of Proposed Technical Specification Change
2. Proposed Technical Specification Changes (mark-up)
3. Changes to TS Bases pages (for information only)
4. Holtec License Report
5. Evaluation of Spent Fuel Pool Structural Integrity for Increased Loads from Spent Fuel Racks
6. Commitments

cc: Mr. Ellis W. Merschoff
Regional Administrator
U. S. Nuclear Regulatory Commission
Region IV
611 Ryan Plaza Drive, Suite 400
Arlington, TX 76011-8064

NRC Senior Resident Inspector
Arkansas Nuclear One
P. O. Box 310
London, AR 72847

U. S. Nuclear Regulatory Commission
Attn: Mr. John L. Minns MS O-7 D1
Washington, DC 20555-0001

U. S. Nuclear Regulatory Commission
Attn: Mr. Thomas W. Alexion MS O-7 D1
Washington, DC 20555-0001

Mr. Bernard R. Bevill
Director Division of Radiation
Control and Emergency Management
Arkansas Department of Health
4815 West Markham Street
Little Rock, AR 72205

Attachment 1

1CAN040302

Analysis of Proposed Technical Specification Change

1.0 DESCRIPTION

This letter is a request to amend Operating License DPR-51 for Arkansas Nuclear One, Unit 1 (ANO-1).

The proposed changes will revise the Technical Specifications (TSs) to:

- Allow insertion of Metamic® poison panels in a newly defined Region 3 of the ANO-1 spent fuel pool (SFP).
- Redefine the loading pattern in the current Region 1, taking no credit for Boraflex®.
- Redefine the loading pattern in the current Region 2.
- Modify the SFP boron concentration from ≥1600 ppm to >1600 ppm.
- Modify the applicability of TS 3.7.14 to specify that the TS is applicable any time fuel assemblies are stored in the SFP regardless of whether a SFP verification has been performed or not.
- Allow an increase in the maximum fuel assembly enrichment of Uranium-235 (U-235) from the current enrichment of 4.1 weight percent (w/o) to a maximum of 5.0 w/o.
- Redefine storage patterns in the new fuel storage racks.

Changes are proposed to the following ANO-1 TSs:

- TS 3.7.14, Spent Fuel Pool Boron Concentration
- TS 3.7.15 and the associated Figure 3.7.15-1.
- TS 4.3, Fuel Storage and the associated Figure 4.3.1.2-1.

Appropriate changes will also be made to the associated TS Bases. These are included for information only as Attachment 3.

The changes are desired in order to address the degradation of Boraflex® and to support the creation of a new Region 3 in which Metamic® poison panel inserts will be installed. In addition the increase in maximum fuel assembly enrichment is desired to support reactor fuel loading capabilities. Approval of the proposed changes is desired by November 15, 2003 to support fuel shuffling in late 2003 or early 2004.

2.0 PROPOSED CHANGE

ANO-1 TS 3.7.14 and Surveillance Requirement 3.7.14.1 define the minimum required SFP boron concentration. The proposed change will result in changing the "greater than or equal to" sign (≥) to a "greater than" sign (>). The proposed change, although minor, results in a more accurate representation of the analysis assumption of greater than 1600 parts per million (ppm) for the boron concentration. In addition the TS 3.7.14 currently applies whenever fuel assemblies are stored in the SFP and a SFP verification has not been performed since the last movement of fuel assemblies in the SFP. The proposed change will modify the applicability to require the designated boron concentration any time fuel assemblies are stored in the SFP regardless of whether a SFP verification has been performed or not. This change is needed to support the new criticality analysis that takes credit for boron to assure the required subcritical margin is maintained.

ANO-1 TS 3.7.15 and Figure 3.7.15-1 define loading restrictions for any fuel assembly that is stored in Region 2 of the ANO-1 SFP. Currently, no loading restrictions are required by TS in SFP Region 1, which allows storage of new and spent fuel. Region 1 contains Boraflex® poison panels. Calculations indicate that the Boraflex® content in Region 1 will degrade below the original Boraflex® content assumed in the criticality analysis (Reference 2). Based on continued projected degradation of Boraflex®, the proposed change will take no credit for Boraflex® in Region 1 and will include loading restrictions for Region 1. This will result in changes to TS 3.7.15 and Figure 3.7.15-1, and the creation of a new Figure 3.7.15-2 based on new criticality analysis for Regions 1 and 2. In addition, a portion of the SFP racks in Region 2 will be modified by the installation of Metamic® poison panel inserts. This will result in the creation of a new Region 3 that will allow unrestricted storage of new and spent fuel. Entergy has submitted a topical report (Reference 1) that describes the physical and chemical properties of Metamic®. Approval of the topical report is required to allow the use of Metamic® in SFP applications.

ANO-1 TS 4.3.1.1a and 4.3.1.2a define a maximum U-235 enrichment of 4.1 w/o. The proposed change will allow the maximum enrichment to be 5.0 w/o.

ANO-1 Figure 4.3.1.2-1 depicts locations in the fresh fuel storage racks in which fuel loading is prohibited. Based on the increase in fuel assembly enrichment from 4.1 w/o to a maximum enrichment of 5.0 w/o, two loading pattern configurations will be proposed, which will result in the addition of a new Figure 4.3.1.2-2. Figure 4.3.1.2-2 will depict the loading pattern associated with fuel assemblies whose enrichment is up to 4.2 w/o and Figure 4.3.1.2-1 will illustrate the loading configuration for fuel assemblies whose enrichment is up to 5.0 w/o. A change is also proposed to TS 4.3.1.2.d and e to state that the fuel storage racks shall be maintained in accordance with the two proposed figures which are based on fuel enrichment.

TS 4.3.1.1 b states that an effective multiplication factor (k_{eff}) of less than or equal to 0.95 is achieved when the SFP racks are fully flooded with unborated water. This subcriticality margin will be maintained by taking credit for boron, which results in the proposed change that states that a k_{eff} of less than or equal to 0.95 is maintained when the pool is flooded with 400 ppm borated water.

A new TS 4.3.1.1 c will be added, which will describe that a k_{eff} less than 1.0 will be maintained when the pool is flooded with unborated water. The addition of TS 4.3.1.1 c will result in the currently designated TSs 4.3.1.1 c, d, and e to be re-indexed as TSs 4.3.1.1 d, e, and f, respectively.

In summary, the proposed change will modify TS 3.7.15 to define Region 3 in which Metamic® poison panels will be inserted and impose new loading restrictions in Region 1 and Region 2. TS 4.3.1 will be changed to support higher fuel assembly enrichment.

3.0 BACKGROUND

3.1 Spent Fuel Pool Racks

The ANO-1 SFP provides 968 storage locations for new and spent fuel assemblies or other items. SFP storage is currently divided into two regions. Region 1 utilizes Boraflex® as a neutron absorbing material. Region 2 does not utilize neutron absorbing materials. Region 1 is designed to accommodate non-irradiated fully enriched fuel. Region 2 is designed to

accommodate irradiated fuel that has sustained approximately 80 percent of the design burnup. Placement of fuel in Region 2 is determined by burnup calculations and controlled administratively. Fuel which does not meet this criterion may be placed in Region 2 in a checkerboard fashion. In these cases, currently vacant spaces adjacent to the faces of any fuel assembly which does not meet the Region 2 burnup criteria (Non-Restricted) are physically blocked before any such fuel assembly may be placed in Region 2. The racks meet the requirements of the NRC Position for Review and Acceptance of Spent Fuel Storage and Handling Applications, dated April 14, 1978, and modified January 18, 1979, with the exception that, for Region 2 storage, credit is taken for fuel burnup based on the proposed Revision 2 of Regulatory Guide 1.13.

The Region 1 storage racks are composed of individual storage cells made of type 304L stainless steel and conform to the requirements of ASME B&PV Code, Section III, Subsection IV. These racks utilize a neutron absorbing material, Boraflex®, which is attached to each cell. The cells within a module are interconnected by grid assemblies to form an integral structure. Each rack module is provided with leveling pads which contact the spent fuel pool floor and are remotely adjustable from above through the cells at installation. The modules are neither anchored to the floor nor braced to the pool walls.

The Region 2 storage racks consist of type 304L stainless steel cells assembled in a checkerboard pattern, producing a honeycomb type structure. Each cell has attached to its outer wall a stainless steel wrapper plate creating a pocket opened at the top and bottom. This is referred to as a "spacer pocket" or "flux trap" design. The flux traps are designed to accept poison inserts if future need arises. This design is also provided with leveling pads which contact the spent fuel pool floor and are remotely adjustable from above through the cells at installation. The modules are neither anchored to the floor nor braced to the pool walls.

3.2 New Fuel Storage Area

The new fuel storage area is a separate and protected area for the dry storage of new fuel assemblies in the fuel storage and handling area. The new fuel storage module consists of a nine by eight array with a 21 inch pitch in both directions. Currently, ten interior storage cells are precluded from use prior to any storage in the new fuel rack.

The new fuel storage racks are structural frames consisting of beams, columns and diagonal bracing acting as a unit to provide both vertical support at the bottom of the fuel element and lateral support at the top and bottom of the element The racks are constructed of aluminum and are designed for gravity loads from the racks and fuel elements as well as the Design Basis Earthquake (DBE) in accordance with ASCE Paper 3341.

Section 9.6 of ANO-1 Safety Analysis Report (SAR) contains a detailed description of the ANO-1 SFP and new fuel storage area.

3.3 Previously Approved Amendments

TS 3.7.15, Figure 3.7.15-1, TS 4.3.1.1.d, and TS 4.3.1.1.e currently define loading restrictions for Region 2 based on the combination of initial enrichment and burnup of each spent fuel assembly. The loading restrictions were defined by the approval of TS Amendment 76 (NRC Safety Evaluation Report (SER) dated April 15, 1983) which allowed modification of the ANO-1 SFP storage capabilities from 589 spaces to 968 spaces. The expansion was accomplished by

replacing the existing racks. The region designated as Region 1 of the new racks contained Boraflex® while the remainder of the racks did not include poison inserts.

TS 4.3.1.1.a and TS 4.3.1.2.a currently define the maximum U-235 enrichment for fuel assemblies that will be stored in the SFP and the new fuel storage racks, respectively. TS 4.3.1.2 and Figure 4.3.1.2-1 currently define the new fuel storage rack loading restrictions based on the new fuel maximum U-235 enrichment of 4.1 w/o. The loading restrictions were defined by the approval of TS Amendment 76 (NRC SER dated April 15, 1983) and TS Amendment 166 (NRC SER dated June 28, 1993).

3.4 Loading Pattern / Storage Procedural Controls

The controls used in determining the storage location for new and irradiated fuel in the new or spent fuel storage racks are governed by procedure. The procedure currently contains guidelines pertaining to restricted and unrestricted fuel storage as reflected by TS Figure 3.7.15-1. The new loading pattern restrictions and the addition of Region 3 will continue to be governed by procedure. Checkerboard storage configurations and vacant spaces will be administratively controlled by procedure.

3.5 Spent Fuel Pool System

The Spent Fuel Cooling (SFC) System is designed to maintain the water quality and clarity and to remove the decay heat from the stored fuel in the spent fuel pool. It is designed to maintain the SFP water at less than or equal to approximately 150°F while removing the total decay heat load from the combination of stored fuel assemblies. This was determined from analysis performed using the guidelines of ASB 9-2, *Residual Decay Energy for Light Water Reactors for Long Term Cooling*. In meeting the foregoing design bases, the system has the capability of maintaining the spent fuel pool water at approximately 120°F with a heat load based on the decay heat generated from approximately one-third of the core fuel assemblies discharged at the end of any given cycle.

In addition to its primary function, the system provides for purification of the SFP water, the fuel transfer canal water, and the contents of the Borated Water Storage Tank (BWST) in order to remove fission and corrosion products and to maintain water clarity for fuel handling operations. The system also provides for filling the fuel transfer canal, the incore instrumentation tank, and the cask loading area from the BWST.

The spent fuel coolers are designed to maintain the temperature of the SFP as noted. The SFP coolers reject heat to the nuclear intermediate cooling water system which subsequently rejects its heat to the service water system.

The two spent fuel pool circulating pumps take suction from the SFP and recirculate the fluid back to the pool after passing through the coolers. Cold water is discharged into the pool through two nozzles simultaneously. One of these nozzles is located near the water surface while the other one is near the bottom of the pool. The suction nozzle for the SFP circulating pumps is located on the opposite end of the pool from the discharge nozzles and is near the water surface. This arrangement provides thermal mixing and insures uniform water temperature. The system provides purification of the SFP water through the SFP demineralizer and SFP filters in order to remove fission and corrosion products and to maintain water clarity for fuel handling operations.

Section 9.4 of the ANO-1 SAR contains a detailed description of the SFP systems. No modifications are proposed to these systems in order to support the proposed change.

4.0 TOPICAL REPORT AND COUPON SAMPLING PROGRAM

Entergy submitted to the Nuclear Regulatory Commission by letter dated August 8, 2002 (Reference 1), a topical report that will support the use of Metamic® poison panel inserts in SFP applications. The topical report describes the manufacturing process, the material composition, the corrosion testing results, and the resistance of Metamic® to radiation damage. The report also describes various coupon sampling programs that have been established at test facilities to monitor the physical and chemical property changes over time. To ensure the physical and chemical properties of Metamic® behave in a similar manner as that found at the test facilities, Entergy will establish a coupon sampling program. Coupons suspended on a mounting tree will be inserted into either an empty fuel cell or an empty flux trap in an ANO-1 SFP rack that is surrounded by spent fuel assemblies. Ten coupons will be created from the same manufacturing lot that will be used to manufacture the Metamic® poison panels and inserted into the SFP. The coupon measurement program is intended to monitor for changes of the following physical properties of the Metamic® absorber material: visual observation and photography, neutron attenuation, dimensional measurements (length, width and thickness), weight and specific gravity. The physical changes observed upon evaluation will reflect the probable changes that are occurring in the Metamic® poison panel inserts and thus provide a method of verifying that the assumptions used in the SFP criticality analyses remain valid.

5.0 TECHNICAL ANALYSIS

The proposed change will result in defining a new region, designated as Region 3, in the SFP in which Metamic® poison panels will be inserted. New loading patterns are proposed in the existing Region 1, in which no credit for Boraflex® will be taken, and in Region 2. In addition, Entergy is proposing to increase the fuel assembly maximum U-235 enrichment. Attachments 4 and 5 to this letter provide detailed technical analyses in support of the proposed change. A brief summary of the content in these attachments is included in sections 5.2 through 5.7.

5.1 Dose Consequences Associated with Increased Fuel Enrichment

An evaluation of the potential offsite and control room dose radiological consequences of a Fuel Handling Accident (FHA) was performed considering the change in radiological consequences associated with the increase in maximum U-235 enrichment from 4.1 w/o to 5.0 w/o. A FHA is a postulated accident involving damage to an irradiated fuel assembly during refueling. Two possibilities exist for this accident: mechanical damage resulting in a release of activates and/or a criticality accident. The enclosed attachment prepared by Holtec International addresses the criticality aspects of the FHA. The following dose consequences for the increase in fuel enrichment were calculated for the FHA.

	With Filtration (1) (rem)	Without Filtration (rem)	25% of 10 CFR 100 Limits (rem)
Exclusion Area Boundary Whole Body Dose	0.3	0.3	6
Exclusion Area Boundary Thyroid Dose	10.4	69.1	75

(1) Filtration is through the charcoal filters in the normal SFP ventilation system.

From the information provided above, it can be seen that the change in dose consequences results in only a small fraction of the 25% 10 CFR 100 limits.

5.2 Material Considerations

It is proposed that Metamic® will be inserted in the newly defined Region 3. The physical and chemical properties of Metamic® have been submitted by letter to the NRC (Reference 1).

5.3 Criticality Considerations

A criticality safety evaluation was performed for storage of fresh and spent fuel in the ANO-1 SFP. The evaluation considered three regions that are designed as Region 1, Region 2, and Region 3. The criticality analysis currently in place for Region 1 assumes the presence of Boraflex®. In the new analyses, no credit was taken for the Boraflex® in Region 1. The new analyses also assume Metamic® poison panel inserts are installed in Region 3. It was concluded that in order to assure K_{eff} remains less than 0.95 in the various storage configurations that are allowed considering the storage of both spent and fresh fuel assemblies, a minimum soluble boron concentration is required. The proposed change to TS 3.7.14 will require a minimum boron concentration in the SFP of greater than 1600 parts per million (ppm). The boron concentrations for each region determined by the analyses to assure K_{eff} remains below 0.95 are bounded by the TS value. The fuel loading patterns are defined by the criticality safety evaluation included in the proposed changes and will be governed by procedure.

The criticality analyses also include consideration for storage of fuel assemblies with a maximum U-235 enrichment of 5.0 w/o. Analyses were performed for the new fuel storage racks and the SFP racks considering storage of the higher enrichment. A new storage configuration is included in the proposed change for the new fuel storage racks.

5.4 Thermal Hydraulic Considerations

A thermal hydraulic analysis conservatively demonstrated that natural circulation of the pool water for the proposed configuration provides adequate cooling of all fuel assemblies in the event of a loss of external cooling. Additionally, corrective actions can be taken prior to SFP boiling. The analysis also demonstrated that fuel cladding will not be subjected to departure from nucleate boiling under the postulated accident scenario of the loss of all SFP cooling and

that cladding integrity would be maintained. None of the temperature limits or corrective actions for the SFP cooling system change.

5.5 Structural/Seismic Analysis

A structural analysis of the spent fuel rack with the new poison panel inserts was considered for all loading configurations. The analysis evaluated normal, seismic, and accident conditions. The evaluations demonstrate large margins of safety in all storage modules.

The structural integrity of the new poison inserts under normal and seismic conditions is essential to maintaining the assumptions of the criticality analysis. The poison insert design has been evaluated for normal and seismic conditions and all safety factors are greater than 1.0. However, it is expected that minor changes to the design will occur during product development and testing. All changes will be reflected in the finalized evaluation of the poison insert structural analysis.

5.6 Mechanical Accident

In line with the current approved philosophies, the postulated fuel assembly drop events for Region 3 of the SFP racks were conservatively evaluated and conclude that the poison inserts, as well as the cell wall of the impacted rack cell could be significantly damaged. Conservatively assuming that all poison inserts in Region 3 were damaged, the evaluation concludes that the racks will remain subcritical when credit is taken for the proposed TS limit of greater than 1600 ppm soluble boron in the pool.

5.7 SFP Structural Integrity for Increased Loads from SFP Racks

An evaluation of the SFP structural integrity for the effects of the increased loads from the SFP racks was performed. The evaluation demonstrated that the structural integrity of the pool structure is maintained.

6.0 REGULATORY ANALYSIS

6.1 Applicable Regulatory Requirements/Criteria

The proposed changes have been evaluated to determine whether applicable regulations and requirements continue to be met. The applicable regulations and requirements used to support the proposed changes and reflection of their continued compliance are included in subsequent attachments to this letter.

Arkansas Nuclear One, Unit 1 (ANO-1) is currently exempt from the requirements of 10 CFR 70.24, *Criticality accident requirements.* The exemption was granted on October 6, 1998 (TAC NOS. MA1278 and MA1279). Upon approval of the proposed change, ANO-1 will fully comply with 10 CFR 50.68 paragraph (b), and the exemption to 10 CFR 70.24 will no longer be required.

Entergy has determined that the proposed changes do not require any exemptions or relief from regulatory requirements, other than the TS, and do not affect conformance with any GDC differently than described in the SAR.

6.2 No Significant Hazards Consideration

The proposed changes will modify the Arkansas Nuclear One, Unit 1 (ANO-1) Technical Specifications (TSs) related to fuel storage and uranium-235 (U-235) fuel assembly enrichment. The ANO-1 spent fuel pool (SFP) is currently divided into two regions (designated as Region 1 and Region 2) in which specific loading restrictions are imposed based on assembly average burnup and initial assembly average U-235 enrichment (up to 4.1 weight percent (w/o) U-235). The SFP racks in Region 1 contain Boraflex® as a neutron absorber while the SFP racks in Region 2 contain no neutron absorbers. Based on calculations which indicate that the neutron absorption characteristics of Boraflex® are degrading, Entergy has determined that the reactivity worth of Boraflex® should no longer be credited in the reactivity analysis and thus more stringent loading restrictions should be imposed in Region 1. Therefore, the proposed changes include modifications to the loading restrictions in Region 1. Changes to the loading restrictions in Region 2 are also proposed. In addition, a portion of the current Region 2 will be designated as a new Region 3. The new region will contain Metamic® poison panel inserts which will provide the neutron absorption capability required to allow storage of various combinations of fuel burnup and enrichment without loading restrictions. In order to accommodate future reactor core loading flexibility, Entergy is also proposing to increase the allowable U-235 fuel assembly enrichment to a maximum of 5.0 w/o. The criticality analyses associated with these changes will require credit for boron in the SFP to assure the SFP remains subcritical with an effective multiplication factor (k_{eff}) less than 0.95. The above proposed changes will result in modifications to TSs covering the SFP boron concentration and the SFP storage and design features related to fuel storage. The proposed change to the SFP boron concentration is a minor editorial change.

Entergy Operations, Inc. has evaluated whether or not a significant hazards consideration is involved with the proposed amendment(s) by focusing on the three standards set forth in 10 CFR 50.92, "Issuance of amendment," as discussed below.

1. Does the proposed change involve a significant increase in the probability or consequences of an accident previously evaluated?

   Response: No.

   The three fuel handling accidents described below can be postulated to increase reactivity. However, for these accident conditions, the double contingency principle of ANS N16.1-1975 is applied. This states that it is unnecessary to assume two unlikely, independent, concurrent events to ensure protection against a criticality accident. Thus, for accident conditions, the presence of soluble boron in the storage pool water can be assumed as a realistic initial condition since its absence would be a second unlikely event.

   Three types of drop accidents have been considered: a vertical drop accident, a horizontal drop accident, and an inadvertent drop of an assembly between the outside periphery of the rack and the pool wall.

   - A vertical drop directly upon a cell will cause damage to the racks in the active fuel region. The current 1600 ppm soluble boron concentration TS limit will ensure that K_{eff} does not exceed 0.95.

- A fuel assembly dropped on top of the rack horizontally will not deform the rack structure such that criticality assumptions are invalidated. The rack structure is such that an assembly positioned horizontally on top of the rack results in a minimum separation distance from the upper end of the active fuel region of the stored assemblies. This distance is sufficient to preclude interaction between the dropped assembly and the stored fuel.
- An inadvertent drop of an assembly between the outside periphery of the rack and the pool wall is bounded by the worst case fuel misplacement accident condition.

The fuel assembly misplacement accident was considered for all storage configurations. An assembly with high reactivity is assumed to be placed in a storage location which requires restricted storage based on initial U-235 loading, cooling time, and burnup. The presence of boron in the pool water assumed in the analysis has been shown to offset the worst case reactivity effect of a misplaced fuel assembly for any configuration. This boron requirement is less than the 1600 ppm currently required by the ANO-1 TS. Thus, a five percent subcriticality margin can be easily met for postulated accidents, since any reactivity increase will be much less than the negative worth of the dissolved boron.

For fuel storage applications, water is usually present. An "optimum moderation" accident is not a concern in spent fuel pool storage racks because the rack design prevents the preferential reduction of water density between the cells of a rack (e.g., boiling between cells). An "optimum moderation" accident in the new fuel pit was previously evaluated and the conclusions of that evaluation have not changed as a result of the fuel enrichment.

Therefore, the proposed change does not involve a significant increase in the probability or consequences of an accident previously evaluated.

2. Does the proposed change create the possibility of a new or different kind of accident from any accident previously evaluated?

Response: No.

The proposed changes will define a portion of the current Region 2 as Region 3. The new region will contain Metamic® poison panel inserts and will allow unrestricted storage of fuel assemblies with various enrichments and burnup. To support the proposed change new criticality analyses have been performed. The analyses resulted in new loading restrictions in Region 1 and Region 2. The presence of boron in the pool water assumed in the analysis is less than the 1600 ppm currently required by the ANO-1 TSs. Thus, a five percent subcriticality margin can be easily met for postulated accidents, since any reactivity increase will be much less than the negative worth of the dissolved boron.

No new or different types of fuel assembly drop scenarios are created by the proposed change. During the installation of the Metamic® panels, the possible drop of a panel is bounded by the current fuel assembly drop analysis. No new or different fuel assembly misplacement accidents will be created. Administrative controls currently exist to assist in assuring fuel misplacement does not occur.

Therefore, the proposed change does not create the possibility of a new or different kind of accident from any previously evaluated.

3. Does the proposed change involve a significant reduction in a margin of safety?

Response: No.

With the presence of a nominal boron concentration, the SFP storage racks will be designed to assure that fuel assemblies of less than or equal to five weight percent U-235 enrichment when loaded in accordance with the proposed loading restrictions will be maintained within a subcritical array with a five percent subcritical margin (95% probability at the 95 % confidence level). This has been verified by criticality analyses.

Credit for soluble boron in the SFP water is permitted under accident conditions. The proposed modification that will allow insertion of Metamic® poison panels does not result in the potential of any new misplacement scenarios. Criticality analyses have been performed to determine the required boron concentration that would ensure the maximum K_{eff} does not exceed 0.95. The ANO-1 TS for the minimum SFP boron concentration is greater than that required to ensure K_{eff} does not exceed 0.95. Therefore, the margin of safety currently defined by taking credit for soluble boron will be maintained.

The structural analysis of the spent fuel racks along with the evaluation of the SFP structure showed that the integrity of these structures will be maintained with the addition of the poison inserts. The structural requirements were shown to be satisfied, so the safety margins were maintained.

Therefore, the proposed change does not involve a significant reduction in a margin of safety.

Based on the above, Entergy concludes that the proposed amendment(s) present no significant hazards consideration under the standards set forth in 10 CFR 50.92(c), and, accordingly, a finding of "no significant hazards consideration" is justified.

6.3 Environmental Considerations

The proposed amendment does not involve (i) a significant hazards consideration, (ii) a significant change in the types or significant increase in the amounts of any effluent that may be released offsite, or (iii) a significant increase in individual or cumulative occupational radiation exposure. Accordingly, the proposed amendment meets the eligibility criterion for categorical exclusion set forth in 10 CFR 51.22(c)(9). Therefore, pursuant to 10 CFR 51.22(b), no environmental impact statement or environmental assessment need be prepared in connection with the proposed amendment.

Attachment 2

1CAN040302

Proposed Technical Specification Changes (mark-up)

3.7 PLANT SYSTEMS

3.7.14 Spent Fuel Pool Boron Concentration

LCO 3.7.14 The spent fuel pool boron concentration shall be ≥ ≥1600 ppm.

APPLICABILITY: When fuel assemblies are stored in the spent fuel pool ~~and a spent fuel pool verification has not been performed since the last movement of fuel assemblies in the spent fuel pool~~.

ACTIONS

CONDITION	REQUIRED ACTION	COMPLETION TIME
A. Spent fuel pool boron concentration not within limit.	----------NOTE---------- LCO 3.0.3 is not applicable. ----------	
	A.1 Suspend movement of fuel assemblies in the spent fuel pool.	Immediately
	AND	
	A.2.1 Initiate action to restore spent fuel pool boron concentration to within limit.	Immediately
	~~OR~~	
	~~A.2.2 Initiate action to perform a spent fuel pool verification.~~	~~Immediately~~

SURVEILLANCE REQUIREMENTS

SURVEILLANCE		FREQUENCY
SR 3.7.14.1	Verify the spent fuel pool boron concentration is ≥≥ 1600 ppm.	7 days

3.7 PLANT SYSTEMS

3.7.15 Spent Fuel Pool Storage

LCO 3.7.15 The combination of initial enrichment, cooling time, and burnup of each spent fuel assembly stored in Region 1 and Region 2 shall be within the acceptable range of Figures 3.7.15-1 and 3.7.15-2, respectively, or in accordance with Specification 4.3.1.1.

APPLICABILITY: Whenever any fuel assembly is stored in Region 1 or Region 2 of the spent fuel pool.

ACTIONS

CONDITION	REQUIRED ACTION	COMPLETION TIME
I. Requirements of the LCO not met.	A.1 ----------NOTE---------- LCO 3.0.3 is not applicable. ---------- Initiate action to move the noncomplying fuel assembly from Region 2the affected Region.	Immediately

SURVEILLANCE REQUIREMENTS

SURVEILLANCE		FREQUENCY
SR 3.7.15.1	Verify by administrative means the initial enrichment, cooling time, and burnup of the fuel assembly is in accordance with Figure 3.7.15-1, Figure 3.7.15-2, or Specification 4.3.1.1.	Prior to storing the fuel assembly in Region 1 or 2.

~~Figure 3.7.15-1~~
~~Burnup versus Enrichment Curve for~~
~~Spent Fuel Storage Racks~~

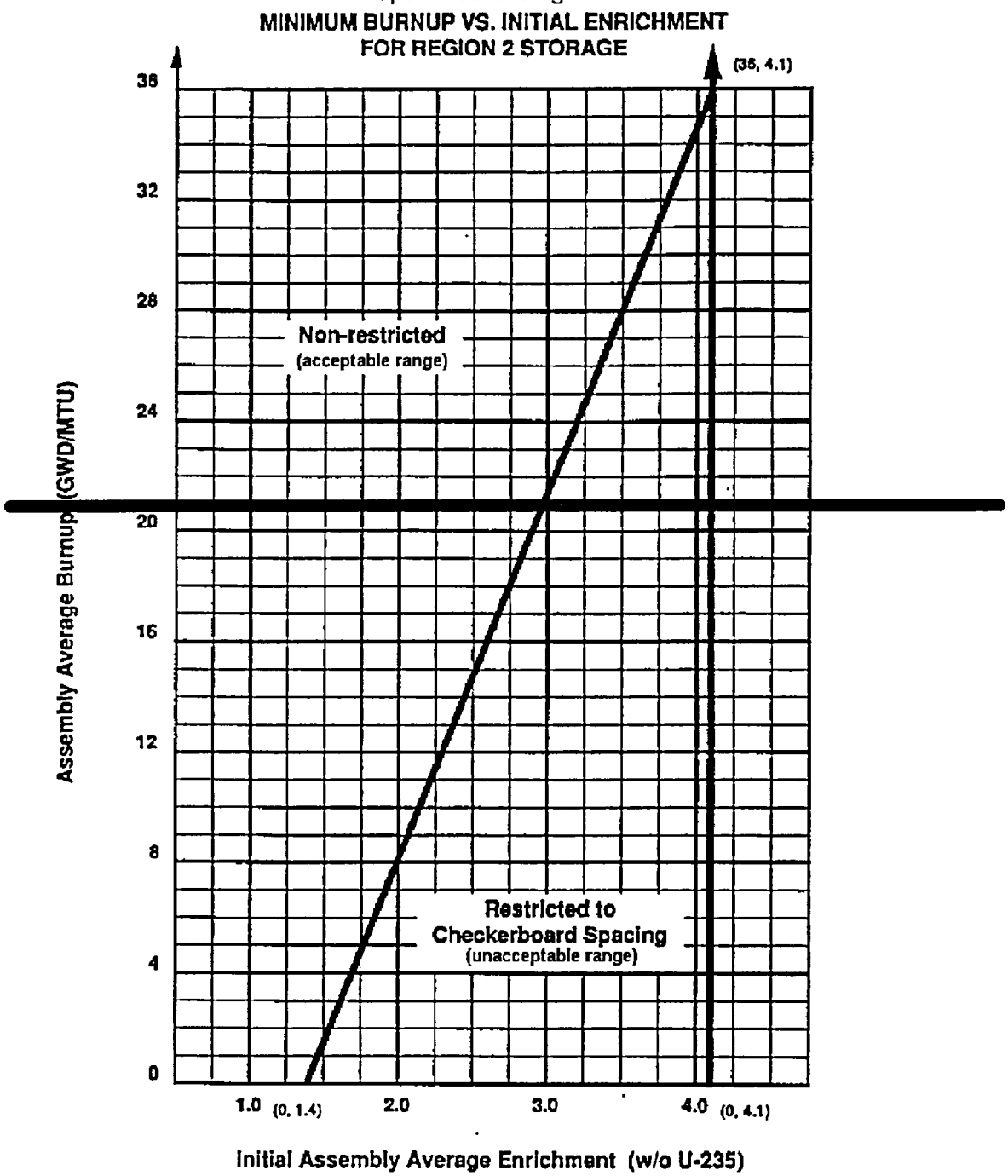

Figure 3.7.15-1
Burnup versus Enrichment Curve for
SFP Storage Racks Region 1

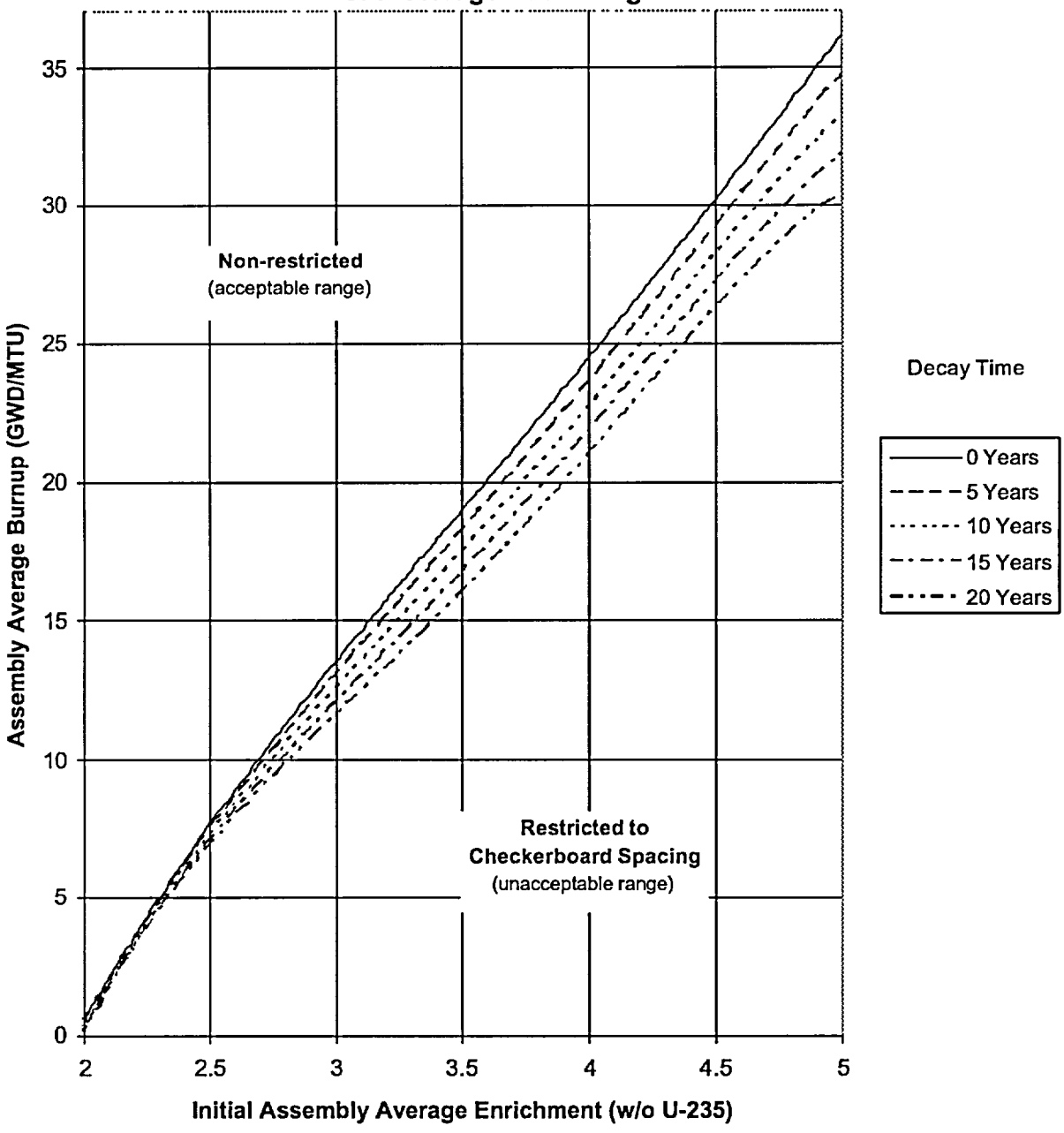

Figure 3.7.15-2
Burnup versus Enrichment Curve For SFP Storage Racks
Region 2

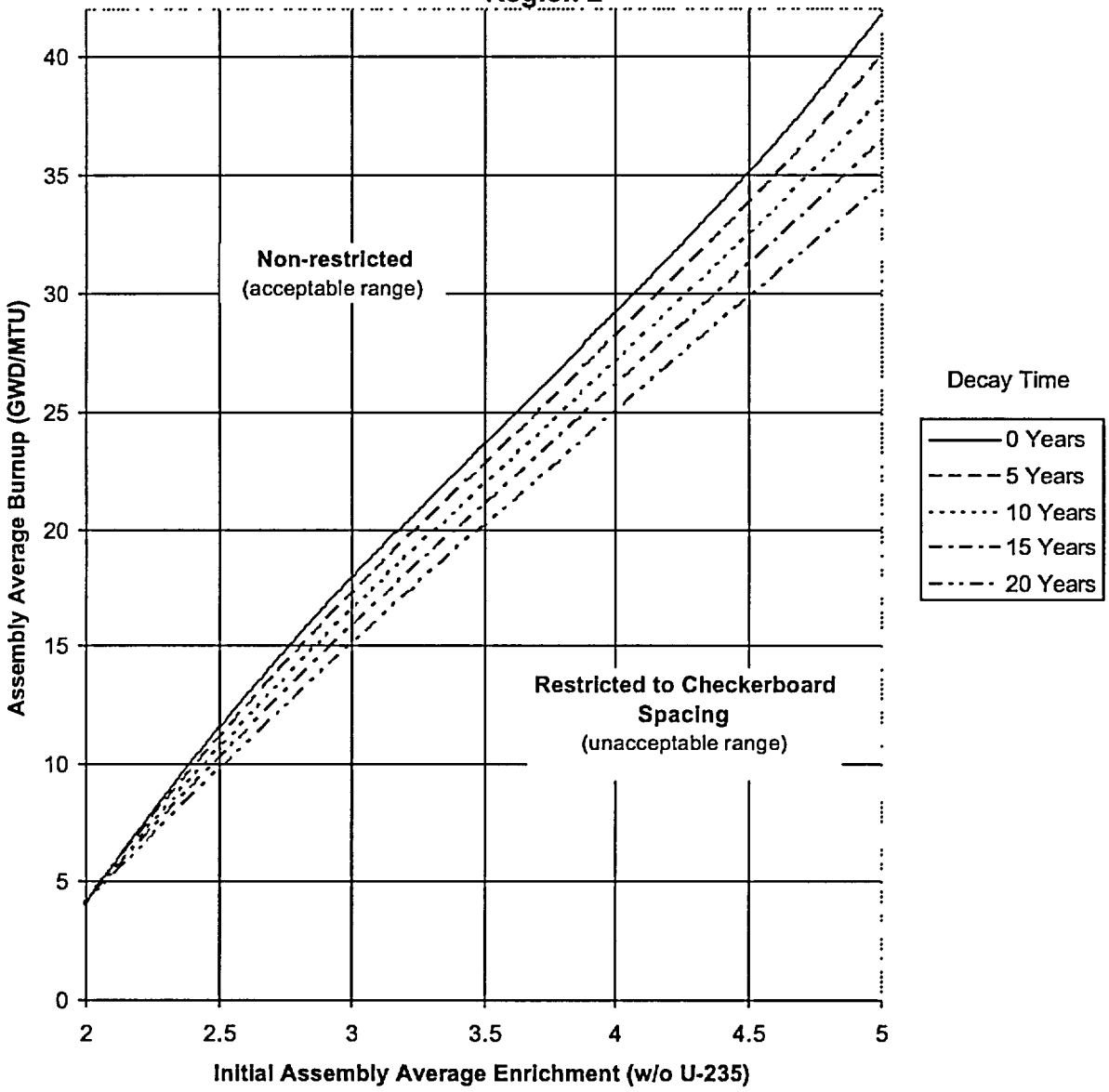

4.0 DESIGN FEATURES

4.3 Fuel Storage

4.3.1 Criticality

4.3 1.1 The spent fuel storage racks are designed and shall be maintained with:

a. Fuel assemblies having a maximum U-235 enrichment of ~~4.15~~5.0 weight percent;

b. $k_{eff} \leq 0.95$ if fully flooded with 400 ppm of ~~un~~borated water, which includes an allowance for uncertainties as described in Section 9.6.2.4.3 of the SAR;

c. $k_{eff} < 1.0$ if fully flooded with unborated water, which includes an allowance for uncertainties as described in Section 9.6.2.4.3 of the SAR;

~~c~~d. A nominal 10.65 inch center to center distance between fuel assemblies placed in the storage racks;

~~d~~e. New or partially spent fuel assemblies with cooling times and a discharge burnup in the "acceptable range" of Figure 3.7.15-1 or Figure 3.7.15-2 allowed unrestricted storage in either fuel storage rack Region 1, ~~or~~ Region 2; or Region 3, and

~~e~~f. New or partially spent fuel assemblies with cooling times and a discharge burnup in the "unacceptable range" of Figure 3.7.15-1 or Figure 3.7.15-2 stored in Region ~~1~~3, or in checkerboard configuration in either Region ~~1~~ or Region 2.

4.3 1.2 The new fuel storage racks are designed and shall be maintained with:

a. Fuel assemblies having a maximum U-235 enrichment of ~~4.15~~5.0 weight percent;

b. $k_{eff} \leq 0.95$ under normal conditions, which includes an allowance for uncertainties as described in Section 9.6.2.4.3 of the SAR;

c. $k_{eff} \leq 0.98$ with optimum moderation, which includes an allowance for uncertainties as described in Section 9.6.2.4.3 of the SAR;

d. A nominal 21 inch center to center distance between fuel assemblies placed in the storage racks; and

e. ~~Ten interior storage cells, as shown in~~ Fuel loading prohibited in interior storage cells as depicted in Figures 4.3.1.2-1 and 4.3.1.2-2, based on fuel enrichment ~~precluded from use during~~ fuel storage

Figure 4.3.1.2-1

Fresh Fuel Storage Rack
Loading Pattern for a Maximum Enrichment of 5.0 w/o U-235

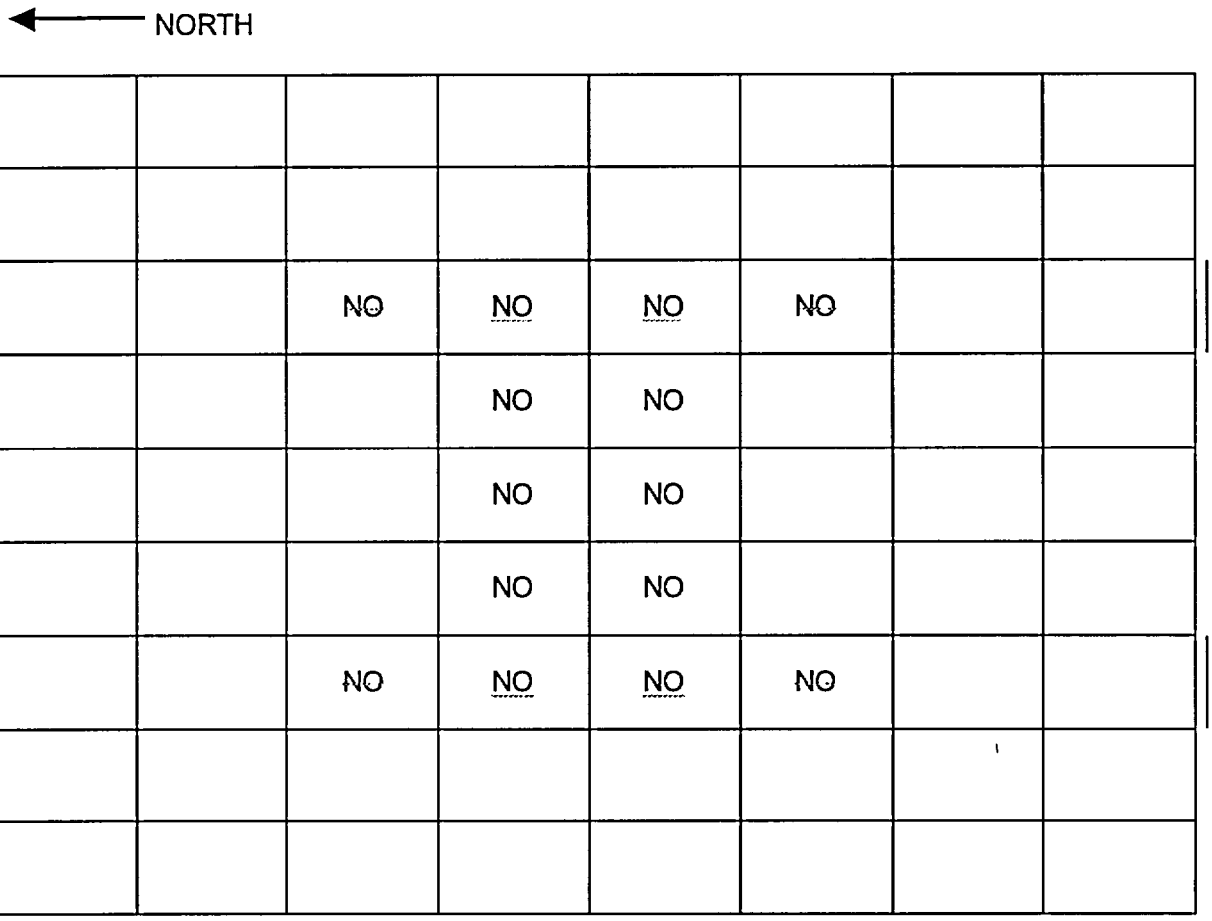

"NO" Indicates a location in which fuel loading is prohibited.

Figure 4.3.1.2-2

Fresh Fuel Storage Rack
Loading Pattern for a Maximum Enrichment of 4.2 w/o U-235

← NORTH

			NO	NO			
		NO	NO	NO	NO		
			NO	NO			

"NO" Indicates a location in which fuel loading is prohibited.

Attachment 3

1CAN040302

Changes to Technical Specification Bases Pages
For Information Only

B 3.7 PLANT SYSTEMS

B 3.7.14 Spent Fuel Pool Boron Concentration

BASES

BACKGROUND

As described in the Bases for LCO 3.7.15, "Spent Fuel Pool Storage," fuel assemblies are stored in the spent fuel pool racks in accordance with criteria based on initial enrichment, cooling time, and discharge burnup. Although the water in the spent fuel pool is normally borated to ≥≥ 1600 ppm, the criteria that limit the storage of a fuel assembly to specific rack locations are conservatively developed without taking credit for boron in the spent fuel pool water.

The spent fuel storage pool is divided into ~~two~~ three separate and distinct regions as shown in SAR Figure 9-53 which, for the purpose of criticality considerations, are considered as separate ~~pools~~ infinite arrays. Region ~~1~~ 3 is designed to accommodate new fuel with a maximum enrichment of ~~4.10~~5.0 wt% U-235, or spent (irradiated) fuel regardless of the discharge fuel burnup. Region 1 and 2 ~~is~~ are designed to accommodate fuel of various initial enrichments which have accumulated minimum cooling times and burnups within the acceptable domain according to Figure 3.7.15-1 and 3.7.15-2. Fuel assemblies not meeting the criteria of Figure 3.7.15-1 or 3.7.15-2 shall be stored in accordance with Specification 4.3.1.1.~~e~~f.

The water in the spent fuel storage pool normally contains soluble boron, which results in large subcriticality margins under actual operating conditions. However, the NRC guidelines specify that the limiting k_{eff} of ~~0.95~~1.0 be evaluated in the absence of soluble boron. Hence, the design of ~~both~~ the three regions is based on the use of unborated water, which maintains each region in a subcritical condition during normal operation with the regions fully loaded. The double contingency principle discussed in ANSI N-16.1-1975 and the April 1978, NRC letter (Ref. 1) allows credit for soluble boron under other abnormal or accident conditions, since only a single accident need be considered at one time. Thus, for accident conditions, the presence of soluble boron in the spent fuel pool water can be assumed as a realistic condition. For example, accident scenarios are postulated which could potentially increase the reactivity and reduce the margin to criticality. To mitigate these postulated criticality related accidents, boron is dissolved in the pool water. Safe operation of the high density storage racks with no movement of assemblies may therefore be achieved by controlling the location of each assembly in accordance with LCO 3.7.15, "Spent Fuel Pool Storage." Prior to movement of an assembly, it is necessary to perform SR 3.7.15.1.

APPLICABLE SAFETY ANALYSES

Most accident conditions will not result in an increase in K_{eff} of the rack. Examples are the loss of cooling systems (reactivity decreases with decreasing water density) and dropping a fuel assembly on top of the rack (the rack structure pertinent for criticality is not deformed and the assembly has more that eight inches of water separating it from the active fuel in the rest of the rack which precludes interaction). However, Aaccidents can be postulated which would increase reactivity such as inadvertent drop of an assembly between the outside periphery of the rack and the pool wall. Thus, for accident conditions, the presence of soluble boron in the storage pool water is assumed as a realistic initial condition.

The presence of greater than 1600 ppm boron in the pool water will decrease reactivity byis to assure the fuel assemblies will be maintained in a subcritical array with approximately 30% ΔK. Thus $K_{eff} \leq 0.95$ can be easily met for postulatedin the event of a postulated drop accidents. , since any reactivity increase will be much less than the negative worth of the dissolved boron. Analysis has shown that, during a postulated misplacement accident with the fuel stored within the limits of this specification, a $K_{eff} \leq 0.95$ will be maintained when the boron concentration is at or above 800 ppm.

The concentration of dissolved boron in the fuel storage pool satisfies Criterion 2 of 10 CFR 50.36 (Ref. 4)

LCO

The specified concentration ≥ 1600 ppm of dissolved boron in the spent fuel pool conservatively preserves the assumption used in the analyses of the potential accident scenarios. This concentration of dissolved boron is the minimum required concentration for fuel assembly storage and movement within the spent fuel pool.

APPLICABILITY

This LCO applies whenever fuel assemblies are stored in the spent fuel pool, until a complete spent fuel pool verification has been performed following the last movement of fuel assemblies in the spent fuel pool. This LCO does not apply following the verification since the verification would confirm that there are no misloaded fuel assemblies. With no further fuel assembly movement in progress, there is no potential for a misloaded fuel assembly or a dropped fuel assembly.

ACTIONS

A 1, and A.2.1, and A 2.2

The Required Actions are modified by a Note indicating that LCO 3.0.3 does not apply. If moving irradiated fuel assemblies while in MODE 5 or 6, LCO 3.0.3 would not specify any action. If moving irradiated fuel assemblies while in MODE 1, 2, 3, or 4, the fuel movement is independent of reactor operation. Therefore, inability to suspend movement of fuel assemblies is not a sufficient reason to require a reactor shutdown.

ACTIONS (continued)

A.1, and A 2.1, and A.2.2 (continued)

When the concentration of boron in the spent fuel pool is less than required, immediate action must be taken to preclude the occurrence of an accident or to mitigate the consequences of an accident in progress. This is most efficiently achieved by immediately suspending the movement of the fuel assemblies. This does not preclude movement of a fuel assembly to a safe position. In addition, action must be immediately initiated to restore the spent fuel pool boron concentration to within its limit. An acceptable alternative is to immediately initiate performance of a spent fuel pool verification to ensure proper locations of the fuel since the last movement of fuel assemblies in the spent fuel pool. However, prior Prior to resuming movement of fuel assemblies, the concentration of boron must be restored. Either of these actions are acceptable, and once initiated must be continued until the action is completed. The immediate Completion Time for initiation of these this actions reflects the importance of maintaining a controlled environment for irradiated fuel.

SURVEILLANCE REQUIREMENTS

SR 3.7.14.1

This SR verifies that the concentration of boron in the spent fuel pool is within the required limit. As long as this SR is met, the analyzed incidents are fully addressed. The 7 day Frequency is appropriate because no major replenishment of pool water is expected to take place over a short period of time.

REFERENCES

1. Double contingency principle of ANSI N16.1-1975, as specified in the April 14, 1978, NRC letter (Section 1.2) and implied in the proposed revision to Regulatory Guide 1.13 (Section 1.4, Appendix A).

2. SAR, Section 14.2.2.3.

3. Safety Evaluation Report, Section 2.1.3, License Amendment No. 76, April 15, 1983.

4. 10 CFR 50.36.

5. 10 CFR 50.68

B.3.7 PLANT SYSTEMS

B 3.7.15 Spent Fuel Pool Storage

BASES

BACKGROUND

The spent fuel assembly storage facility is designed to store either new (nonirradiated) nuclear fuel assemblies, or burned (irradiated) fuel assemblies in a vertical configuration underwater. The spent fuel pool is sized to store 968 fuel assemblies. The spent fuel storage cells are installed in parallel rows with center to center spacing of 10.65 inches in each direction.

The spent fuel storage pool is divided into two three separate and distinct regions as shown in SAR Figure 9-53 which, for the purpose of criticality considerations, are considered as separate pools. Region 1 is designed to accommodate new fuel with a maximum enrichment of 4.10 wt% U-235, or spent (irradiated) fuel regardless of the discharge fuel burnup. and Region 2 is are designed to accommodate fuel of various initial enrichments which have accumulated minimum burnups within the acceptable domain according to Figures 3.7.15-1 and 3.7.15-2. Region 3 is designed to accommodate new fuel with a maximum enrichment of 5.0wt% U-235 or spent (irradiated) fuel regardless of the discharge fuel burnup. Fuel assemblies not meeting the criteria acceptable range of Figures 3.7.15-1 or 3.7.15-2 shall be stored in accordance with paragraph 4.3.1.1.e f in SAR TS Section 4.3, Fuel Storage.

APPLICABLE SAFETY ANALYSES

Criticality of fuel assemblies in the spent fuel storage rack is prevented by the design of the rack which limits fuel assembly interaction. This is done by fixing the minimum separation between assemblies and inserting neutron poison between assemblies in Region 1. Region 1 and Region 2 controls fuel assembly interaction by fixing the minimum separation between assemblies and by setting enrichment and burnup criterion to limit fissile materials. Region 3 controls fuel assembly interaction with the insertion of Metamic poison panels. This is sufficient to maintain Aa k_{eff} of ≤ 0.95 for spent fuel of original enrichment of up to 4.105.0wt% is accomplished by taking credit for boron (nominal conditions require 400 ppm for all regions). A k_{eff} of < 1.0 is accomplished when no credit for boron is taken. However, fuel assemblies to be stored in the spent fuel pool Region 2 which do not meet enrichment and burnup criterion must be stored in a checkerboard pattern to maintain a k_{eff} of 0.95 or less. In order to prevent inadvertent fuel assembly insertion into two adjacent storage locations, vacant spaces adjacent to the faces of any fuel assembly which does not meet the Region 2 burnup criteria (unrestricted) are physically blocked before any such fuel assembly is placed in Region 2 (Ref. 1). In addition, the area designated for checkerboard arrangement is divided from the normal storage in Region 2 by a row of vacant storage spaces (Ref. 2.)

Region 1 and Region 2

Fresh or spent fuel with enrichments up to 5.0 wt% U-235 may be stored in Region 1 and/or Region 2 per TS 3.7.15 Figures 3.7.15-1 (Region 1) and 3.7.15-2 (Region 2). The figures use initial U-235 enrichment and burnup to determine loading restrictions. The five curves on each figure represent decay time in years. Decay time is based on the time at which an assembly is permanently placed in the pool (i.e., if an assembly is placed in the pool one cycle and then returned to the core, the initial time in the pool is not included in the decay time once the assembly is permanently removed from the core.) The following equations were used to generate the decay curves and may be used to interpolate fuel placement in restricted or non-restricted regions:

Region 1 Decay Time Curves:

Decay Time, Years	Burnup, GWD/MTU
0	$(-0.1661*E^4) + (2.791*E^3) - (17.013*E^2) + (55.795*E) - 62.57$
5	$(-0.3014*E^4) + (4.6636*E^3) - (26.447*E^2) + (75.84*E) - 77.88$
10	$(-0.443*E^4) + (6.6239*E^3) - (36.324*E^2) + (96.837*E) - 93.94$
15	$(-0.5782*E^4) + (8\ 4965*E^3) - (45.758*E^2) + (116.88*E) - 109.27$
20	$(-0.7198*E^4) + (10.457*E^3) - (55.635*E^2) + (137.88*E) - 125.3$

Region 2 Decay Time Curves:

Decay Time, Years	Burnup, GWD/MTU
0	$(0.6257*E^3) - (6.8758*E^2) + (36.293*E) - 46.0$
5	$(0.4934*E^3) - (5.5023*E^2) + (31.23*E) - 40.3$
10	$(0.3634*E^3) - (4.1511*E^2) + (26.244*E) - 34.7$
15	$(0.2311*E^3) - (2.776*E^2) + (21.186*E) - 29.0$
20	$(0.1011*E^3) - (1.4265*E^2) + (16.19*E) - 23.4$

Region 1 and Region 2 Restricted Loading Pattern

If restricted loading in either Region 1 or Region 2 storage cells is required by Figures 3.7.15-1 and/or 3.7.15-2, then a checkerboard loading arrangement is required (alternate storage cells filled only with water or non-fuel bearing materials checkerboarded with cells containing fuel assemblies).

Region 1 is comprised of two separate modules and Region 2 has four separate modules with a water gap separating each module from the others. If it is desired to load part of a module in the checkerboard loading pattern and part of the module without loading restrictions, then a single row of empty cells (cells filled only with water or non-fuel bearing materials) must be maintained as a barrier between the two loading patterns. The row of empty cells serves as the water gap between the modules to prevent neutron interaction between the two loading patterns and thereby ensures proper criticality control.

If a checkerboard loading arrangement is not desirable, then the fuel assembly may be stored in Region 3.

Region 3

Fresh fuel assemblies with enrichments up to a maximum of 5 wt% U-235 or spent fuel of any burnup may be stored in any cell in Region 3 without restriction.

Required Soluble Boron Concentrations for Accident Conditions

TS 3.7.14 includes the requirement for great than 1600 ppm boron concentration to assure the fuel assemblies will be maintained in a subcritical array with $K_{eff} \leq 0.95$ in the event of a postulated drop accident. Analysis has shown that, during a postulated misplacement accident with the fuel stored within the limits of this specification, that a $K_{eff} \leq 0.95$ will be maintained when the boron concentration is at or above 800 ppm.

The spent fuel pool storage satisfies Criterion 2 of 10 CFR 50.36 (Ref. 3).

LCO

The restrictions on the placement of fuel assemblies within the fuel pool, according to Figures 3.7.15-1 and 3.7.15-2, ensure that the k_{eff} of the spent fuel pool will always remain ≤ 0.95 assuming the pool to be flooded with 400 ppm unborated water. The restrictions are consistent with the criticality safety analysis performed for the spent fuel pool. Fuel assemblies not meeting the enrichment and burnup criteria shall be stored in accordance with Specification 4.3.1.1.

The k_{eff} of the spent fuel pool will remain below 1.0 when the pool is flooded with unborated water.

In the event a checkerboard storage configuration is deemed necessary for a portion of Region 1 or 2, spaces, void of fissionable material, adjacent to the faces of any fuel assembly which does not meet the Region 1 or 2 burnup criteria (non-restricted) shall be physically blockedconfirmed before any such fuel assembly may be placed in Region 1 or 2. This will prevent inadvertent fuel assembly insertion into two adjacent storage locations.

APPLICABILITY

This LCO applies whenever any fuel assembly is stored in Region 1 or 2 of the spent fuel pool.

ACTIONS

A.1

Required Action A.1 is modified by a Note indicating that LCO 3.0.3 does not apply. If moving irradiated fuel assemblies while in MODE 5 or 6, LCO 3.0.3 would not specify any action. If moving irradiated fuel assemblies while in MODE 1, 2, 3, or 4, the fuel movement is independent of reactor operation. Therefore, in either case, inability to move fuel assemblies is not sufficient reason to require a reactor shutdown.

When the configuration of fuel assemblies stored in the spent fuel pool is not in accordance with Figure 3.7.15-1 or 3.7.15-2, immediate action must be taken to make the necessary fuel assembly movement(s) to bring the configuration into compliance with Figure 3.7.15-1, Figure 3.7.15-2, or Specification 4.3.1.1.

SURVEILLANCE REQUIREMENTS

SR 3.7.15.1

This SR verifies by administrative means that the initial enrichment, cooling time, and burnup of the fuel assembly is in accordance with Figure 3.7.15-1 or Figure 3.7.15-2 in the accompanying LCO or Specification 4.3.1.1. For fuel assemblies in the unacceptable range of Figure 3.7.15-1 or 3.7.15-2, performance of the SR will ensure compliance with Specification 4.3.1.1.

REFERENCES

1. SAR, Section 9.6.2.

2. SER for ANO-1 License Amendment No. 76, Section 2.1 (0CNA048314), dated April 15, 1983.

3. 10 CFR 50.36.

Attachment 4

1CAN040302

Holtec License Report

HOLTEC
INTERNATIONAL

Holtec Center, 555 Lincoln Drive West, Marlton, NJ 08053
Telephone (856) 797-0900
Fax (856) 797-0909

SPENT FUEL POOL RACKS MODIFICATIONS WITH POISON MATERIAL INSERTS IN ANO UNIT-1

FOR

ENTERGY

Holtec Report No: HI-2022867

Holtec Project No: 1196

Report Class: SAFETY RELATED

TABLE OF CONTENTS

TABLE OF CONTENTS

TABLE OF CONTENTS

TABLE OF CONTENTS

Tables

TABLE OF CONTENTS

Figures

1.0 INTRODUCTION

Arkansas Nuclear One, Unit 1 (ANO-1), operated by Entergy Operations, is located approximately 70 miles northwest of Little Rock, Arkansas and about five miles west of Russellville. ANO-1 is a Babcock & Wilcox pressurized water reactor and has been in commercial operation since 1974. The ANO-1 reactor is licensed for a thermal power level of 2568 megawatts The reactor core contains 177 fuel assemblies and the spent fuel pool (SFP) is licensed for the storage of 968 assemblies.

The racks in the SFP of ANO-1 are free-standing and self supporting racks of Westinghouse design. The principal fabrication materials are ASTM A-240, Type 304 stainless steel for the structural members and shapes. "Boraflex", a product of BISCO (a division of Brand, Inc.) was originally used to augment reactivity control.

The ANO-1 SFP was designed to hold spent fuel assemblies (or rod cluster control assemblies) in underwater storage for long-term decay after their removal from the reactor core. The structures are seismic Category I, heavy walled, reinforced concrete pool, located on grade outside the containment structure. The interior of the pool is lined with stainless steel plate (Type 304L).

The ANO-1 spent fuel racks consist of individual cells with a square pitch of 10.65 inches, each of which accommodates a single B&W 15x15 fuel assembly or equivalent. The ANO-1 SFP is divided into two regions, designated Region 1 and Region 2. Region 1 racks employ Boraflex as the poison material and are presently qualified to store fresh fuel assemblies with enrichments up to 4.1 weight percent (wt%) ^{235}U. Region 2 racks are designed with flux-traps and are currently used to store spent fuel assemblies with various initial enrichments that have accumulated certain minimum burn-ups. These racks do not have any poison material. Some of the Region 2 racks will be modified by the insertion of Metamic® absorber panels into the flux trap region to create a Region 3. These different regions are depicted in Figure 1-1. These poison inserts will have two borated Aluminum (Metamic®) panels as neutron absorbers. Each poison insert panel will be held in the flux trap along the cell wall by a spring mechanism. The insertion of the Metamic® poison panels into the new region, as shown by analyses later in this report, will enable storage of fresh fuel with a maximum enrichment up to 5.0 weight percent (wt%) in the ANO-1 SFP. The Region 3 flux traps will be fitted with lead-ins on the top of the flux traps, which will act to prevent any possible uplifting of the poison panel insert. The lead-in devices will also help guide the fuel assemblies into the storage cells.

The existing Region 1 racks have been reanalyzed to establish new fuel storage requirements without crediting the presence of Boraflex. The Region 2 racks, which will not be converted to Region 3 racks, were re-analyzed to establish more flexible fuel storage requirements. These racks have been re-analyzed to establish their capability for fresh fuel storage in a 2-of-4 checkerboard arrangement or to store spent fuel assemblies of specified enrichment-burnup limits. The New Fuel Vault and fuel handling equipment is also analyzed to confirm acceptability of fuel with initial enrichment up to 5.0 wt% ^{235}U.

Sections 2.0 and 3.0 of this report provide an abstract of the design and material information on the poison inserts and the racks.

Section 4.0 provides a summary of the methods and results of the criticality evaluations performed for the spent fuel storage racks. Credit for soluble boron in the pool has been taken, in accordance with 10CFR50.68, to assure the criticality safety of the spent fuel storage racks. The analyses show that the neutron multiplication factor (k_{eff}) for the stored fuel array are subcritical under assumed condition of the loss of all soluble boron in the pool water. Additional analyses are required to determine the soluble boron requirements to maintain k_{eff} below 0.95 for both normal storage and accident conditions. The criticality safety analysis sets the requirements on the Metamic® poison insert panel length and the amount of B_4C (i.e., loading density) of the Metamic® inserts for the Region 3 SFP racks.

Thermal-hydraulic considerations require that fuel cladding will not fail due to excessive thermal stress. The thermal-hydraulic analyses carried out in support of the modification of some of the existing Region 2 racks are described in Section 5.0.

Rack module structural criteria require that the primary stresses in the rack module structure will remain below the ASME B&PV Code (Subsection NF) [1] allowables. Demonstrations of seismic and structural adequacy are presented in Section 6.0. The structural qualification also requires that the subcriticality of the stored fuel be maintained under all postulated mechanical accident scenarios. The structural consequences of these postulated accidents are evaluated and presented in Section 7.0 of this report.

Results of the analyses presented in this report establish acceptable restrictions on combinations of initial enrichment and discharge burnups for Region 1 and Region 2, as well as showing that the insertion of poison inserts into the newly defined Region 3 racks will permit storage of fresh fuel assemblies in these racks. The storage racks meet all requirements of the applicable USNRC guidelines and regulations, and applicable ANSI/ANS standards (References 2 – 6). The analysis

methodologies employed are a direct evolution of previous license applications reviewed and approved by the USNRC, including nuclear subcriticality, thermal-hydraulic safety, seismic and structural adequacy, and mechanical integrity.

All computer programs utilized to perform the analyses documented in section 1.0 through 7.0 are benchmarked and verified. These programs have been utilized by Holtec International in numerous license applications over the past decade. The analyses presented herein clearly demonstrate that the rack module arrays with the addition of the poison inserts and the lead-ins possess wide margins of safety in respect to all considerations of safety specified in the OT Position Paper [3], namely, nuclear subcriticality, thermal-hydraulic safety, seismic and structural adequacy, and mechanical integrity.

1.1 REFERENCES

[1] American Society of Mechanical Engineers (ASME), Boiler & Pressure Vessel Code, Section III, 1989 Edition, Subsection NF, and Appendices.

[2] General Design Criterion 62, Prevention of Criticality in Fuel Storage and Handling.

[3] USNRC, "OT Position for Review and Acceptance of Spent Fuel Storage and Handling Applications, April 14, 1978, and Addendum dated January 18, 1979.

[4] Code of Federal Regulations 10CFR50.68, Criticality Accident Requirements

[5] ANSI-8.17-1984, Criticality Safety Criteria for the Handling, Storage and Transportation of LWR Fuel Outside Reactors.

[6] L. I. Kopp, "Guidance on the Regulatory Requirements for Criticality Analysis Of Fuel Storage At Light-Water Reactor Plants", USNRC Internal Memorandum L. Kopp to Timothy Collins, August 19 1998.

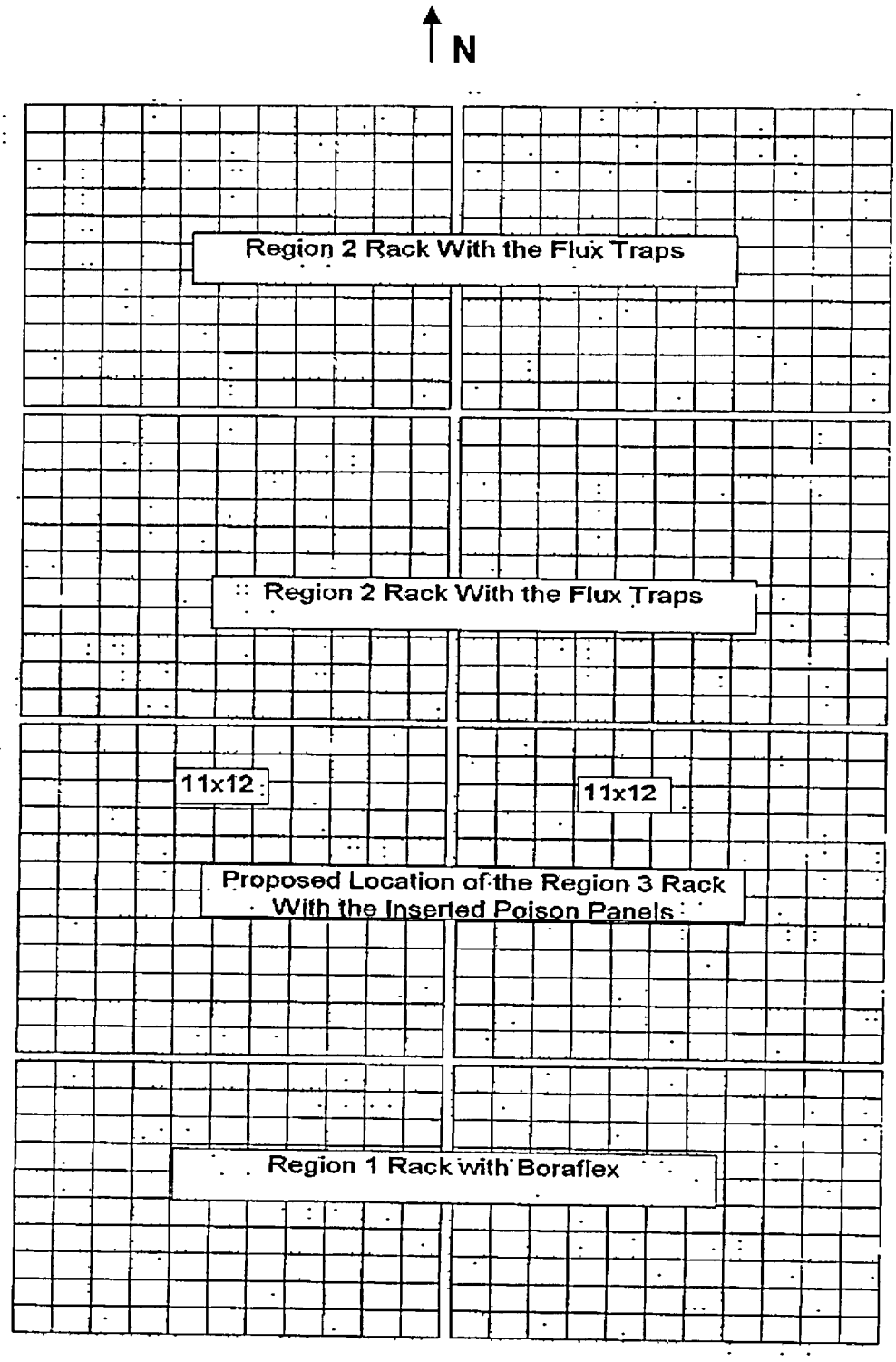

Figure 1.1: Location of the Different Rack Types in the Spent Fuel Pool

2.0 SPENT FUEL RACK FLUX TRAP GAP POISON INSERT DESIGN

2.1 INTRODUCTION

The ANO-1 Spent Fuel Pool contains eight fuel racks with a total storage capacity of 968 fuel assemblies. As described in Section 1.0, there are currently two regions in the ANO-1 SFP that are designated as Region 1, which contains Boraflex, and Region 2, which does not contain poison inserts. A portion of Region 2 will be designated as Region 3 in which panels of Metamic® containing a high loading of the B_4C (up to 25% by weight of B_4C) will be inserted into the flux traps to provide appropriate neutron attenuation between adjacent storage cells. With the insert of Metamic®, it is proposed to allow the initial enrichment limit for fresh fuel storage in Region 3 racks to be 5.0 wt% (4.95 ±0.05 wt%).

In addition to the poison inserts, the Region 3 racks will also be fitted with independent lead-in devices to help guide the fuel assemblies into the storage cells and prevent debris from entering the flux trap.

2.2 SUMMARY OF PRINCIPAL DESIGN CRITERIA

The key design criteria for the spent fuel racks are set forth in the USNRC memorandum entitled "OT Position for Review and Acceptance of Spent Fuel Storage and Handling Applications," dated April 14, 1978 as modified by amendment dated January 18, 1979. The individual sections of this report expound on the specific design bases derived from the above-mentioned "OT Position Paper." The design bases for the spent fuel racks with the poison inserts in them are summarized below:

a. Kinematic Stability: All freestanding modules must be kinematically stable (against tipping or overturning) if a seismic event is imposed on any module.

b. Structural Compliance: All primary stresses in the rack modules must satisfy the limits postulated in Section III subsection NF of the ASME B & PV Code.

c. Thermal-Hydraulic Compliance: The spatial average bulk pool temperature is required to remain below 150 °F. No localized boiling is permitted.

d. Criticality Compliance: The New Fuel Storage Racks (NFSR) and Spent Fuel Storage Racks (SFSR) must be able to store Zircaloy clad fuel of 5.0 weight percent maximum enrichment while maintaining the reactivity (k_{eff}) less than 0.95.

e. Accident Events: In the event of postulated drop events (uncontrolled lowering of a fuel assembly, for instance), it is necessary to demonstrate that the stored fuel remains subcritical.

The foregoing design bases are further articulated in Sections 4.0 through 7.0 of this report.

2.3 APPLICABLE CODES AND STANDARDS

The following codes, standards and practices are used as applicable for the design, construction, and assembly of the poison inserts. Additional specific references related to detailed analyses are given in each section.

a. Design Codes

(1) ASME B & PV Code Section III, 1998 Edition.

(2) American Society for Nondestructive Testing SNT-TC-1A, June 1980, Recommended Practice for Personnel Qualifications and Certification in Non-destructive Testing.

(3) ASME Y14.5M, Dimensioning and Tolerancing

(4) ASME B & PV Code, Section II-Part D, 1998 Edition.

b. Standards of American Society for Testing and Materials (ASTM)

(1) ASTM A240 - Standard Specification for Heat-Resisting Chromium and Chromium-Nickel Stainless Steel Plate, Sheet and Strip for Pressure Vessels.

(2) ASTM A262 - Standard Practices for Detecting Susceptibility to Intergranular Attack in Austenitic Stainless Steel.

(3) ASTM C750 - Standard Specification for Nuclear-Grade Boron Carbide Powder.

(4) ASTM A380 - Standard Practice for Cleaning, Descaling, and Passivation of Stainless Steel Parts, Equipment and Systems.

(5) ASTM C992 - Standard Specification for Boron-Based Neutron Absorbing Material Systems for Use in Nuclear Spent Fuel Storage Racks.

(6) ASTM E3 - Standard Practice for Preparation of Metallographic Specimens.

(7) ASTM E190 - Standard Test Method for Guided Bend Test for Ductility of Welds.

c. Welding Code:

(1) ASME B & PV Code, Section IX - Welding and Brazing Qualifications, latest applicable edition and addenda.

d. Quality Assurance, Cleanliness, Packaging, Shipping, Receiving, Storage, and Handling

(1) ANSI N45.2.1 - Cleaning of Fluid Systems and Associated Components during Construction Phase of Nuclear Power Plants - 1980 (R.G. 1.37)

(2) ANSI N45.2.2 - Packaging, Shipping, Receiving, Storage and Handling of Items for Nuclear Power Plants - 1978 (R.G. 1.38).

(3) ANSI N45.2.6 - Qualifications of Inspection, Examination, and Testing

Personnel for the Construction Phase of Nuclear Power Plants - 1973. (R.G. 1.58).

(4) ANSI N45.2.8 - Supplementary Quality Assurance Requirements for Installation, Inspection and Testing of Mechanical Equipment and Systems for the Construction Phase of Nuclear Plants - 1975 (R.G. 1.116).

(5) ANSI N45.2.11 - Quality Assurance Requirements for the Design of Nuclear Power Plants - 1978 (R.G. 1.64).

(6) ANSI N45.2.12 - Requirements for Auditing of Quality Assurance Programs for Nuclear Power Plants - 1977 (R.G 1.144).

(7) ANSI N45.2.13 - Quality Assurance Requirements for Control of Procurement of Items and Services for Nuclear Power Plants - 1976 (R.G. 1.123).

(8) ANSI N45.2.23 - Qualification of Quality Assurance Program Audit Personnel for Nuclear Power Plants - 1978 (R.G. 1.146).

(9) ASME B & PV Code, Section V, Nondestructive Examination, 1983 Edition.

(10) ANSI N16.9-75 - Validation of Calculation Methods for Nuclear Criticality Safety.

(11) ASME NQA-1 – Quality Assurance Program Requirements for Nuclear Facilities.

(12) ASME NQA-2 – Quality Assurance Requirements for Nuclear Power Plants.

e. USNRC Documents

(1) "OT Position for Review and Acceptance of Spent Fuel Storage and Handling Applications," dated April 14, 1978, and the modifications to this document of January 18, 1979.

(2) NUREG 0612, "Control of Heavy Loads at Nuclear Power Plants", USNRC, Washington, D.C., July, 1980.

(3) NUREG 0800, "Standard Review Plan for the Review of Safety Analysis Reports for Nuclear Power Plants", USNRC, Washington, D.C., July, 1981.

f. Other ANSI Standards (not listed in the preceding)

(1) ANSI/ANS 8.1 - Nuclear Criticality Safety in Operations with Fissionable Materials Outside Reactors, 1983.

(2) ANSI N45.2.9 - Requirements for Collection, Storage and Maintenance of Quality Assurance Records for Nuclear Power Plants - 1974.

(3) ANSI N45.2.10 - Quality Assurance Terms and Definitions - 1973

(4) ANSI/ASME N626-3 -- Qualification and Duties of Specialized Professional Engineers, 1977.

g. Code-of-Federal Regulations (CFR)

(1) 10 CFR 20 - Standards for Protection Against Radiation.

(2) 10 CFR 21 - Reporting of Defects and Non-compliance.

(3) 10 CFR 50 Appendix A - General Design Criteria for Nuclear Power Plants.

(4) 10 CFR 50 Appendix B - Quality Assurance Criteria for Nuclear Power Plants and Fuel Reprocessing Plants.

(5) 10 CFR 100 – Reactor Site Criteria

h. Regulatory Guides (RG)

(1) RG 1.13 - Spent Fuel Storage Facility Design Basis (Revision 2 Proposed).

(2) RG 1.25 - Assumptions Used for Evaluating the Potential Radiological Consequences of a Fuel Handling Accident in the Fuel Handling and Storage Facility for Boiling and Pressurized Water Reactors, Rev. 0 - March, 1972.

(3) RG 1.28 - Quality Assurance Program Requirements - Design and Construction, Rev. 2 - February, 1979 (endorses ANSI N45.2).

(4) RG 1.33 – Quality Assurance Program Requirements.

(5) RG 1.29 - Seismic Design Classification, Rev. 2 - February, 1976.

(6) RG 1.31 - Control of Ferrite Content in Stainless Steel Weld Metal, Rev. 3.

(7) RG 1.38 - Quality Assurance Requirements for Packaging, Shipping, Receiving, Storage and Handling of Items for Water-Cooled Nuclear Power Plants, Rev. 2 - May, 1977 (endorses ANSI N45.2 2).

(8) RG 1.44 - Control of the Use of Sensitized Stainless Steel.

(9) RG 1.58 – Qualification of Nuclear Power Plant Inspection, Examination, and Testing Personnel, Rev. 1 – September 1980 (endorses ANSI N45.2.6)

(10) RG 1.60 – Design Response Spectra for Seismic Design of Nuclear Power Plants

(11) RG 1.61 - Damping Values for Seismic Design of Nuclear Power Plants, Rev. 0, 1973.

(12) RG 1.64 - Quality Assurance Requirements for the Design of Nuclear Power Plants, Rev. 2 - June, 1976 (endorses ANSI N45.2.11).

(13) RG 1.71 - Welder Qualifications for Areas of Limited Accessibility.

(14) RG 1.74 - Quality Assurance Terms and Definitions, Rev. 2 - February, 1974 (endorses ANSI N45.2.10).

(15) RG 1.85 - Materials Code Case Acceptability - ASME Section III, Division 1.

(16) RG 1.88 - Collection, Storage and Maintenance of Nuclear Power Plant Quality Assurance Records, Rev. 2 - October, 1976 (endorses ANSI N45.2.9).

(17) RG 1.92 - Combining Modal Responses and Spatial Components in Seismic Response Analysis, Rev. 1 - February, 1976.

(18) RG 1.116 - Quality Assurance Requirements for Installation, Inspection and Testing of Mechanical Equipment and Systems, Rev. 0-R - May,1977 (endorses ANSI N45.2.8-1975)

(19) RG 1.123 - Quality Assurance Requirements for Control of Procurement of Items and Services for Nuclear Power Plants, Rev. 1 - July, 1977 (endorses ANSI N45.2.13).

(20) RG 1.124 - Service Limits and Loading Combinations for Class 1 Linear-Type Component Supports, Rev. 1 - January,1978.

(21) RG 1.144 - Auditing of Quality Assurance Programs for Nuclear Power Plants, Rev.1 - September, 1980 (endorses ANSI N45.2.12-1977)

(22) RG 8.8 - Information Relative to Ensuring that Occupational Radiation Exposures at Nuclear Power Stations will be as Low as Reasonably Achievable (ALARA).

(23) IE Information Notice 83-29 - Fuel Binding Caused by Fuel Rack Deformation.

(24) RG 8.38 - Control of Access to High and Very High Radiation Areas in Nuclear Power Plants, June, 1993.

i Branch Technical Position

(1) CPB 9.1-1 - Criticality in Fuel Storage Facilities.

(2) ASB 9-2 - Residual Decay Energy for Light-Water Reactors for Long-Term Cooling - November, 1975.

j American Welding Society (AWS) Standards

(1) AWS D1.1 - Structural Welding Code - Steel.

(2) AWS D1.3 - Structure Welding Code - Sheet Steel.

(3) AWS D9.1 - Sheet Metal Welding Code.

(4) AWS A2.4 - Standard Symbols for Welding, Brazing and Nondestructive Examination.

(5) AWS A3.0 - Standard Welding Terms and Definitions.

(6) AWS A5.12 - Specification for Tungsten and Tungsten Alloy Electrodes for Arc-Welding and Cutting

(7) AWS QC1 - Standard for AWS Certification of Welding Inspectors.

(8) AWS 5.4 – Specification for Stainless Steel Electrodes for Shielded Metal Arc Welding.

(9) AWS 5 9 – Specification for Bare Stainless Steel Welding Electrodes and Rods.

k. Other References

(1) ANO Unit 1 & 2 Operating Licenses and Technical Specifications, License No. DPR-51 & NPF-6.

(2) ANO Unit 1 & 2 Updated Final Safety Analysis Report (UFSAR).

2.4 QUALITY ASSURANCE PROGRAM

The governing quality assurance requirements for design and fabrication of the poison inserts are stated in 10 CFR 50 Appendix B. Holtec's Nuclear Quality Assurance program complies with this regulation and is designed to provide a system for the design, analysis, and licensing of customized components in accordance with various codes, specifications, and regulatory requirements.

The Quality Assurance System that will be used by Entergy Operations to install the poison inserts is controlled by the ANO-1 Quality Assurance Program.

2.5 MECHANICAL DESIGN

The mechanical design of the poison insert consists of two poison panels separated by a mechanism to maintain the water gap specified by criticality considerations. The poison panels

are independent flat panels sized to cover the active fuel region. The poison panels will extend all the way to the SFP rack base plate. The poison panel will be nominally 0.10 inch thick 6061 aluminum plus boron carbide metal matrix manufactured by Metamic®.

The poison panels will be held together with a frame that is fabricated from SA240-304 stainless steel. A schematic of the arrangement is shown in Figure 2.5.1. The poison panels and the mechanical framework form the poison insert. The poison insert will be able to collapse smaller than the flux trap opening prior to installation. Figure 4.3.2 depicts the current Region 2 cell with four flux traps. The insert is designed to expand in the flux trap once fully inserted.

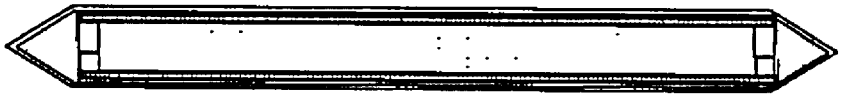

Figure 2.5.1 Schematic of the Poison Insert Mechanism

The lead-in device, which is depicted in Figure 2.5.2, is fabricated from SA240-304L stainless steel. The device is designed to rest on top of the flux trap, and it is secured in place by two slotted plates, which straddle the cell wall at the corners external to the flux trap. The size and shape of the lead-in is such that it will not interfere with the square opening of the cell. Each lead-in device weighs less than 3 lb. The lead-in contains flow holes in the mounting plate to provide an uninterrupted flow path for the water entering at the bottom of the flux trap and exiting at the top of the flux trap.

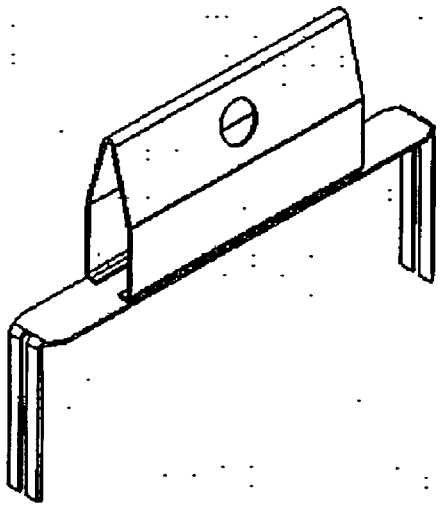

Figure 2.5.2 Lead-in Device

2.6 FABRICATION

The object of this section is to provide a brief description of the poison insert construction activities, which enable an independent appraisal of the adequacy of design. The pertinent methods used in manufacturing the poison inserts may be stated as follows:

1. The poison panels are extruded and rolled from a powder metallurgy billet then cut to the specified rectangular size.

2. The fabrication process involves operational sequences that permit immediate accessibility for verification by the inspection staff.

3. The poison inserts are fabricated per the manufacturer's Appendix B Quality Assurance program, which ensures, and documents that the fabricated poison inserts meet all of the requirements of the design and fabrication documents.

2.7 INSTALLATION

The poison insert is placed in an upending cradle on the fuel bridge. The poison insert is then upended and connected to the poison insert handling tool. All installation activities will be performed remotely, from the fuel bridge, using long handled installation tools. Subsequent to the upending process, the poison insert is lowered into the spent fuel pool and guided into the appropriate flux trap with installation tools. Then, the lead-ins are installed onto a flux trap that received a poison insert.

3.0 MATERIAL CONSIDERATIONS

3.1 INTRODUCTION

Safe storage of nuclear fuel in the pool requires that the materials utilized in the poison inserts be of proven durability and compatible with the pool water environment. This section provides a synopsis of the considerations with regard to long-term design service life of 60 years.

3.2 STRUCTURAL MATERIALS

The only structural material utilized in the fabrication of the poison inserts is SA240 Type 304 stainless steel.

3.3 NEUTRON ABSORBING MATERIAL

In addition to the structural materials, the poison inserts employ Metamic®, a patented product of Metamic®, Inc., as the neutron absorber material A brief description of Metamic® follows.

Metamic® is a neutron absorber material developed by the Reynolds Aluminum Company in the mid-1990s for spent fuel reactivity control in dry and wet storage applications [3.3.1]. Metallurgically, Metamic® is a metal matrix composite (MMC) consisting of a high purity 6061 aluminum matrix reinforced with Type 1 ASTM C750-89, isotopically graded boron carbide (B_4C). Metamic® is characterized by an extremely fine aluminum spherical powder (325 mesh or better) and boron carbide powder (average particle size under 10 microns). The high performance reliability of Metamic® derives from the particle size distribution of its constituents, namely, high purity aluminum 6061 alloy powder and isotopically graded B_4C particulate, rendered into an isotropic metal matrix composite state by the powder metallurgy process which yields excellent homogeneity, and which prevents B_4C from clustering in the final product.

The powders are carefully blended together without binders, chelating agents, or other additives that could potentially become retained in the final product and deleteriously influence performance. The maximum percentage of B_4C that will be dispersed in the aluminum alloy 6061 matrix is 25% by weight. The pure blend of powders is cold isostatically compacted into a green billet and vacuum sintered to a

high theoretical density[1]. An extrusion process is used to bring the matrix into final density. Billets can vary in diameter, size and weight depending on a number of variables including loading and final panel dimensions.

Metamic® has been subjected to an extensive array of tests sponsored by the Electric Power Research Institute (EPRI) that evaluated the functional performance of the material at elevated temperatures (up to 900 °F) and radiation levels (1E+11 rads gamma). The results of the tests documented in an EPRI report [3.3.2] indicate that Metamic® maintains its physical and neutron absorption properties with little variation in its properties from the unirradiated state. The main conclusions provided in the above-referenced EPRI report are summarized below:

- The isotropic metal matrix configuration produced by the powder metallurgy process with a complete absence of interconnected internal porosity in Metamic® ensures that its density is essentially equal to the maximum theoretical density.

- Measurements of boron carbide particle distribution show extremely small particle-to-particle distance[2] and near-perfect homogeneity.

- The physical and neutronic properties of Metamic® are essentially unaltered under exposure to elevated temperatures (750 °F – 900 °F).

- No detectable change in the neutron attenuation characteristics under accelerated test conditions has been observed.

Holtec International's Q.A. program ensures that Metamic® is manufactured under the control and surveillance of a Quality Assurance/Quality Control Program that conforms to the requirements of 10 CFR 50 Appendix B, "Quality Assurance Criteria for Nuclear Power Plants".

3.3 1 METAMIC® Material Characteristics

Aluminum: Aluminum is a silvery-white, ductile metallic element. The 6061 alloy aluminum is used

[1] The theoretical density of Metamic®, before being hot worked, is 82% to 98% depending on the B_4C content.
[2] Medium measured neighbor-to-neighbor distance is 10.08 microns according to the article, "METAMIC Neutron Shielding" [3.3.3].

extensively in heat exchangers, pressure and storage tanks, chemical equipment, reflectors, and sheet metal work.

It has high resistance to corrosion in industrial and marine atmospheres. Aluminum has atomic number of 13, atomic weight of 26.98, specific gravity of 2.69 and valence of 3. The physical, mechanical and chemical properties of the 6061 alloy aluminum are listed in Table 3.3.1.

The excellent corrosion resistance of the 6061 alloy aluminum is provided by the protective oxide film that quickly develops on its surface from exposure to the atmosphere or water. This film prevents the loss of metal from general corrosion or pitting corrosion.

Boron Carbide: The boron carbide contained in Metamic® is a fine granulated powder that conforms to ASTM C750-89 nuclear grade Type I. The material conforms to the chemical composition and properties listed in Table 3.3.2.

References [3.3.1] and [3.3.2] provide further discussion as to the suitability of these materials for use in spent fuel storage applications.

3.4 COMPATIBILITY WITH ENVIRONMENT

All materials used in the construction of the poison inserts have been determined to be compatible with the ANO Spent Fuel Pools, and have an established history of in-pool usage. Austenitic stainless steel (e.g., Type 304) is a widely used stainless alloy in nuclear power plants, and it has an established history of in-pool usage. Metamic® is likewise an excellent material for spent fuel applications based on its high resistance to corrosion and its functional performance at elevated temperatures and radiation levels.

3.5 HEAVY LOAD CONSIDERATIONS

There are no heavy loads involved in the proposed installation of poison inserts. The estimated weight of a single poison insert is less than 40 pounds

3.6 REFERENCES

[3.3.1] "Use of METAMIC in Fuel Pool Applications," Holtec International, HI-2022871, Revision 1, August 2002.

[3.3.2] "Qualification of METAMIC for Spent Fuel Storage Application," EPRI, 1003137, Final Report, October 2001.

[3.3.3] K Anderson et al., "METAMIC Neutron Shielding," EPRI Boraflex Conference, November 19-20, 1998.

Table 3.3.1 Chemical Composition and Physical Properties of Aluminum (6061 Alloy)	
Chemical Composition	
0.8-1.2%	Magnesium
0.40-0.8%	Silicone
0.15-0.40%	Copper
0.15% max.	Iron
0.25% max.	Zinc
0.15% max.	Titanium
50 ppm max.	Nickel
10 ppm max.	Cobalt
10 ppm max.	Manganese
10 ppm max.	Chromium
0.15% max.	Other
Remainder	Aluminum
Physical Properties	
Density	0.098 lb/in^3 2.71 g/cm^3
Melting Range	1080 °F – 1205 °F 582 °C – 652 °C
Thermal Conductivity (77 °F)	1250 BTU/hr-ft^2-°F/in 1.55 kcal/hr-cm^2-°C/cm

Table 3.3.2 Chemical Composition and Physical Properties of Boron Carbide	
Chemical Composition (Weight Percent)	
Total boron	76.5 min.
B^{10} isotope	19.9 ± 0.30 a/o
HNO_3 soluble boron	0.5 max.
Water soluble boron	0.2 max.
Fluoride	25 µg/g max.
Chloride	75 µg/g max.
Calcium	0.3 max.
Iron	1.0 max.
Total boron plus total carbon	98.0 min.
Physical Properties	
Chemical formula	B_4C
Boron content (weight percent)	78.28%
Carbon content (weight percent)	21.72%
Crystal structure	rhombohedral
Density	0.0907 lb/in^3 2.51 g/cm^3
Melting Point	4442 °F 2450 °C
Boiling Point	6332 °F 3500 °C

4.0 CRITICALITY SAFETY EVALUATION

4.1 DESIGN BASES

This section of the report documents the criticality safety evaluation for the storage of fresh and spent nuclear fuel assemblies in the ANO-1 high-density spent fuel storage racks. ANO-1 spent fuel pool currently has two regions of storage, which are currently licensed to store fuel assemblies with a maximum enrichment of 4.1 wt%.

1. Region 1 racks: These racks were originally designed with Boraflex as the poison material in a flux-trap configuration.

2. Region 2 racks: These racks are designed to store spent fuel assemblies of a specified combination of initial enrichment and discharge burnup. These racks do not currently have any poison material within the water gap between cells.

Due to the Boraflex degradation in the Region 1 racks, future credit for Boraflex is not feasible in these racks. The proposed resolution is to re-evaluate the criticality safety of the racks without credit for Boraflex and to insert poison material strips into the flux trap region of some of the Region 2 type racks. These modified Region 2 racks are identified as Region 3 racks. The new Region 3 racks will enable unrestricted fresh fuel (maximum enrichment of 5.0 wt% or nominally 4.95 $\pm$0.05 wt%) storage capability in that region. The calculations are performed with no credit for Boraflex in the Region 1 racks and with poison inserts in the Region 3 racks All racks, including the remaining Region 2 racks were re-evaluated under the provisions of 10 CFR 50.68.

Specifically, the following evaluations were performed for ANO-1:

- The Region 1 racks were evaluated for storage of spent fuel assemblies with specific burnup requirements for the spent fuel assemblies, as a function of initial enrichments and decay times (up to 20 years). Results are summarized in Figure 4.1.1 and tabulated in Table 4.2.1, 4.2.2, and 4.2.3.

- Fresh fuel storage in Region 1 has been assessed based in a "2-of-4" checkerboard loading with empty storage cells. (i.e., filled only with water or non-fuel bearing materials). Results are shown in Table 4.2.4 for fuel of 4.95 ±0.05 wt% ^{235}U enrichment.

- Region 2 racks were evaluated for storage of spent fuel assemblies with burnup requirements for the spent fuel assemblies, determined as a function of initial enrichments and decay times (up to 20 years). Results are summarized in Figure 4.1.2 and Tables 4.2.5, 4.2.6, and 4.2.7.

- Fresh fuel storage in Region 2 has been assessed based on a "2- of -4" checkerboard loading with empty storage cells (i.e., filled only with water or non-fuel bearing materials). Results are shown in Table 4.2.8 for fuel assemblies of 4.95 ±0.05 wt% ^{235}U enrichment.

- The new Region 3 racks were evaluated with Metamic® panels inserted in the water gap, for storage of fresh fuel assemblies, with ^{235}U enrichments up to 4.95 ±0.05 wt%. Results are shown in Table 4.2.9. Region 3 may also accommodate spent fuel of any burnup for fuel assemblies up to 4.95 ±0.05 wt% ^{235}U enrichment.

The racks have been evaluated for Babcox & Wilcox (B&W) 15x15 spent and fresh fuel assemblies with an initial average uniform enrichment up to 5.0 wt% ^{235}U (4.95 ±0.05 wt%). Credit is taken for poison inserts, fuel burnup, cooling time, and soluble boron in pool water as applicable per 10 CFR 50.68 and Reference 4.1.2.

The objective of this analysis is to ensure, per 10 CFR 50.68, that the racks shall remain subcritical under normal conditions with no credit for soluble boron and less than or equal to 0.95 when partial credit is taken for soluble boron in pool water, including calculation uncertainties and effects of mechanical tolerances. Reactivity effects of abnormal and accident conditions have also been evaluated to determine the required soluble boron concentration in the pool to assure that under all credible abnormal and accident conditions, the maximum reactivity will not exceed the regulatory limit of 0.95. The required soluble boron concentrations are summarized in Table 4.9.1. In this context "abnormal" refers to conditions, which may reasonably be expected to occur during the lifetime of the plant and "accident" refers to conditions, which are not expected to occur but nevertheless must be protected against. The double contingency principle [4.1.2] allows full credit for soluble boron under other abnormal or accident conditions, since only a single independent accident need be considered at one time.

Applicable codes, standards, and regulations or pertinent sections thereof, include the following:

- Code of Federal Regulations, Title 10, Part 50, Appendix A, General Design Criterion 62, "Prevention of Criticality in Fuel Storage and Handling."

- Code of Federal Regulations 10 CFR 50.68, "Criticality Accident Requirements"

- USNRC Standard Review Plan, NUREG-0800, Section 9.1.2, "Spent Fuel Storage," Rev. 1 - July 1981.

- USNRC letter of April 14, 1978, to all Power Reactor Licensees – "OT Position for Review and Acceptance of Spent Fuel Storage and Handling Applications," including modification letter dated January 18, 1979.

- L. I. Kopp, "Guidance on the Regulatory Requirements for Criticality Analysis of Fuel Storage at Light-Water Reactor Power Plants," NRC Memorandum from L. Kopp to T. Collins, August 19, 1998.

- USNRC Regulatory Guide 1.13, "Spent Fuel Storage Facility Design Basis," Rev. 2 (proposed), December 1981.

- ANSI ANS-8.17-1984, "Criticality Safety Criteria for the Handling, Storage and Transportation of LWR Fuel Outside Reactors."

To assure the true reactivity will be less than the calculated reactivity, the following conservative design criteria and assumptions have been employed:

- Criticality safety analyses were based upon an infinite radial array of cells; i.e., no credit was taken for radial neutron leakage, except for evaluating accident conditions along the rack outer boundary where neutron leakage is inherent.

- Minor structural materials were neglected; i.e., spacer grids were conservatively assumed to be replaced by water.

- Because the temperature coefficient of reactivity is positive in the absence of neutron absorber panels, the analyses for Region 1 (no credit is taken in the current evaluations for the existing Boraflex poison material in these racks) and Region 2 (no poison material currently exists in these racks) type racks assumed a temperature of 150 °F. This is the design basis maximum pool water temperature. Higher temperatures would be an accident condition for which full soluble boron credit is permitted and the reactivity effects would be mitigated by the presence of the large amounts of soluble boron in the pool water.

- For Region 3 type racks, the moderator is assumed to be un-borated water at a temperature within the operating range (4 °C or 39 °F) that results in highest reactivity. Criticality calculations were performed at 20 °C (68 °F) and temperatures below 20 °C (68 °F) were assumed to be abnormal events and the reactivity effects combined additively with other uncertainties.

- Manufacturing tolerances of the Metamic® neutron absorber (width, thickness and B_4C loading) is included in the criticality safety evaluation. Steel components associated with the inserts are replaced with water in the analysis.

- The analyses used a B&W 15x15 fuel assembly, with a maximum ^{235}U enrichment of 4.95 ±0.05 wt%.

- No axial blankets were assumed to be present in the fuel rods. The entire active fuel length was assumed to be of uniform enrichment.

- In-core depletion calculations have assumed conservative operating conditions, conservative fuel and moderator temperature, and an allowance for the average soluble boron concentrations during in-core operations.

The spent fuel storage racks are designed to accommodate the fuel assembly type listed in Table 4.1.1 with a maximum nominal initial enrichment of 4.95 ±0.05 wt% ^{235}U.

4.2 SUMMARY OF CRITICALITY ANALYSES

4.2.1 Normal Operating Conditions

The criticality analyses for each of the three separate regions of the spent fuel storage pool for the design basis storage conditions are summarized in Tables 4.2.1 through 4.2.9. For the fuel acceptance criteria defined in the previous section, the maximum effective neutron multiplication factor (k_{eff}) values are shown to be less than 1.0 (95% probability at the 95% confidence level) in each of the regions when no credit is taken for the presence of soluble boron in the pool. Credit for soluble boron is required to ensure k_{eff} is maintained less than 0.95. The required soluble boron concentrations are summarized in Table 4.9.1.

4.2.1.1 Region 1

The maximum k_{eff} values for storage of spent fuel were determined assuming an infinite radial array of storage cells with a finite axial length, water reflected. For each spent fuel cooling time, minimum burnup values were determined that assure the maximum k_{eff}, including calculational and manufacturing uncertainties, remains subcritical under the assumed accident condition of the loss of all soluble boron. Table 4.2.1 summarizes the results of these analyses at zero cooling time for spent fuel assemblies with an initial enrichment of 4.95 ±0.05 wt% ^{235}U. Figure 4.1.1 and Table 4.2.2 show the minimum acceptable burnup for storage of fuel assemblies of various initial enrichments and cooling times in the spent fuel. The calculated maximum reactivity includes the reactivity effect of the axial distribution in burnup and provides an additional margin for the uncertainty in the depletion calculations. The minimum soluble boron concentration required to maintain k_{eff} below 0.95, including all manufacturing and calculational tolerances, for the storage of spent fuel in the Region 1 racks, is 225 ppm.

For convenience, the minimum (limiting) burnup data shown in Table 4.2.2 may be described as a function of the nominal initial enrichment, E, in wt% ^{235}U by a bounding polynomial expression as shown in Table 4.2.3 Fuel assemblies with enrichments less than 2.0 wt% ^{235}U will conservatively be required to meet the burnup requirements of 2.0 wt% ^{235}U assemblies. Since the data is nearly linear, linear interpolation between the points listed in Table 4.2.2 is acceptable.

The maximum k_{eff}, for storage of fresh fuel assemblies of 4.95 ±0.05 wt% initial enrichment in the Region 1 type racks in a 2-of-4 checkerboard pattern with the alternate cells remaining empty of fuel, is 0.9443. Table 4.2.4 summarizes the results of this analysis. Based on this result, this arrangement is

acceptable for storage of fresh fuel with no credit for soluble boron or for spent fuel regardless of burnup.

4.2.1.2 Region 2

The maximum k_{eff} values for storage of spent fuel were determined assuming an infinite radial array of storage cells with a finite axial length, water reflected. For each spent fuel cooling time, minimum burnup values were determined that assure the maximum k_{eff}, including calculational and manufacturing uncertainties, remains subcritical under the assumed accident condition of the loss of all soluble boron. Table 4.2.5 summarizes the results of these analyses at zero cooling time for spent fuel assemblies with an initial enrichment of 4.95 ±0.05 wt%. Figure 4.1.2 and Table 4.2.6 show the minimum acceptable burnup for storage of fuel assemblies of various initial enrichments and cooling times in the SFP. The calculated maximum reactivity includes the reactivity effect of the axial distribution in burnup and provides an additional margin for the uncertainty in the depletion calculations. The minimum soluble boron concentration required to maintain k_{eff} below 0.95, including all manufacturing and calculational tolerances, for the storage of spent fuel allowed in the Region 2 racks is 180 ppm.

For convenience, the minimum (limiting) burnup data shown in Table 4.2.6 may be described as a function of the nominal initial enrichment, E, in wt% ^{235}U by a bounding polynomial expression as shown in Table 4.2.7. Fuel assemblies with enrichments less than 2.0 wt% ^{235}U will conservatively be required to meet the burnup requirements of 2.0 wt% ^{235}U assemblies. Since the data is nearly linear, linear interpolation between the points listed in Table 4.2.6 is acceptable.

The maximum k_{eff}, for storage of fresh unburned fuel assemblies of enrichment 4.95 ±0.05 wt% in the Region 2 in a 2-of-4 checkerboard pattern with the alternate cells remaining empty of fuel, is 0.9621. Table 4.2.8 summarizes the results of this analysis and confirms that this arrangement is acceptable for storage of fresh fuel or spent fuel regardless of burnup, without requiring any credit for soluble boron. The minimum soluble boron concentration required to maintain k_{eff} below the 0.95 limit, including all manufacturing and calculational tolerances, for the storage of fresh fuel assemblies in this configuration in the Region 2 racks is 180 ppm.

4.2.1.3 Region 3

The Region 3 racks were analyzed for the storage of 4.95 ±0.05 wt% fresh fuel assemblies. The maximum k_{eff}, for storage of fresh fuel assemblies in the Region 3 racks is 0 9939. Table 4.2.9 summarizes the results of this analysis, and confirms that this arrangement is acceptable for storage of fresh unburned fuel or spent fuel regardless of burnup. The minimum soluble boron concentration required in Region 3 to maintain k_{eff} below 0.95, including all manufacturing and calculational tolerances, is 400 ppm.

4.3 REFERENCE DESIGN INPUT DATA

4.3.1 Reference Fuel Assembly

The spent fuel storage racks are designed to accommodate B&W 15x15 fuel assemblies. The design specifications for the B&W fuel assembly designs, as used for this analysis, are given in Table 4.1.1.

4.3.2 Region 1 Fuel Storage Cells

Figure 4.3.1 shows the calculational model of the nominal Region 1 spent fuel storage cell. The Region 1 storage cells are composed of stainless steel boxes separated by a gap. The 0.075 ±0.004 thick steel walls define the storage cells, which have an 8.970 -0.05/+0.025 inch inside dimension. A 0.020 inch stainless steel sheath is around the gap and defines the boundary of the flux-trap water-gap used to augment reactivity control. The cells are located on a lattice spacing of 10.65 inches in both directions. Stainless steel channels connect the storage cells in a rigid structure and define the flux-trap of 1.31 inches, between the sheathing of adjacent cells.

4.3.3 Region 2 Fuel Storage Cells

Figure 4.3.2 shows the calculational model of the nominal Region 2 spent fuel storage cell. The Region 2 storage cells area also have a flux trap between adjacent cells and are composed of stainless steel boxes separated by a gap. The straight portion of the flux trap is 7.5 inches. The measured flux trap water gap of 1.456 +0.12/-0.08 inches was used in the analysis. The 0.062 ±0.004 thick steel walls define the storage cells, which have an 8.97 +0.050/-0.025 inch nominal inside dimension. The measured value of the flux trap water gap corresponded to a Box inside dimension (ID) of 9.07 inches because of the bow in the cell walls. This value of the Box ID was used in the analysis. The cells are

located on a lattice spacing of 10.65 inches in both directions. No additional water gaps exist between adjacent Region 2 cells in a rack.

4.3.4 Region 3 Fuel Storage Cells

The Region 3 storage cells are identical to Region 2 storage cells except that the Metamic® Poison panels will be inserted into the flux trap gaps. The poison panels are designed to be 7.0 ±0.0625 inches wide with a with a minimum Boron Carbide (B_4C) content of 25 weight percent. The criticality safety analysis conservatively assumes the poison panels are 6.7 inches wide. These Metamic® panels are held by appropriate mechanisms to remain close to the straight portion of the flux trap walls.

4.4 ANALYTICAL METHODOLOGY

4.4.1 Reference Design Calculations

The principal methods for the criticality analyses of the storage racks include the following codes: (1) MCNP4a [4.4.1], (2) KENO Va [4.4.2], and (3) CASMO-4 [4.4.5-4.4.7]. MCNP4a is a continuous energy three-dimensional Monte Carlo code developed at the Los Alamos National Laboratory. KENO Va is a three-dimensional multi-group Monte Carlo code developed at the Oak Ridge National Laboratory as part of the SCALE 4.3 package [4.4.3]. The KENO Va calculations used the 238-group SCALE cross-section library and NITAWL [4.4.4] for ^{238}U resonance shielding effects (Nordheim integral treatment). Benchmark calculations, presented in Appendix 4A, indicate a bias of 0.0009 with an uncertainty of ±0.0011 for MCNP4a and 0.0030 ±0.0012 for KENO Va, both evaluated with the 95% probability at the 95% confidence level [4.1.1].

Fuel depletion analyses during core operation were performed with CASMO-4, two-dimensional multi-group transport theory codes based on transmission probabilities [4.4.5 - 4.4.7]. Restarting the CASMO-4 calculations in the storage rack geometry yields the two-dimensional infinite multiplication factor (k_∞) for the storage rack. CASMO-4 was also used to determine the reactivity uncertainties (differential calculations) of manufacturing tolerances and the reactivity effects of variations in the water temperature and density.

In the geometric models used for the calculations, each fuel rod and its cladding were described explicitly and reflecting boundary conditions were used in the radial direction, which has the effect of

creating an infinite radial array of storage cells. Monte Carlo calculations inherently include a statistical uncertainty due to the random nature of neutron tracking. To minimize the statistical uncertainty of the MCNP4a and KENO Va calculated reactivity and to assure convergence, a minimum of 1 million neutron histories were accumulated in each calculation. Three-dimensional MCNP calculations were necessary to describe the geometry of the checkerboard cases. However, MCNP cannot perform depletion calculations, and depletion calculations were performed with CASMO-4. Explicit description of the fission product nuclide concentrations in the spent fuel was determined from the CASMO-4 calculations and used in the MCNP calculations. To compensate for those few fission product nuclides that are not in the MCNP library, an equivalent boron-10 concentration in the fuel was determined which produced the same reactivity in MCNP as the CASMO-4 result. This methodology explicitly incorporates approximately 40 of the most important fission products, accounting for all but about 1% in reactivity. The remaining ~1 % in reactivity is included by the equivalent B-10 concentration in the fuel.

4.4.2 Fuel Burnup Calculations and Uncertainties

CASMO-4 was used for burnup calculations in the hot operating condition. Conservatively bounding moderator and fuel temperatures and the average operating soluble boron concentrations (900 ppm) were used to assure the high plutonium production and hence conservatively high values of reactivity. Since critical experiment data with spent fuel is not available for determining the uncertainty in depletion calculations, an allowance for uncertainty in reactivity was assigned based upon other considerations [4.1.2]. Assuming the uncertainty in depletion calculations is less than 5% of the total reactivity decrement, a burnup dependent uncertainty in reactivity for burnup calculations was assigned. Thus, the burnup uncertainty varies (increases) with burnup. This allowance for burnup uncertainty was included in determination of the acceptable burnup versus enrichment combinations.

4.4.3 Effect of Axial Burnup Distribution

Initially, fuel loaded into the reactor will burn with a slightly skewed cosine power distribution. As burnup progresses, the burnup distribution will tend to flatten, becoming more highly burned in the central regions than in the upper and lower regions. At high burnup, the more reactive fuel near the ends of the fuel assembly (less than average burnup) occurs in regions of high neutron leakage. Consequently, it is expected that over most of the burnup history, fuel assemblies with distributed burnups will exhibit a slightly lower reactivity than that calculated for the uniform average burnup. As burnup progresses, the distribution, to some extent, tends to be self-regulating as controlled by the axial power distribution, precluding the existence of large regions of significantly reduced burnup.

Among others, Turner [4.4.8] has provided generic analytic results of the axial burnup effect based upon calculated and measured axial burnup distributions. These analyses confirm the minor and generally negative reactivity effect of the axially distributed burnups at values less than about 30 GWD/MTU with small positive reactivity effects at higher burnup values. Calculations were performed based upon a burnup distribution provided by ANO. These calculations were performed in MCNP4a with 10 zone axial calculations, using specific (CASMO-4) concentrations of actinides and fission product nuclides in each zone. Results of these calculations, therefore, inherently include the effect of the axial distribution in burnup.

4.4.4 BPRAs and APSRs

The fuel assemblies used at the ANO-1 Nuclear Power Plant contain poison rods such as the Burnable Poison Rods Assemblies (BPRAs) and Axial Power Shaping Rods (APSRs). These rods are inserted into the guide tubes during the in-core depletion process and are stored in fuel assemblies in the rack cells. Analyses show that the fuel assemblies, which contained the BPRAs during depletion in the core, are more reactive in the racks than those that contained APSRs or no burnable absorber in the burnup range of interest in this analysis. CASMO-4 calculations performed to obtain the isotopic compositions of the spent fuel assemblies, which were subsequently used in the MCNP calculations, were performed with BPRAs in the fuel assemblies during core operation.

4.4.5 MCNP4a Temperature Correction

The reactivity for non-poisoned racks in the spent fuel pool increases with pool water temperature. The maximum bulk pool water temperature is 150 °F. However, since the Doppler treatment and cross-sections in MCNP4a are valid only at 20 °C (68 °F), the delta-k determined in CASMO-4 from 20 °C (68 °F) to the limiting temperature described in section 4.8.1 is included in the final k_{eff} calculation.

4.4.6 Long-Term Changes in Reactivity

At reactor shutdown, the reactivity of the fuel initially decreases due to the growth of Xe-135. Subsequently, the Xenon decays and the reactivity increase to a maximum at about a hundred hours when the Xenon is gone. Therefore, for conservatism, the Xe is set to zero in the calculations to assure maximum reactivity. During the next 50 years, the reactivity continuously decreases due primarily to

^{241}Pu decay and ^{241}Am growth. Credit for this decay and for changes in fission product concentrations is included in calculations of the decrease in reactivity in long-term storage (up to 20 years). The CASMO-4 code includes the capability of tracking the decay of the actinides and the most significant product nuclides during long-term storage.

4.5 REGION 1 CRITICALITY ANALYSES AND TOLERANCES

4.5.1 Nominal Design Case

For the nominal storage cell design in Region 1, the criticality safety analyses for the two different storage patterns are summarized in Tables 4.2.1, 4.2.2, and 4.2.4. This data confirms that the maximum reactivity in Region 1 remains subcritical (less than the regulatory limit $k_{eff} \leq 1.0$) under the assumed condition of the loss of all soluble boron in the pool water. Figure 4.1.1 shows the limiting burnup values for fuel of other enrichments and cooling times (see also Table 4.2.2).

4.5.2 Uncertainties Due to Tolerances

The reactivity effects of manufacturing tolerances are summarized in Tables 4.2.1 and 4.2.4. All of the individual reactivity allowances were separately calculated for the reference fuel assembly and a statistical combination of uncertainties was used. The tolerances include the fuel storage area I.D., rack material thickness, water gap, fuel enrichment and density.

4.5.3 Eccentric Fuel Positioning

The fuel assembly is assumed to be normally located in the center of the storage rack cell. However, calculations were also made with the fuel assemblies assumed to be in the corner of the storage rack cell (four-assembly cluster at closest approach). These calculations indicated that the reactivity effect is slightly positive. Therefore, the uncertainty for eccentricity is included in the calculations for the final k_{eff} in Tables 4.2.1 and 4.2.4.

4.6 REGION 2 CRITICALITY ANALYSES AND TOLERANCES

4.6.1 Nominal Design Case

For the nominal storage cell design in Region 2, the criticality safety analyses are summarized in Tables 4.2.5, 4.2.6, and 4.2.8. This data confirms that the maximum reactivity in Region 2 remains subcritical (less than the regulatory limit $k_{eff} \leq 1.0$) under the assumed condition of the loss of all soluble boron in the pool water. Figure 4.1.2 (and table 4 2.6) summarizes the limiting fuel burnups for fuel assemblies of other enrichments and cooling times.

4.6.2 Uncertainties Due to Tolerances

The reactivity effects of manufacturing tolerances are summarized in Tables 4.2.5 and 4.2.8. All of the individual reactivity allowances were separately calculated for the reference fuel assembly and a statistical combination of uncertainties was used. The tolerances include the fuel storage area I.D , rack material thickness, water gap, fuel enrichment and density.

4.6.3 Eccentric Fuel Positioning

The fuel assembly is assumed to be normally located in the center of the storage rack cell. However, calculations were also made with the fuel assemblies assumed to be in the corner of the storage rack cell (four-assembly cluster at closest approach). These calculations indicate that the reactivity effect is slightly positive. Therefore, the uncertainty for eccentricity is included in the calculations for the final k_{eff} in Tables 4.2.5 and 4.2.8.

4.7 REGION 3 CRITICALITY ANALYSES AND TOLERANCES

4.7.1 Nominal Design Case

For the nominal storage cell design in Region 3, the criticality safety analyses are summarized in Table 4.2.9. This data confirms that the maximum reactivity in Region 3 remains subcritical (less than the regulatory limit $k_{eff} \leq 1.0$) under the assumed condition of the loss of all soluble boron in the pool water.

4.7.2 Uncertainties Due to Tolerances

The reactivity effects of manufacturing tolerances are tabulated in Table 4.2.9. All of the individual reactivity allowances were separately calculated for the reference fuel assembly and a statistical combination of uncertainties was used. The tolerances include the fuel storage area I.D., rack material thickness, water gap, poison panel width, poison panel thickness, boron loading in the poison panel, fuel enrichment, and density.

4.7.3 Eccentric Fuel Positioning

The fuel assembly is assumed to be normally located in the center of the storage rack cell. However, calculations were also made with the fuel assemblies assumed to be in the corner of the storage rack cell (four-assembly cluster at closest approach). These calculations indicate that the reactivity effect is slightly negative, so it is conservatively not included.

4.8 ABNORMAL AND ACCIDENT CONDITIONS IN THE SPENT FUEL POOL RACKS

4 8.1 Temperature and Water Density Effects

The moderator temperature coefficient of reactivity in both Region 1 and Region 2 is positive. A moderator temperature of 20 °C (68 °F) was assumed for the reference MCNP4a calculations and the increase in reactivity to the maximum permissible bulk pool water temperature of 150 °F is included (CASMO-4 calculation) as a bias in the calculation of the maximum k_{eff}. This assures that the true reactivity will always be lower over the expected range of water temperatures. The reactivity effects of the pool water temperature effects on reactivity have been evaluated using CASMO-4.

The moderator temperature coefficient of reactivity for the Region 3 racks is negative and, therefore, the reference MCNP4a calculation provides the maximum reactivity. The effect of a reduction in temperature to 4 °C (39 °F) is included as an uncertainty in Table 4.2.9.

4.8.2 Lateral Rack Movement

Lateral motion of the storage racks under postulated seismic conditions could potentially alter the spacing between racks. Under these conditions, credit for the soluble boron (permitted under accident

conditions) would maintain the k_{eff} at a value well below the maximum allowable. The double contingency principle requires the consideration of only one accident at one time. Nevertheless, the separation (water-gap) between rack modules is sufficiently large that even for the maximum movement expected under seismic excitation, the water gap remains larger than the water gap within the Region 1 modules. In the Region 2 and the Region 3 racks, the k_{eff} is independent of the inter-module water gap and is not sensitive to any potential seismic induced movement of the modules. The water-gap structure in each cell is included in the analysis and precludes any closer proximity between modules.

4.8.3 Abnormal Location of a Fuel Assembly

The misplacement of a fresh unburned fuel assembly of the highest permissible reactivity, would, in the absence of soluble poison, result in exceeding the regulatory limit ($k_{eff} \leq 1.0$). This could occur if a fresh fuel assembly of the highest permissible initial enrichment (4.95 ±0.05 wt% ^{235}U) were to be inadvertently loaded into a Region 1 or Region 2 storage cell, which are intended to store spent fuel assemblies or remain empty. Calculations confirmed that the highest reactivity, including uncertainties, for the worst case postulated fuel mis-loading accident condition (fresh fuel assembly in Region 2 cell intended to remain empty) would exceed the limit on reactivity in the absence of soluble boron. Soluble boron in the spent fuel pool water, for which credit is permitted under these accident conditions, would assure that the reactivity is maintained substantially less than the design limitation. Calculations indicate that a soluble boron concentration of 800 ppm is adequate to assure that the maximum k_{eff} does not exceed 0.95.

In addition, the mislocation of a fresh unburned fuel assembly could occur if a fresh fuel assembly of the highest permissible initial enrichment (4.95 ±0.05 wt%) were to be accidentally mislocated outside of a Region 1 or Region 2 storage rack, with the rack fully loaded. However, this is an area of high neutron leakage and the reactivity effect would be bounded by that of a fuel assembly accidentally misloaded internal to Region 1 or Region 2 storage module. The gaps between the racks are sufficiently small to preclude the accidental mislocation of a fuel assembly in between storage rack modules.

4.8.4 Dropped Fuel Assembly

For the case in which a fuel assembly is assumed to be dropped horizontally on top of a rack, the fuel assembly will come to rest horizontally on top of the rack with a minimum separation distance from the active fuel region sufficient to preclude neutron coupling (with fuel in the storage rack). Consequently,

the horizontal fuel assembly drop accident will not result in a significant increase in reactivity. Furthermore, the soluble boron in the spent fuel pool water assures that the true reactivity is always less than the limiting value for this dropped fuel accident.

Analyses were performed to evaluate the potential loss of Metamic® poison panels in the Region 3 racks by means of a dropped fuel assembly. A very conservative bounding accident condition was analyzed postulating the loss of all Metamic® absorber material throughout the entire Region 3 storage racks. For this accident analysis, the Tech Spec limit of 1600 ppm soluble boron was assumed. The results of this postulated accident condition show that the maximum k_{eff} is well below 0.95, including bias and tolerance uncertainties. This is a very conservative evaluation since an actual dropped assembly at most, would be expected to only damage a maximum of eight Metamic® panels (4 inserts).

It is also possible to vertically drop an assembly into a location occupied by another assembly. Such a vertical impact, would, at most cause a small compression of the stored assembly, reducing the water-to-fuel ratio and thereby reducing reactivity. In addition the distance between the active fuel regions of both assemblies will be more than sufficient to ensure no neutron interaction between the two assemblies.

Dropping of an assembly into an unoccupied cell could result in a localized deformation of the baseplate of the rack. The immediate eight surrounding fuel cells could also be affected. However, the amount of deformation for these cells would be considerably less. The resultant effect would be the lowering of a few fuel assemblies in the area near the deformation. Since the Metamic inserts in Region 3 are designed to sit on the baseplate, the localized deformation of the baseplate was considered. The Metamic® poison panel inserts in the Region 3 type racks are designed to sit on the baseplate and could potentially move downward and uncover a portion of the active fuel. The resulting geometry is bound by the previously discussed configuration in which a complete loss of all Metamic® inserts was assumed with no change in the active fuel region alignment. Therefore, the presence of the boron concentration assures the maximum k_{eff} is well below the 0.95 acceptance criteria.

4.9 SOLUBLE BORON DILUTION EVALUATION

The soluble boron in the spent fuel pool water is normally a minimum of 1600 ppm under operating conditions. Significant loss or dilution of the soluble boron concentration is extremely unlikely, if not incredible. Nonetheless, an evaluation was performed based on the ANO spent fuel pool data. The minimum required soluble boron concentration in the spent fuel pool water for various conditions is

summarized in Table 4.9.1.

The required minimum soluble boron concentration is 400 ppm under normal conditions and 800 ppm for the most serious credible accident scenario. The volume of water in the pool is 256,860 gallons. Large amounts of unborated water would be necessary to reduce the boron concentration from 1600 ppm to 800 ppm or 400 ppm. Abnormal or accident conditions are discussed below for either low dilution rates (abnormal conditions) or high dilution rates (accident conditions). It should be noted that routine surveillances to measure the soluble boron concentrations in the pool water are required by Technical Specifications.

Small failures or mis-aligned values could possibly occur in the normal soluble boron control system or related systems. Such failures might not be immediately detected. These flow rates would be of the order of 2 gpm (comparable to normal evaporative loss) and the increased frequency of makeup flow might not be observed. However, an assumed loss flow-rate of 2 gpm dilutions flow rate would require some 123 days to reduce the boron concentration to the minimum required 400 ppm required under normal conditions or 62 days to reach the 800 ppm required for the most severe fuel handling accident. Routine surveillance measurements of the soluble boron concentration would readily detect the reduction in soluble boron concentration with ample time for corrective action.

Under certain accident conditions, it is conceivable that a high flow rate of unborated water could flow onto the top of the pool. Such an accident scenario could result from rupture of a demineralized water supply line or possibly the rupture of a fire protection system header, both events potentially allowing unborated water to spray onto the pool. A flow rate of up to 2500 gpm could possibly flow onto the spent fuel pool as a result of a rupture of the fire protection line. This would be the most serious condition and bounds all other accident scenarios. Conservatively assuming that all the unborated water from the break poured onto the top of the pool and further assuming instantaneous mixing of the unborated water with the pool water, it would take approximately 142 minutes to dilute the soluble boron concentration to 400 ppm, which is the minimum required concentration to maintain k_{eff} below 0.95 under normally operating conditions. In this dilution accident, some 355,000 gallons of water would spill on the auxiliary building floor. Well before the spilling of such a large volume of water, multiple alarms would have alerted the control room of the accident consequences (including the fuel pool high-level alarm, the fire protection system pump operation alarm, and the floor drain receiving tank high level alarm). For this high flow rate condition, 71 minutes would be required to reach the 800 ppm required for the most severe fuel handling accident.

Instantaneous mixing of pool water with the water from the rupture of the demineralized water supply line is an extremely conservative assumption. Water falling on to the pool surface would mix with the top layers of pool water and the portions of the mixed volumes would continuously spill out of the pool. The density difference between water at 150°F (maximum permissible pool bulk water temperature) and at the temperature of the demineralizer water supply is small. This density difference will not cause the water falling on to the pool surface to instantaneously sink down into the racks overcoming the principal driving force for the flow in the pool, which is the buoyancy force generated in the spent fuel pool racks region due to the heat generation from the spent fuel in the racks. This would further enhance the mixing process between the pool water and spilled water above the racks

For the fire water system line break, upon the initial break, the fire protection system header pressure would drop to the auto start setpoint of the fire protection pumps. The start is accompanied with an alarm in the main control room. The annunciator response is to dispatch an operator to find the source of the pump start. Approximately 5 minutes into the event, a Spent Fuel Pool high level alarm would be received in the main control room, assuming that the Spent Fuel Pool level started at the low alarm. The annunciator response for high Spent Fuel Pool level is to investigate the cause. The coincidence of the 2 alarms would quickly lead to the discovery of the failure of the fire protection system and sufficient time to isolate the failure.

The maximum flow rate for a failure of the demineralized water header would provide approximately 900 gpm into the Spent Fuel Pool. Failure of the demineralized water header is not accompanied with an alarm; however, the time to dilute the Spent Fuel Pool from 1600 to 400 ppm is greater than the bounding case described above. In this scenario, there is sufficient time to isolate the failure and to prevent the spilling of some 355,000 gallons of water.

The analysis assume that for a double-ended break in the fire water system piping, the stream of water will arch through the air some 40 feet falling on top of the pool. This is virtually an incredible event. Should the stream of water fall upon the pool deck, a 3 inch high curb would channel some of the water to the pool drain and prevent all of the water from reaching the pool. Furthermore, the evaluation also assumes at least 3 independent and concurrent accidents occur simultaneously:

- Large amount of water flowing from the double-ended pipe break would remain un-detected and is ignored.

- Pool water high level alarms either fail or are ignored.

- Alarms indicating large amounts of water flowing into the floor drain have failed or are ignored.

Considering all related facts, a significant dilution of the pool soluble boron concentration in a short period of time without corrective action is not considered a credible event.

It is not considered credible that multiple alarms would fail or be ignored or that the spilling of large volumes of water would not be observed. Therefore, such a major failure would be detected in sufficient time for corrective action to avoid violation of an administrative guideline and to assure that the health and safety of the public is protected.

4.10 NEW FUEL STORAGE RACKS CRITICALITY ANALYSIS

The New Fuel Storage Vault is intended for the receipt and storage of fresh fuel under normally dry conditions where the reactivity is very low. To assure criticality safety under accident conditions and to conform to the requirements of General Design Criterion 62, "Prevention of Criticality in Fuel Storage and Handling," two separate criteria must be satisfied as defined in NUREG-0800, Standard Review Plan 9.1.1, "New Fuel Storage." These criteria are as follows:

- When fully loaded with fuel of the highest anticipated reactivity and flooded with clean unborated water, the maximum reactivity, including uncertainties, shall not exceed a k_{eff} of 0.95.

- With fuel of the highest anticipated reactivity in place and assuming the optimum hypothetical low density moderation, (i.e., fog or foam), the maximum reactivity shall not exceed a k_{eff} of 0.98.

The New Fuel Storage Vault provides two 4 x 9 storage rack modules with cell array of storage locations arranged on a 21.00 inch lattice spacing. Calculations were made with the 238-group NITAWL KENO Va code package (SCALE 4.3), a three-dimensional Monte Carlo analytical technique, with fresh fuel assemblies with 4.95 wt% initial enrichment. These calculations were made for various moderator densities and the results shown in Figure 4.10 1, shows that the peak reactivity (optimum moderation) occurs at 9% moderator density. The calculations for the configuration illustrated in Figure 4.10.2 confirm that five locations in each of the storage racks are required to remain empty in order to meet the regulatory limits. Results of the criticality safety analyses are summarized in Table 4.10.1 for the two accident conditions for fuel assemblies of 4.95 ±0.05 wt% initial enrichment. The maximum reactivity at

9% moderator density is 0.9708, including uncertainties, which is within the regulatory limit of 0.98, thus confirming the acceptability of the New Fuel Vault for 4.95 ±0.05 wt% fuel.

Additional calculations at 9% moderator density, performed for the storage pattern depicted in Figure 4.10.3, show that this storage configuration is acceptable for storage of fresh fuel assemblies of up to 4.20 wt% enrichment with four locations in each rack array required to remain empty.

In the flooded condition (clean unborated water), the storage locations are essentially isolated from each other (neutronically). Under these conditions and with fuel of 4.95 ±0.05 wt% enrichment, the maximum reactivity, including all known uncertainties is less than the regulatory limit of 0.95 for k_{eff}, thus confirming the acceptability of the NFV for 4.95 wt% fuel in the fully flooded accident condition. At 4.2 wt% enrichment in the flooded condition, the reactivity will be substantially lower than that for 4.95 ± 0.05 wt% enrichment and would therefore be acceptable for storage. (Note: in the fully flooded conditions the fuel assemblies are neutronically isolated from each other and the reactivity is independent of the presence or number of blanked-off cells.)

4.11 FUEL HANDLING EQUIPMENT

Criticality safety evaluations were also performed for handling of fresh fuel assemblies during transfer from the new fuel vault to the reactor core, including the new-fuel elevator, the up-ender and fuel carriage, and the temporary storage rack within the transfer canal. The new fuel elevator is located on the south wall of the pool facing the Region 1 spent fuel storage racks This device can position a fresh fuel assembly 16 inches (assembly center line) from the wall. The distance from the wall to the edge of the rack is 24.5 inches A distance of 7.845 inches exists between the centerline of the assembly in the elevator and the edge of the closest fuel storage cell in the rack. For normal operation, the maximum reactivity with fuel in the New Fuel Elevator (with Region 1 loaded) is 0.9512 in unborated water. This is reduced to 0.9271 with credit for 100 ppm soluble boron. Additional calculations were performed to evaluate the effect of accidentally dropping or misplacing an assembly adjacent to the New Fuel Elevator while it is loaded. A most reactive location for the dropped assembly was determined. A credit of 700 ppm boron will ensure k-effective remains below 0.95 should such an event occur. The New Fuel Elevator therefore meets the criticality acceptance criteria defined in 10 CFR 50.68. The Upender/ Fuel Carriage device handles a single assembly. The maximum reactivity of a single fresh assembly containing 4.95 wt% ±0.05 enriched fuel in water is 0.9425. Furthermore for a postulated accident in which a second fresh assembly was positioned near the Upender/Fuel Carriage, the presence of soluble

boron (1600 ppm minimum) excludes the possibility of any criticality concern.

The transfer canal incorporates a 7-cell temporary storage rack on a linear array at a 21-1/8 inch spacing (6 locations for fuel assemblies and 1 location for a damaged fuel). The maximum k-effective for normal operation of this rack was determined to be 0.9413. Evaluations of a potential mis-placement of a fresh fuel assembly at a position of closest approach to another assembly in the spent fuel rack, separated only by the structure of the temporary rack, shows that the maximum k_{eff} (in the absence of any soluble boron) would be 0.9698. The presence of 200 ppm soluble boron would be sufficient to maintain the maximum k-effective below 0.95. However, the transfer canal, during operations, would always contain the minimum 1600 ppm boron (or usually more), significantly reducing reactivity and further eliminating any criticality concern.

4.12 REFERENCES

[4.1.1] M. G. Natrella, Experimental Statistics, National Bureau of Standards Handbook 91, August 1963.

[4.1.2] L. I. Kopp, "Guidance on the Regulatory Requirements for Criticality Analysis of Fuel Storage at Light-Water Reactor Power Plants," NRC Memorandum from L. Kopp to T. Collins, August 19, 1998.

[4.4.1] J. F. Briesmeister, Editor, "MCNP - A General Monte Carlo N-Particle Transport Code, Version 4A," LA-12625, Los Alamos National Laboratory (1993).

[4.4.2] L. M. Petrie and N.F. Landers, "KENO Va - An Improved Monte Carlo Criticality Program with Supergrouping," Volume 2, Section F11 from "SCALE: A Modular System for Performing Standardized Computer Analysis for Licensing Evaluation" NUREG/CR-0200, Rev. 4, January 1990.

[4 4.3] "SCALE 4.3: A Modular System for Performing Standardized Computer Analysis for Licensing Evaluation For Workstations and Personal Computers, Volume 0," CCC-545, ORNL-RSICC, Oak Ridge National Laboratory (1995).

[4.4.4] N. M. Greene, L. M. Petrie and R. M. Westfall, "NITAWL-II: Scale System Module for Performing Shielding and Working Library Production," Volume 1, Section F1 from "SCALE: A Modular System for Performing Standardized Computer Analysis for Licensing Evaluation" NUREG/CR-0200, Rev. 4, January 1990.

[4.4.5] M. Edenius, K. Ekberg, B. H. Forssén, and D. Knott, "CASMO-4 A Fuel Assembly Burnup Program User's Manual," Studsvik/SOA-95/1, Studsvik of America, Inc. and Studsvik Core Analysis AB (proprietary).

[4.4.6] D. Knott, "CASMO-4 Benchmark Against Critical Experiments", SOA-94/13, Studsvik of America, Inc., (proprietary).

[4.4.7] D. Knott, "CASMO-4 Benchmark Against MCNP," SOA-94/12, Studsvik of America, Inc., (proprietary).

[4.4.8] S E. Turner, "Uncertainty Analysis - Burnup Distributions", presented at the DOE/SANDIA Technical Meeting on Fuel Burnup Credit, Special Session, ANS/ENS Conference, Washington, D.C., November 2, 1988.

Table 4.1.1

Fuel Assembly Specifications

Assembly Data	
Rod Array Size	15x15
Rod Pitch (inches)	0.5680
Active Fuel Length (inches)	144
Fuel Rod Data	
Total Number of Fueled Rods	208
Fuel Rod Outer Diameter (inches)	0.430
Fuel Rod Inner Diameter (inches)	0.377
Cladding Thickness (inches)	0.0265
Cladding Material	Zircaloy
Pellet Diameter (inches)	0.370
UO_2 Stack Density, gms/cc	10.412 ±0.20
Guide Tube Data	
Number of Tubes	16
Outer Diameter (inches)	0.530
Wall Thickness (inches)	0.016
Material	Zircaloy
Instrument Tube Data	
Number of Tubes	1
Outer Diameter (inches)	0.493
Wall Thickness (inches)	0.026
Material	Zircaloy

Table 4.2.1

Summary of the Criticality Safety Analyses for Storage of Spent Fuel Assemblies in Region 1 Racks

Reference k_{eff}	0.9710
Burnup, MWD/KgU	35.4
MCNP4a Bias	±0.0009
Temperature Bias	0.0100
MCNP4a Bias Uncertainty	±0.0011
MCNP4a Statistical (95/95) Uncertainty	±0.0007
Manufacturing Tolerance Uncertainty	±0.0041
Enrichment Tolerance Uncertainty	±0.0027
Depletion Uncertainty	±0.0119
Fuel Eccentric Positioning Uncertainty	±0.0020
Statistical Combination of Uncertainties	±0.0131
Maximum k_{eff}	0.9950
Regulatory Limiting k_{eff}	1.0000

Table 4.2.2

Minimum Burnup Required for Storage of Spent Fuel Assemblies
in the Region 1 Racks

BURNUP, MWD/KgU					
Average Enrichment, wt% ^{235}U	0 Years Cooling Time	5 Years Cooling Time	10 Years Cooling Time	15 Years Cooling Time	20 Years Cooling Time
2	0.50	0.375	0.25	0.125	0.00
2.5	7.50	7.35	7.20	7.05	6.90
3.0	13.60	13.10	12.60	12.10	11.60
3.5	18.70	18.03	17.35	16.68	16.00
4.0	24.27	23.45	22.64	21.82	21.00
4.5	30.00	29.05	28.10	27.15	26.20
4.95	35.40	34.08	32.75	31.43	30.10

Table 4.2.3

Bounding Polynomial Fits to Determine Minimum Acceptable Burnup for Storage of Spent Fuel Assemblies Storage in Region 1 Racks as a Function of Initial Average Enrichment

Decay Time, Years	Burnup, MWD/KgU
0	$-0.1661*E^4+2.791*E^3-17.013*E^2+55.795*E-62.57$
5	$-0.3014*E^4+4.6636*E^3-26.447*E^2+75.84*E-77.88$
10	$-0.443*E^4+6.6239*E^3-36.324*E^2+96.837*E-93.94$
15	$-0.5782*E^4+8.4965*E^3-45.758*E^2+116.88*E-109.27$
20	$-0.7198*E^4+10.457*E^3-55.635*E^2+137.88*E-125.30$

Note: E = Initial average enrichment in wt% ^{235}U

Table 4.2.4

Summary of the Criticality Safety Analyses for a 2-of-4 Checkerboard Storage of Fresh Fuel Assemblies and Empty Cells in Region 1 Racks

Reference k_{eff}	0.9264
MCNP4a Bias	±0.0009
Temperature Effect	+0.0117
Axial Burnup Distribution Penalty	Not Applicable
MCNP4a Bias Uncertainty	±0.0011
MCNP4a Statistics (95/95) Uncertainty	±0 0007
Manufacturing Tolerance Uncertainty	±0.0044
Enrichment Tolerance Uncertainty	±0.0019
Depletion Uncertainty	Not Applicable
Fuel Eccentric Positioning Uncertainty	±0.0017
Statistical Combination of Uncertainties	±0.0053
Maximum k_{eff}	0.9443
Regulatory Limiting k_{eff}	1.0000

Table 4.2.5

Summary of the Criticality Safety Analyses for Storage of Spent Fuel Assemblies in Region 2 Racks

Initial Enrichment, wt% ^{235}U	4.95±0.05
Burnup, MWD/KgU	41.00
Cooling Time, years	0
Reference k_{eff}	0 9619
MCNP4a Bias	±0.0009
Temperature Effect	0.0112
MCNP4a Bias Uncertainty	±0.0011
MCNP4a Statistics (95/95) Uncertainty	±0.0007
Manufacturing Tolerance Uncertainty	±0.0094
Enrichment Tolerance Uncertainty	±0.0028
Depletion Uncertainty	±0.0133
Fuel Eccentric Positioning Uncertainty	±0.0088
Statistical Combination of Uncertainties	±0.0188
Maximum k_{eff}	0.9928
Regulatory Limiting k_{eff}	1.0000

Table 4.2.6

Minimum Burnup Required for Storage of Spent Fuel Assemblies in the Region 2 Racks

BURNUP, MWD/KgU					
Average Enrichment, wt% ^{235}U	0 Years Cooling Time	5 Years Cooling Time	10 Years Cooling Time	15 Years Cooling Time	20 Years Cooling Time
2.00	4.00	4.00	4.00	4.00	4.00
2.50	11.50	11.00	10.50	10.00	9.50
3.00	17.80	17.10	16.40	15.70	15.00
3.50	23.50	22.63	21.75	20.88	20.00
4.00	29.20	28.15	27.10	26.05	25.00
4.50	35.00	33.63	32.25	30.88	29.50
4.95	41.00	39.25	37.50	35.75	34.00

Table 4.2.7

Bounding Polynomial Fits to Determine Minimum Acceptable Burnup for Storage of Spent Fuel Assemblies Storage in Region 2 Racks as a Function of Initial Enrichment

Decay Time, Years	Burnup, MWD/KgU
0	$0.6257E^3 - 6.8758E^2 + 36.293E - 46.0$
5	$0.4934*E^3 - 5.5023*E^2 + 31.23*E - 40.3$
10	$0.3634*E^3 - 4.1511*E^2 + 26.244*E - 34.7$
15	$0.2311*E^3 - 2.776*E^2 + 21.186*E - 29.0$
20	$0.1011*E^3 - 1.4265*E^2 + 16.19*E - 23.4$

Note: E = Initial average enrichment in wt% ^{235}U

Table 4.2.8

Summary of the Criticality Safety Analyses for a 2-of-4 Checkerboard Storage of Fresh Fuel Assemblies and Empty Cells in Region 2 Racks

Reference k_{eff}	0.9359
MCNP4a Bias	±0.0009
Temperature Effect	0.0129
MCNP4a Bias Uncertainty	±0.0011
MCNP4a Statistics (95/95) Uncertainty	±0.0007
Manufacturing Tolerance Uncertainty	±0.0119
Enrichment Tolerance Uncertainty	±0.0020
Depletion Uncertainty	Not Applicable
Fuel Eccentricity Positioning Uncertainty	±0.0026
Statistical Combination of Uncertainties	±0.0124
Maximum k_{eff}	0.9621
Regulatory Limiting k_{eff}	1.0000

Table 4.2.9

Summary of the Criticality Safety Analyses for Storage of Fresh Fuel Assemblies in ANO Unit 1 Region 3 Racks

Reference k_{eff}	0.9776
MCNP4a Bias	±0.0009
MCNP4a Bias Uncertainty	±0.0011
MCNP4a Statistics (95/95) Uncertainty	±0.0007
Manufacturing Tolerance Uncertainty	±0.0152
Enrichment Tolerance Uncertainty	±0.0016
Depletion Uncertainty	Not Applicable
Fuel Eccentric Positioning Uncertainty	Negative
Pool Water Temperature Uncertainty	±0.0012
Statistical Combination of Uncertainties	±0.0154
Maximum k_{eff}	0.9939
Regulatory Limiting k_{eff}	1.0000

Table 4.9.1

Required Soluble Boron Concentrations in the SFP Water.

Condition	Soluble Boron Required for k<1	Soluble Boron Required for k<0.95 (ppm)
Region 1: All Spent Fuel Assemblies	0	225
Region 1: Accident condition of 1 fresh fuel assembly mis-placed into a cell intended to store spent fuel	-	475
Region 1: Accident condition of 1 fresh fuel assembly mis-placed into a cell intended to remain empty	-	675
Region 2: All Spent Fuel Assemblies	0	180
Region 2: Accident condition of 1 fresh fuel assembly mis-placed into a cell intended to store spent fuel	-	450
Region 2: Checkerboard Arrangement	0	100
Region 2: Accident condition of 1 fresh fuel assembly mis-placed into a cell intended to remain empty	-	800
Region 3: All Fresh Fuel Assemblies	-	400
Region 3: Dropped fuel assembly with all fresh fuel assemblies with no poison inserts.	-	1600

Table 4.10.1

Summary of New Fuel Vault Criticality Safety Analysis

	Optimum Moderation (Figure 4.10.1)	Flooded Moderation (Figure 4.10.1)	Optimum* Moderation (Figure 4.10.2)
Initial Enrichment, wt%	4.95± 0.05	4.95± 0.05	4.20 ± 0.05
Temperature for analysis	20 °C (68 °F)	20 °C (68 °F)	20 °C (68 °F)
Reference k_{eff}	0.9639	0.9350	0.9650
Calculational bias, Δk	0.0030	0.0030	0.0030
Uncertainties			
KENO Bias	±0.0012	±0.0012	±0.0012
KENO Statistics	±0.0004	±0.0004	±0.0004
Lattice Spacing	±0.0019	±0.0016	±0.0018
Fuel Density	±0.0025	±0.0026	±0.0022
Fuel Enrichment	±0.0019	±0.0030	±0.0028
Statistical Combination	±0.0039	±0.0045	±0.0042
Total k_{eff}	0.9669 ± 0.0039	0.9380 ± 0.0045	0.9680 ± 0.0042
Maximum k-eff	0.9708	0.9425	0.9722
Regulatory Limit	0.98	0.95	0.98

* At 4.2 wt% enrichment, the flooded condition reactivity is much lower than the 4.95 wt% case.

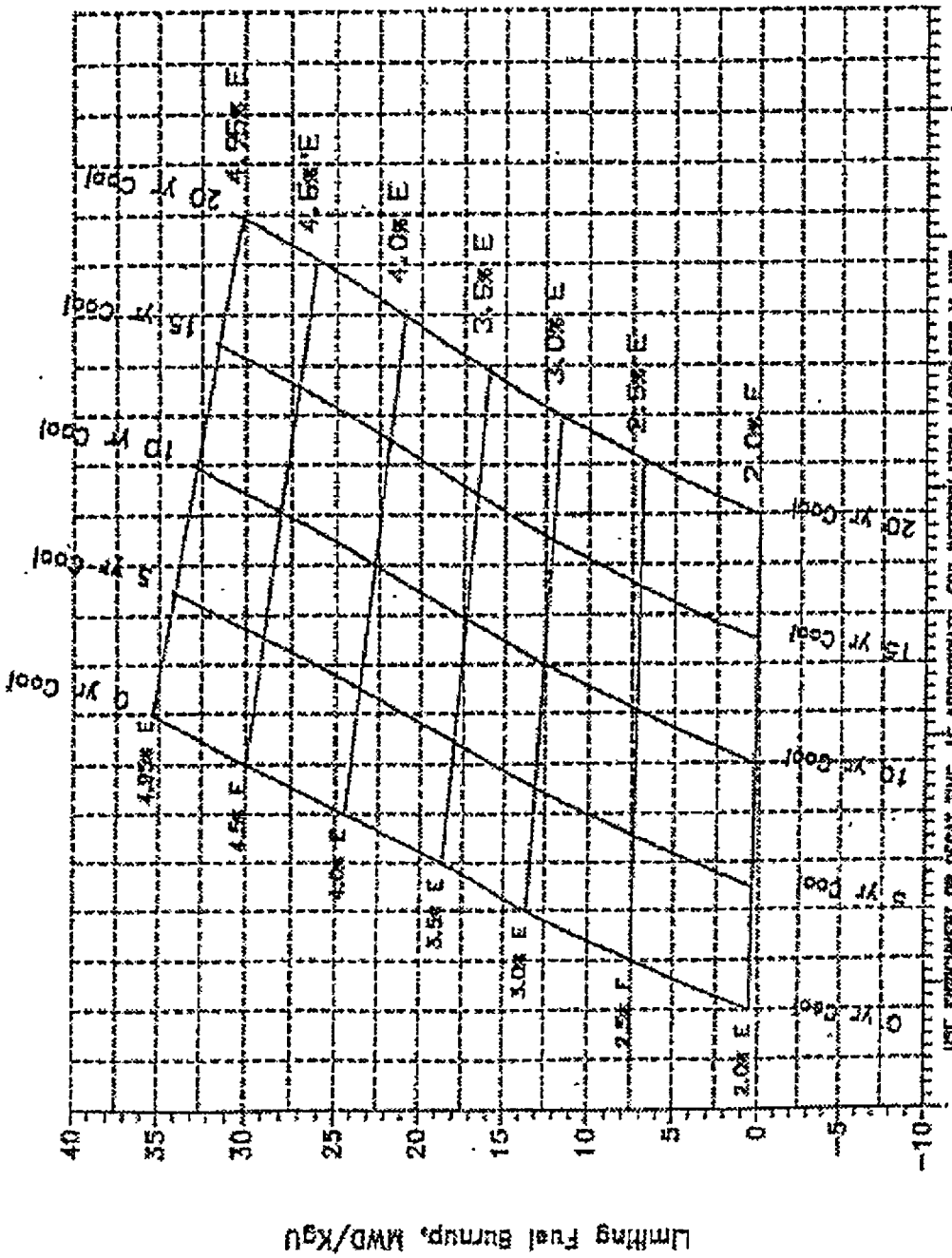

Fig. 4.1.1 3-Dimensional Plot of Minimum Fuel Burnups for Fuel In Unit 1 Region 1 for Enrichments and/or Cooling Times

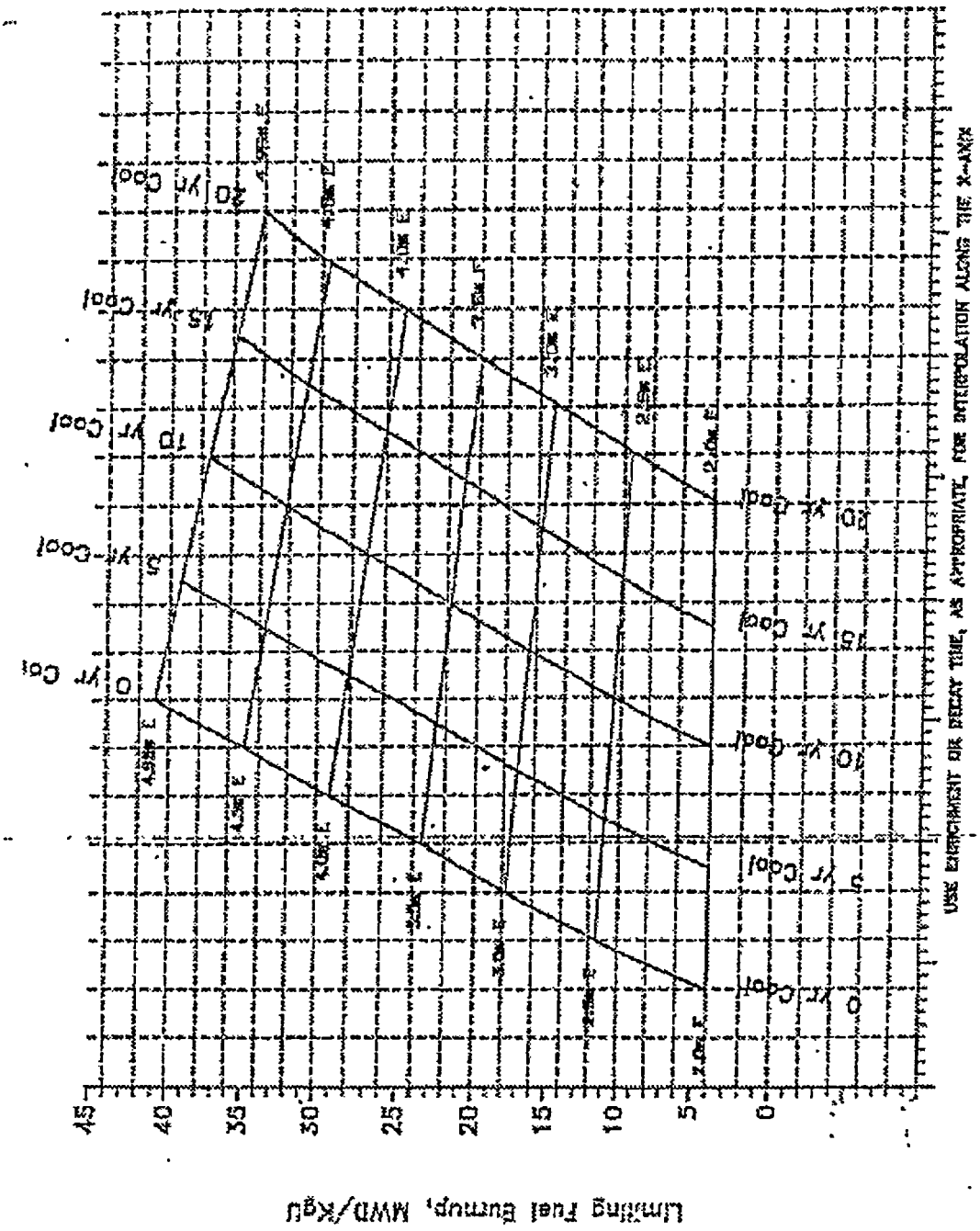

Fig. 4.1.2 3—Dimensional Plot of Minimum Fuel Burnups for Fuel In Unit 1 Region 2 for Enrichments and/or Cooling Times

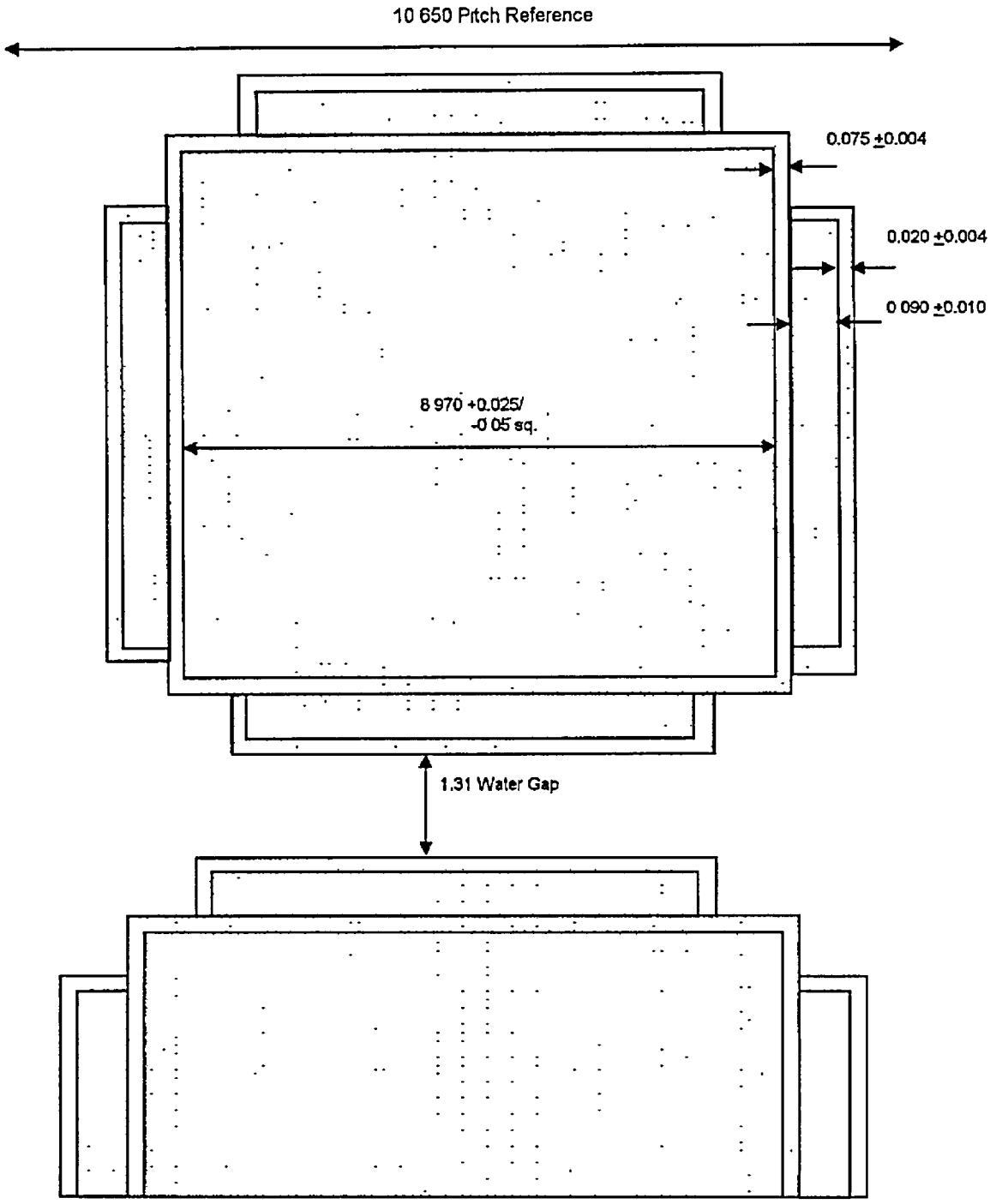

Figure 4.3.1: A Cross-Sectional View of the Calculational Model Used for the Region 1 Rack Analysis (NOT TO SCALE).

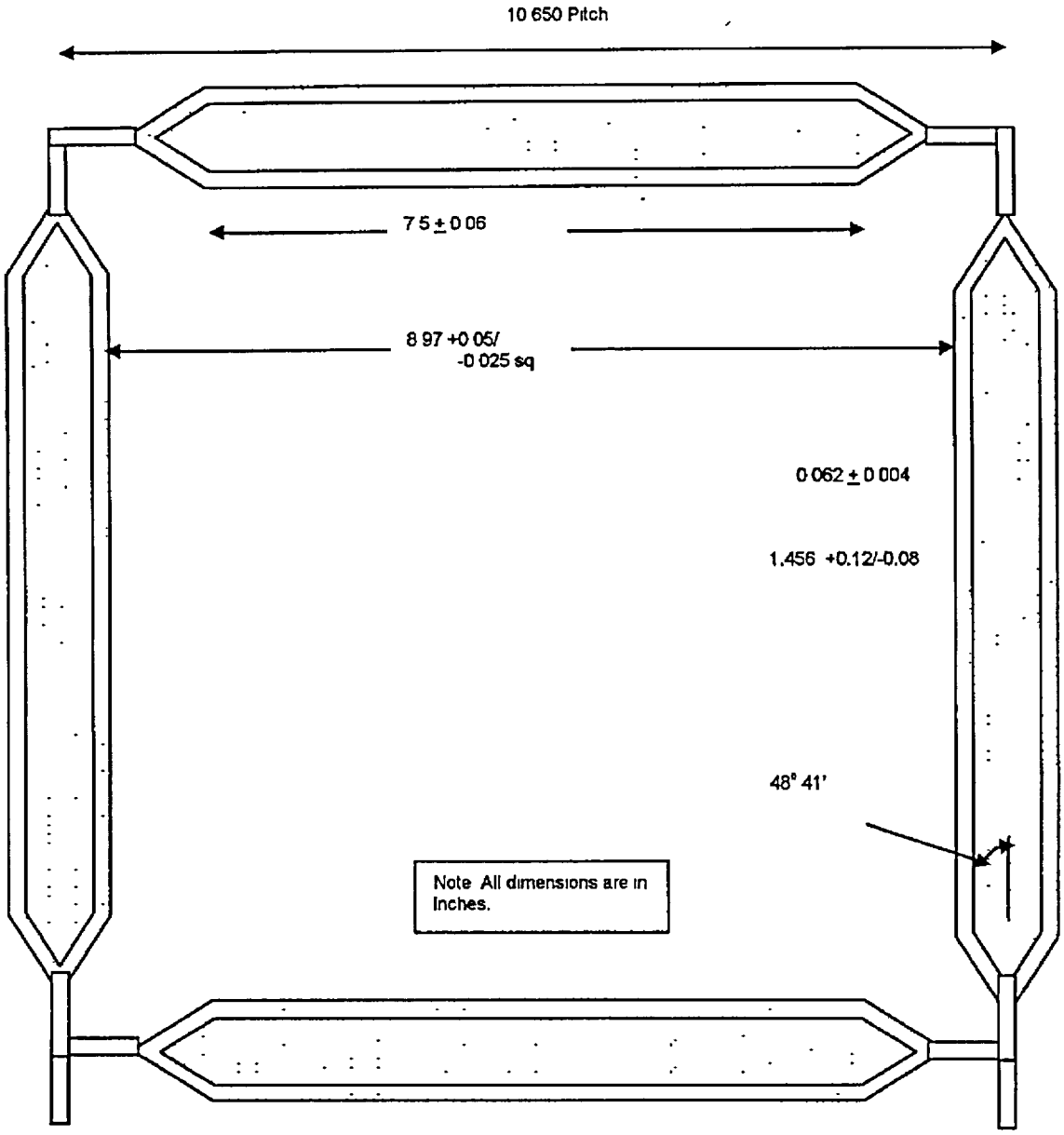

Figure 4.3.2: A Cross-Sectional View of the Calculational Model Used for the Region 2 Rack Analysis (NOT TO SCALE).

Note: The straight portion of the flux trap is modeled as 7.2 inches. In order to preserve the pitch due to a conservative reduction of the flux trap gap width from a design reference value of 1.556 inches to 1.456 inches (based on measurements which accounts for the bow in the cell walls), the cell ID was modeled as 9.07 +0.050/-0.025 inches.

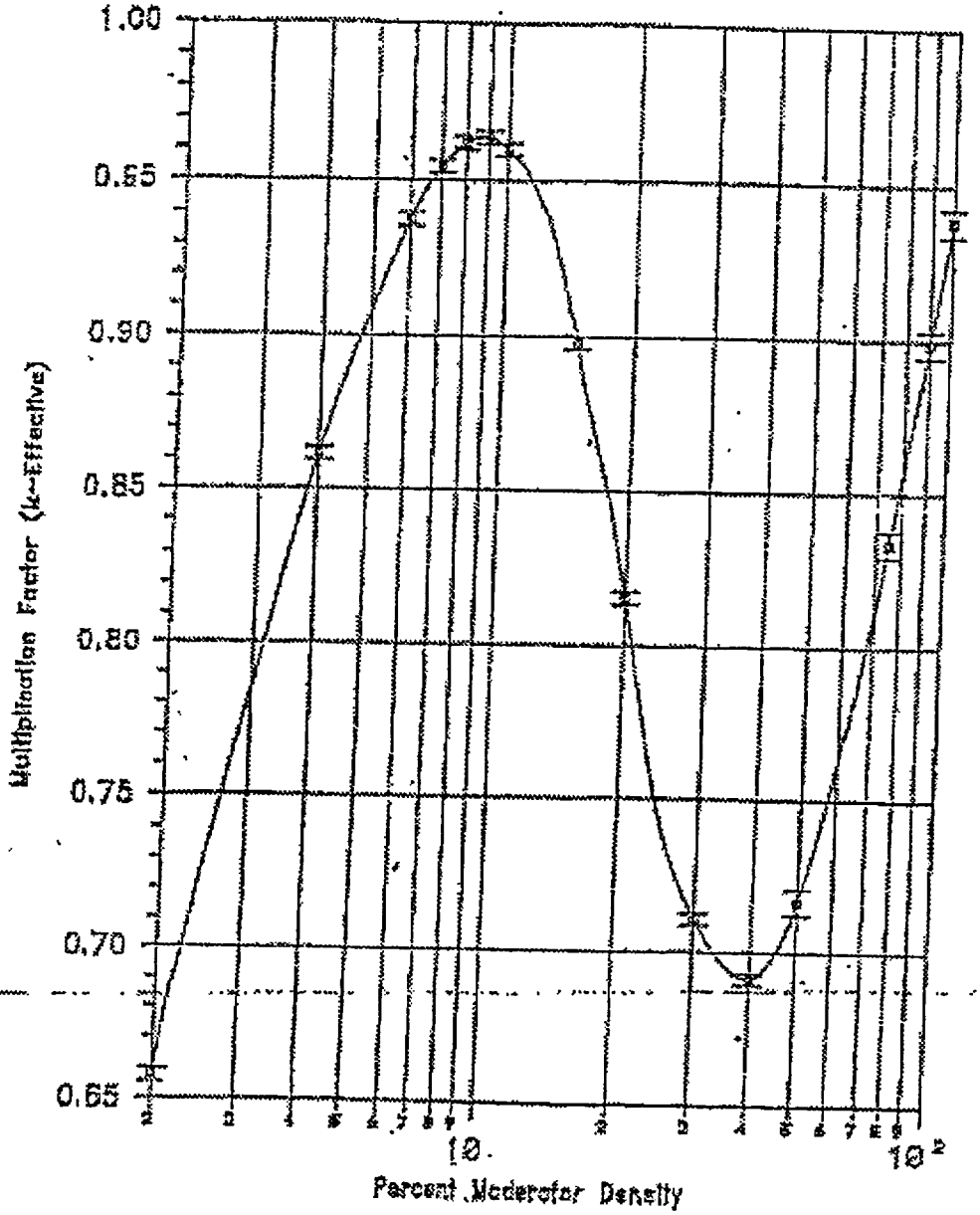

Figure 4.10.1 Reactivity of the New Fuel Vault as a Function of Moderator Density (4.95% ±0.05 Enrichment).

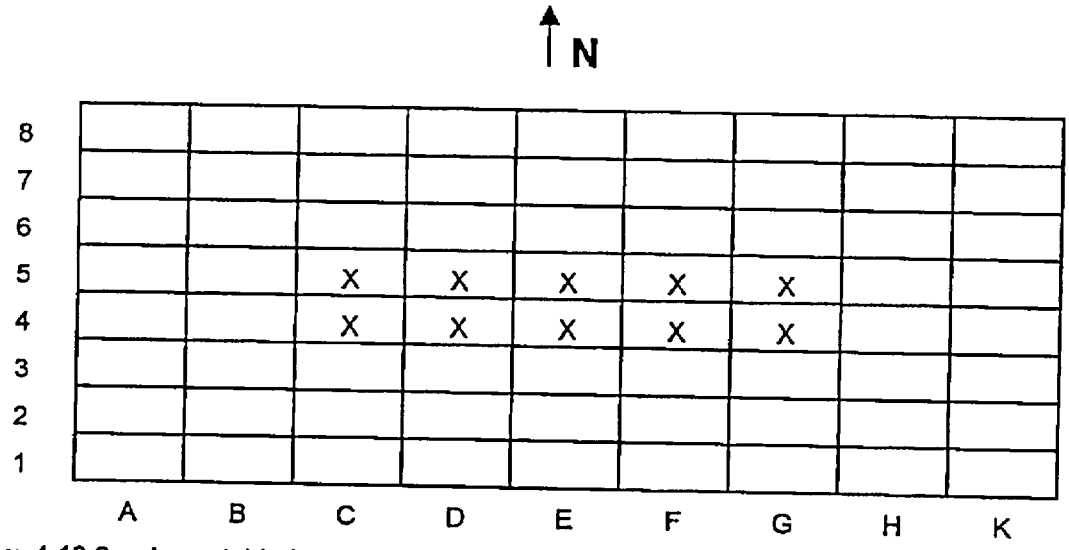

Figure 4.10.2: Acceptable New Fuel Storage Vault Configuration for up to 4.95 wt% Enrichment Fresh Fuel

Note: X's show the locations where fuel assemblies will not be stored.

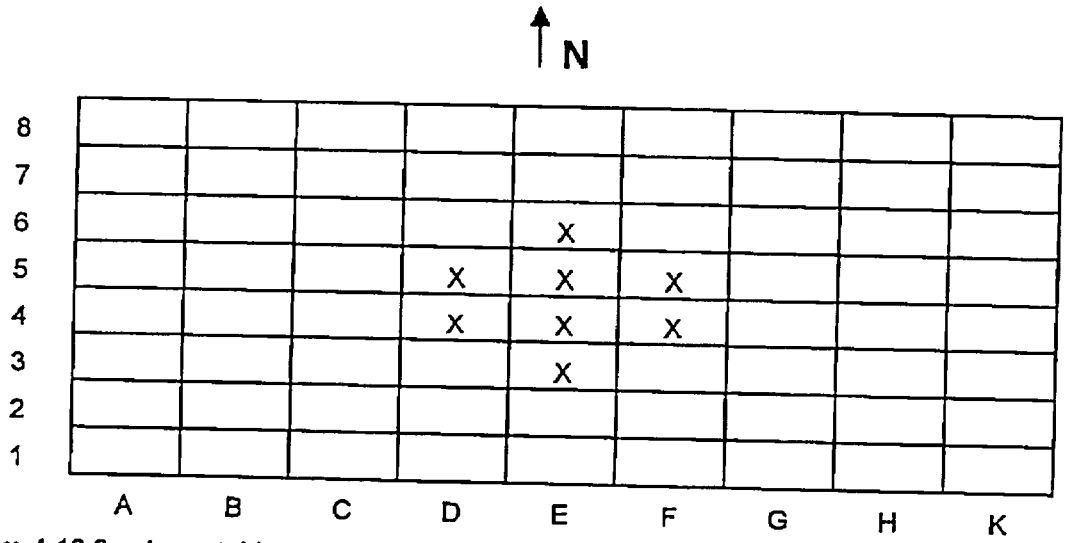

Figure 4.10.3: Acceptable New Fuel Storage Vault Configuration for up to 4.2 wt% Enrichment Fresh Fuel.

Note: X's show the locations where fuel assemblies will not be stored.

5.0 THERMAL-HYDRAULIC CONSIDERATIONS

5.1 INTRODUCTION

This document requests an operating license amendment to modify the spent fuel storage capacity at the ANO-1 nuclear power plant to preserve the capability of storing fresh fuel assemblies in the SFP racks. As discussed in Section 1.0, this will be achieved by placing poison inserts into the flux trap area of some of the existing Region 2 spent fuel storage racks (SFSRs). This section provides a summary of the analyses performed to demonstrate the compliance of the SFP and its attendant cooling system with the provisions of USNRC Standard Review Plan (SRP) 9.1.3 (Spent Fuel Pool Cooling and Cleanup System, Rev. 1, July 1981) and Section III of the USNRC "OT Position Paper for Review and Acceptance of Spent Fuel Storage and Handling Applications," (April 14, 1978). Similar methods of thermal-hydraulic analysis have been used in the licensing evaluations for other SFP capacity expansion projects.

The thermal-hydraulic qualification analyses for the modified rack array may be broken down into the following categories:

i. Evaluation of bounding maximum decay heat versus time profiles, used as input to subsequent analyses.

ii. Evaluation of loss-of-forced cooling scenarios, to establish minimum times to perform corrective actions and the associated makeup water requirements.

iii. Determination of the maximum local water temperature, at the instant when the pool decay heat reaches its maximum value, to establish that localized boiling in the SFSRs is not possible while forced cooling is operating. The bulk pool temperature is postulated to be at the maximum limit.

iv. Evaluation of the maximum fuel rod cladding temperature, at the instant when the pool decay heat reaches its maximum value, to establish that nucleate boiling is not possible while forced cooling is operating. The bulk pool temperature is postulated to be at the maximum limit.

The following sections present plant system descriptions, analysis methodologies and assumptions, a synopsis of the input data employed, and summaries of the calculated results.

5.2 COOLING SYSTEMS DESCRIPTION

The Spent Fuel Cooling (SFC) System is designed to maintain the water quality and clarity and to remove the decay heat from the stored fuel in the spent fuel pool. It is designed to maintain the spent fuel pool water at less than or equal to approximately 150 °F. This is accomplished by recirculating spent fuel coolant water from the spent fuel pool through the pumps and coolers and back to the pool. The spent fuel pool coolers reject heat to the nuclear intermediate cooling water system, which subsequently rejects its heat to the service water system. The spent fuel coolant pumps take suction from the spent fuel pool and deliver the water through the tube side of two coolers arranged in parallel back to the pool. In addition to its primary function, the system provides for purification of the spent fuel pool water, the fuel transfer canal water, and the contents of the Borated Water Storage Tank (BWST) in order to remove fission and corrosion products and to maintain water clarity for fuel handling operations. A bypass purification loop is provided to maintain the purity of the water in the spent fuel pool. This loop is also utilized to purify the water in the BWST following refueling and to maintain clarity in the fuel transfer canal during refueling. Water from the BWST or fuel transfer canal can be purified by using the borated water recirculation pump. The system also provides for filling the fuel transfer canal, the incore instrumentation tank, and the cask loading area from the BWST.

The spent fuel storage pool is provided with a makeup system design which meets the intent of Safety Guide 13. That is, the Borated Water Storage Tank (BWST) is a Seismic Category 1 vessel; all connecting piping is located in a Seismic Category 1 structure; a backup system for supplying water to the pool is provided through a temporary connection to the Seismic Category 1 service water system; and, there is sufficient time to rig a temporary makeup water supply to the pool in the event of failure of the normal source. The service water system can be supplied from either the Dardanelle Reservoir or the emergency cooling pond.

5.3 SPENT FUEL POOL DECAY HEAT LOADS

The decay heat in the SFP is generated in the spent fuel assemblies stored therein. In order to conservatively simplify the decay heat calculations, the total decay heat is considered as coming from two different groups of assemblies:

i. Fuel assemblies from previous offloads already stored in the SFP

ii. Fuel assemblies that are being offloaded from the reactor to the SFP

The fuel assemblies in the first group are referred to as previously offloaded fuel. Over the relatively short transient evaluation periods of this report the heat generation rate of these assemblies reduces very slowly with time, due to the exponential nature of radioactive decay and their relatively long decay periods. The decay heat contribution of these assemblies can therefore be conservatively treated as constant, neglecting any reduction in their decay heat contribution during the evaluation period. The fuel assemblies in the second group are referred to as recently offloaded fuel. The heat generation rate of these assemblies reduces rapidly with time, so the decay heat contribution of these assemblies is treated as time varying. The following equation defines the total decay heat generation in the SFP.

$$Q_{GEN}(\tau) = Q_P + F(\tau) \times Q_R(\tau) \qquad (5\text{-}1)$$

where:

$Q_{GEN}(\tau)$ is the total time-varying decay heat generation rate in SFP, Btu/hr
Q_P is the decay heat contribution of the previously offloaded fuel, Btu/hr
$F(\tau)$ is the fraction of the recently offloaded fuel transferred to the SFP
$Q_R(\tau)$ is the decay heat contribution of the recently offloaded fuel, Btu/hr
τ is the fuel decay time after reactor shutdown, hrs

Prior to the start of fuel transfer from the reactor to the SFP, $F(\tau)$ is equal to zero and the total decay heat in the SFP will be equal to the invariant portion Q_P. During the fuel transfer, $F(\tau)$ will increase linearly from zero to one, and the total decay heat in the SFP will increase to $Q_P+Q_R(\tau)$. Following the completion of fuel transfer, the total decay heat in the SFP will decrease as $Q_R(\tau)$ decreases.

The decay heat contributions of both the previously and recently offloaded fuel are determined using the Holtec QA validated computer program DECOR [5.3.1]. This computer program incorporates the Oak Ridge National Laboratory (ORNL) ORIGEN2 computer code [5.3.2] for performing decay heat calculations. The ORIGEN2 code is not modified for its incorporation into the Holtec program and should give the same results as DECOR.

Based on the input data provided in Tables 5.3.1 and 5.3.2, the fuel decay heat is determined for the following two offload scenarios:

1. Partial Core Offload - A refueling batch of 76 assemblies is offloaded from the plant's reactor into the SFP, completely filling all available storage locations. The total SFP inventory prior to the offload is 912 fuel assemblies, for a final post-offload inventory of 988 fuel assemblies. This slightly exceeds the storage capacity of the ANO-1 SFP (and the ANO-1 TS 4.3.3 limit of 968 assemblies) and is used for calculation of decay heat loads, which is conservative.

2. Full Core Offload - The full core of 177 assemblies is offloaded from the plant's reactor into the SFP, completely filling all available storage locations. The total SFP inventory prior to the offload is 836 fuel assemblies, for a final post-offload inventory of 1013 fuel assemblies. This slightly exceeds the storage capacity of the ANO-1 SFP (and the ANO-1 TS 4.3 3 limit of 968 assemblies) and is used for calculation of decay heat loads, which is conservative.

5.4 MINIMUM TIME-TO-BOIL AND MAXIMUM BOILOFF RATE

In this section, we present the methodology for calculating the minimum time-to-boil and corresponding maximum boiloff rate.

The following conservatisms and assumptions are applied in the time-to-boil and boiloff rate calculations:

- The initial SFP bulk temperature is assumed to be equal to the bulk temperature limit of 150 °F.

- The thermal inertia (thermal capacity) of the SFP is based on the net water volume only. This conservatively neglects the considerable thermal inertia of the fuel assemblies, stainless steel racks and stainless steel SFP liners.

- During the loss of forced cooling evaluations, it is assumed that makeup water is not available. This minimizes the thermal capacity of the SFP as water is boiled off, thus increasing the water level drop rate.

- The loss of forced cooling is assumed to occur coincident with the peak SFP bulk temperature and the maximum pool decay heat. Maximizing the initial temperature and the pool decay heat conservatively minimizes the calculated time-to-boil.

The governing enthalpy balance equation for this condition, subject to these conservative assumptions, can be written as:

$$C(\tau)\frac{dT}{d\tau}=Q_{gen}(\tau+\tau_0) \qquad (5\text{-}2)$$

where:

$C(\tau)$ = Time-varying SFP thermal capacity (BTU/°F)

τ = Time after cooling is lost (hr)

τ_0 = Loss of cooling time after shutdown (hr)

T=Pool water temperature, (°F)

Equation 5-2 is solved to obtain the bulk pool temperature as a function of time, the time-to-boil, boil-off rate and water depth versus time. The major input values for these analyses are summarized in Table 5 4.1.

5.5 MAXIMUM SFP LOCAL WATER TEMPERATURE

In this section, a summary of the methodology for evaluating the maximum SFP local water temperature is presented. The results of these evaluations are maximum local water temperatures.

In order to determine an upper bound on the maximum local water temperature, a series of conservative assumptions are made. The most important of these assumptions are:

- The walls and floor of the SFP are all modeled as adiabatic surfaces, thereby neglecting conduction heat loss through these items.

- Heat losses by thermal radiation and natural convection from the hot SFP surface to the environment are neglected.

- No downcomer flow is assumed to exist between the rack modules.

- The hydraulic resistance parameters for the rack cells, permeability and inertial resistance, are conservatively adjusted by 10%.

- The bottom plenum heights used in the model are less than the actual heights.

- The hydraulic resistance of every SFSR cell is determined based on the most restrictive water inlet geometry of the cells over rack support pedestals (i.e., all baseplate holes are completely blocked). These cells have a reduced water entrance area, caused by the pedestal blocking the baseplate hole, and a correspondingly increased hydraulic resistance.

- The hydraulic resistance of every SFSR cell includes the effects of blockage due to an assumed dropped fuel assembly lying horizontally on top of the SFSRs.

The objective of this study is to demonstrate that the thermal-hydraulic criterion of ensuring local subcooled conditions in the SFP is met for all postulated fuel offload scenarios. The local thermal-hydraulic analysis is performed such that slight fuel assembly variations are bounded. An outline of the Computational Fluid Dynamics (CFD) approach is described in the following.

There are several significant geometric and thermal-hydraulic features of the ANO-1 SFP that need to be considered for a rigorous CFD analysis. From a fluid flow modeling standpoint, there are two regions to be considered. One region is the SFP bulk region where the classical Navier-Stokes equations [5.5.1] are solved, with turbulence effects included. The other region is the SFSRs containing heat generating fuel assemblies, located near the bottom of the SFP. In this region, water flow is directed vertically upwards due to buoyancy forces through relatively small

flow channels formed by the B&W 15x15 fuel assemblies in each SFSR cell. This situation is modeled as a porous region with pressure drop in the flowing fluid governed by Darcy's Law as:

$$\frac{\partial P}{\partial X_i} = -\frac{\mu}{K(i)} V_i - C \rho |V| \frac{V_i}{2} \qquad (5\text{-}3)$$

where $\partial P/\partial X_i$ is the pressure gradient, K(i), V_i and C are the corresponding permeability, velocity and inertial resistance parameters and μ is the fluid viscosity. These terms are added as sink terms to the classic Navier-Stokes equations. The permeability and inertial resistance parameters for the rack cells loaded with B&W 15x15 fuel assemblies are determined based on friction factor correlations for the laminar flow conditions that would exist due to the low buoyancy induced velocities and the small size of the flow channels.

The ANO-1 SFP geometry requires an adequate portrayal of both large scale and small scale features, spatially distributed heat sources in the SFSRs and water inlet/outlet piping. Relatively cooler bulk water normally flows down between the perimeter of the fuel rack array and wall liner, a clearance known as the downcomer. Near the bottom of the racks the flow turns from a vertical to horizontal direction into the bottom plenum, supplying cooling water to the rack cells. Heated water issuing out of the top of the racks mixes with the bulk water. An adequate modeling of these features on the CFD program involves meshing the large scale bulk SFP region and small scale downcomer and bottom plenum regions with sufficient number of computational cells to capture both the global and local features of the flow field.

The distributed heat sources in the SFP racks are modeled by identifying distinct heat generation zones considering recently offloaded fuel, bounding peaking effects, and the presence of background decay heat from previous offloads. Two heat generating zones are modeled. The first consists of background fuel from previous offloads. The second zone consists of fuel from recently offloaded fuel assemblies. This is a conservative model, since all of the hot fuel assemblies from the recent offload are placed in a contiguous area. A uniformly distributed heat generation rate was applied throughout each distinct zone (i.e., there were no variations in heat generation rate within a single zone).

The CFD analysis was performed on the commercially available FLUENT [5.5.2] Computational Fluid Dynamics program, which has been benchmarked under Holtec's QA program. The

FLUENT code enables buoyancy flow and turbulence effects to be included in the CFD analysis. Buoyancy forces are included by specifying a temperature-dependent density for water and applying an appropriate gravity vector. Turbulence effects are modeled by relating time-varying Reynolds' Stresses to the mean bulk flow quantities with the standard k-ε turbulence model.

Some of the major input values for this analysis are summarized in Table 5.5.1. An isometric view of the assembled CFD model is presented in Figure 5.5.1.

5.6 FUEL ROD CLADDING TEMPERATURE

In this section, the method to calculate the temperature of the fuel rod cladding is presented. The maximum fuel rod cladding temperature is determined to establish that nucleate boiling is not possible while forced cooling is operating. This requires demonstrating that the highest fuel rod cladding temperatures are less than the local saturation temperature of the adjacent SFP water. The maximum fuel cladding superheat above the local water temperature is calculated for two different peak fuel rod heat emission rates.

A fuel rod can produce F_z times the average heat emission rate over a small length, where F_z is the axial peaking factor. The axial heat distribution in a rod is generally a maximum in the central region, and tapers off at its two extremities. Thus, peak cladding heat flux over an infinitesimal rod section is given by the equation:

$$q_c = \frac{Q \times F_z}{A_c} \tag{5-4}$$

where Q is the rod average heat emission and A_c is the total cladding external heat transfer area in the active fuel length region. The axial peaking factor is given in Table 5.5.1.

As described previously, the maximum local water temperature was computed. Within each fuel assembly sub-channel, water is continuously heated by the cladding as it moves axially upwards under laminar flow conditions. Rohsenow and Hartnett [5.6.1] report a Nusselt-number for laminar flow heat transfer in a heated channel. The film temperature driving force (ΔT_f) at the peak cladding flux location is calculated as follows:

$$\Delta T_f = \frac{q_c}{h_f}$$
$$h_f = Nu\frac{Kw}{D_h} \qquad (5\text{-}5)$$

where h_f is the waterside film heat transfer coefficient, D_h is sub-channel hydraulic diameter, Kw is water thermal conductivity and Nu is the Nusselt number for laminar flow heat transfer.

In order to introduce some additional conservatism in the analysis, we assume that the fuel cladding has a crud deposit resistance R_c (equal to 0.0005 ft^2-hr-°F/Btu) which covers the entire surface. Thus, including the temperature drop across the crud resistance, the cladding to water local temperature difference (ΔT_c) is given by the equation $\Delta T_c = \Delta T_f + R_c \times q_c$.

5.7 RESULTS

This section contains results from the analyses performed for the postulated offload scenarios.

5.7.1 Decay Heat

For the offload scenarios described in Section 5.3, the calculated SFP decay heat loads are summarized in Table 5.7.1. Given the conservatisms incorporated into the calculations, actual decay heat loads will be lower than these calculated values. Figures 5.7.1 and 5.7.2 each present profiles of net decay heat load versus time for the evaluated transient scenarios.

5.7.2 Minimum Time-to-Boil and Maximum Boiloff Rate

For the offload/cooling described in Section 5.3, the calculated times-to-boil and maximum boil-off rates are summarized in Table 5.7.2. These results show that, in the extremely unlikely event of a failure of forced cooling to the SFP, there would be at least 3.23 hours available for corrective actions prior to SFP boiling. Given the conservatisms incorporated into the calculations, actual times-to-boil will be higher than these calculated values. It is noted that a complete failure of forced cooling is extremely unlikely. The maximum water boiloff rate is less than 85 gpm.

5.7.3 Local Water and Fuel Cladding Temperatures

Consistent with our approach to make conservative assessments of temperature, the local water temperature calculations are performed for a SFP with a total decay heat generation equal to the calculated decay heat load coincident with the maximum SFP bulk temperature. Thus, the local water temperature evaluation is a calculation of the temperature increment over the theoretical spatially uniform value due to local hot spots (due to the presence of highly heat emissive fuel assemblies). As described in Subsection 5.6, the peak fuel clad superheats (i e., the maximum clad-to-local water temperature difference) are determined. The resultant bounding superheat values were used to calculate bounding maximum fuel clad temperatures.

The numeric results of the maximum local water temperature and the bounding fuel cladding temperature evaluations are presented in Table 5.7.3. Figure 5.7.3 presents converged temperature contours in a vertical slice through the hot fuel region. Figure 5.7.4 presents converged velocity vectors in a vertical slice through the hot fuel region.

Both the maximum local water temperatures and the bounding fuel cladding temperatures are substantially lower than the 240 °F local boiling temperature at the top of the SFSRs. These results demonstrate that boiling, including nucleate boiling on clad surfaces, cannot occur anywhere within the ANO-1 SFP.

Under a postulated accident scenario of the loss of all cooling, the water temperature will rise. Assuming a temperature of 212 °F at the inlet to the rack cells, and conservatively using the bounding bulk-to-local and local-to-clad temperature differences from Table 5.7.3, the maximum possible cladding temperature will be 285.5 °F, which is greater than the saturation temperature at the top of the active fuel length. Due to the low maximum assembly heat flux (approximately 7000 W/m^2) and the critical heat flux required for departure from nucleate boiling (on the order of 10^6 W/m^2), it can be concluded that the fuel cladding will not be subjected to departure from nucleate boiling even under the postulated accident scenario of the loss of all SFP cooling and the cladding integrity would be maintained.

5.8 REFERENCES

[5.3.1] "QA Documentation for DECOR," Holtec Report HI-971734, Revision 0.

[5.3.2] A. G. Croff, "ORIGEN2 - A Revised and Updated Version of the Oak Ridge Isotope Generation and Depletion Code," ORNL-5621, Oak Ridge National Laboratory, 1980.

[5.5.1] Batchelor, G. K., "An Introduction to Fluid Dynamics", Cambridge University Press, 1967.

[5.5.2] "Validation of FLUENT Version 5.1", Holtec Report HI-992276, Revision 0.

[5.6.1] Rohsenow, N. M., and Hartnett, J. P., "Handbook of Heat Transfer", McGraw Hill Book Company, New York, 1973.

Table 5.3.1

Key Input Data for Decay Heat Computations

Input Data Parameter	Value
Reactor Thermal Power (MWt)	2800
Number of Assemblies in Reactor Core	177
Maximum Number of Storage Cells in SFP	968
Bounding Discharge Schedule	Table 5.3.2
Minimum In-Core Hold Time (hr)	100
Fuel Discharge Rate	5 per hour

Table 5.3.2

Offload Schedule

Cycle Number	Offload Date (mm/dd/yyyy)	Number of Assemblies	Average Burnup (MWd/MTU)	Initial ^{235}U Enrichment (wt.%)[4]	Assembly U Weight (kgU)
1	01/01/2002[1]	76	75,000	4.00	463.8
2	01/01/2004	76	75,000	4.00	463.8
3	01/01/2006	76	75,000	4.00	463.8
4	01/01/2008	76	75,000	4.00	463.8
5	01/01/2010	76	75,000	4.00	463.8
6	01/01/2012	76	75,000	4.00	463.8
7	01/01/2014	76	75,000	4.00	463.8
8	01/01/2016	76	75,000	4.00	463.8
9	01/01/2018	76	75,000	4.00	463.8
10	01/01/2020	76	75,000	4.00	463.8
11	01/01/2022	76	75,000	4.00	463.8
12	01/01/2024	76 or 177[2]	75,000	4.00	463.8
13	01/01/2026	76 or 0[3]	75,000	4.00	463.8

Table Notes:

(1) Dates are arbitrarily set to yield two years between offloads. While historic (ca. 2002) offloads were on 18-month cycles, the use of the longer 24-month cycle will have a negligible impact on the total SFP heat load. This is due to the use of bounding burnups and initial enrichments for the historic offloads, as well as the extremely long cooling times for these fuel assemblies at the point in time where the SFP becomes filled.

(2) 76 assemblies for partial core offload (previously discharged fuel), 177 assemblies for full core offload (recently discharged fuel).

(3) 76 assemblies for partial core offload (recently discharged fuel), 0 assemblies for full core offload.

(4) Initial enrichments may be as high as 5.0 wt.%. For a given burnup, a lower enrichment will yield a higher calculated decay heat. Thus, the use of 4.0 wt.% is conservative for the purposes of the thermal analysis.

Table 5.4.1

Key Input Data for Time-To-Boil Evaluation

SFP Surface Area	1012 ft^2
Minimum Pool Water Depth	37.0 feet
SFP Net Water Volume	34,340 ft^3

Note: The net water volume is the gross water volume (i.e., area times depth) minus the volume displaced by the fuel racks and stored fuel assemblies.

Table 5.5.1

Key Input Data for Local Temperature Evaluation

Axial Peaking Factor	1.65
Number of Fuel Assemblies	968
Cooled SFP Water Flow Rate through SFPCS Heat Exchanger	1000 gpm*
Fuel Assembly Type	B&W 15x15
Fuel Rod Outer Diameter	0.430 inches
Active Fuel Length**	140.6 inches
Number of Rods per Assembly	208 rods
Rack Cell Inner Dimension	8.97 inches
Rack Cell Length	162 inches
Modeled Bottom Plenum Height	3 inches

* Conservatively, only one pump flow is credited in the analysis.

** Conservatively, the lowerbound value for the active fuel length for ANO-1 fuel assemblies is used in the analysis.

Table 5.7.1

Result of SFP Decay Heat Calculations

Heat Load Component	Partial Core Offload Value (Btu/hr)	Full Core Offload Value (Btu/hr)
Previously Discharged Fuel	5.739×10^6	5.462×10^6
Recently Discharged Fuel at End of Transfer	15.598×10^5	34.014×10^6
Total Bounding Decay Heat	21.337×10^6	39.476×10^6
SFP Pump Heat (2 operating)	0.204×10^6	0.204×10^6
Total Bounding SFP Heat	21.541×10^6	39.680×10^6

Table 5.7.2

Results of Loss-of-Forced Cooling Evaluations

Calculate Result Parameter	Partial Core Offload Value	Full Core Offload Value
Minimum Time-to-Boil	8.87 hours	3.23 hours
Maximum Boiloff Rate	45.84 gallons per minute	84.80 gallons per minute
Minimum Time for Water to Drop to Top of Racks	63.5 hours	34.3 hours

Table 5.7.3

Results of Maximum Local Water and Fuel Cladding Temperature Evaluations

Parameter	Value
Peak Local Water Temperature	192 °F
Peak Cladding Superheat	31.5 °F
Peak Local Fuel Cladding Temperature	223.5 °F

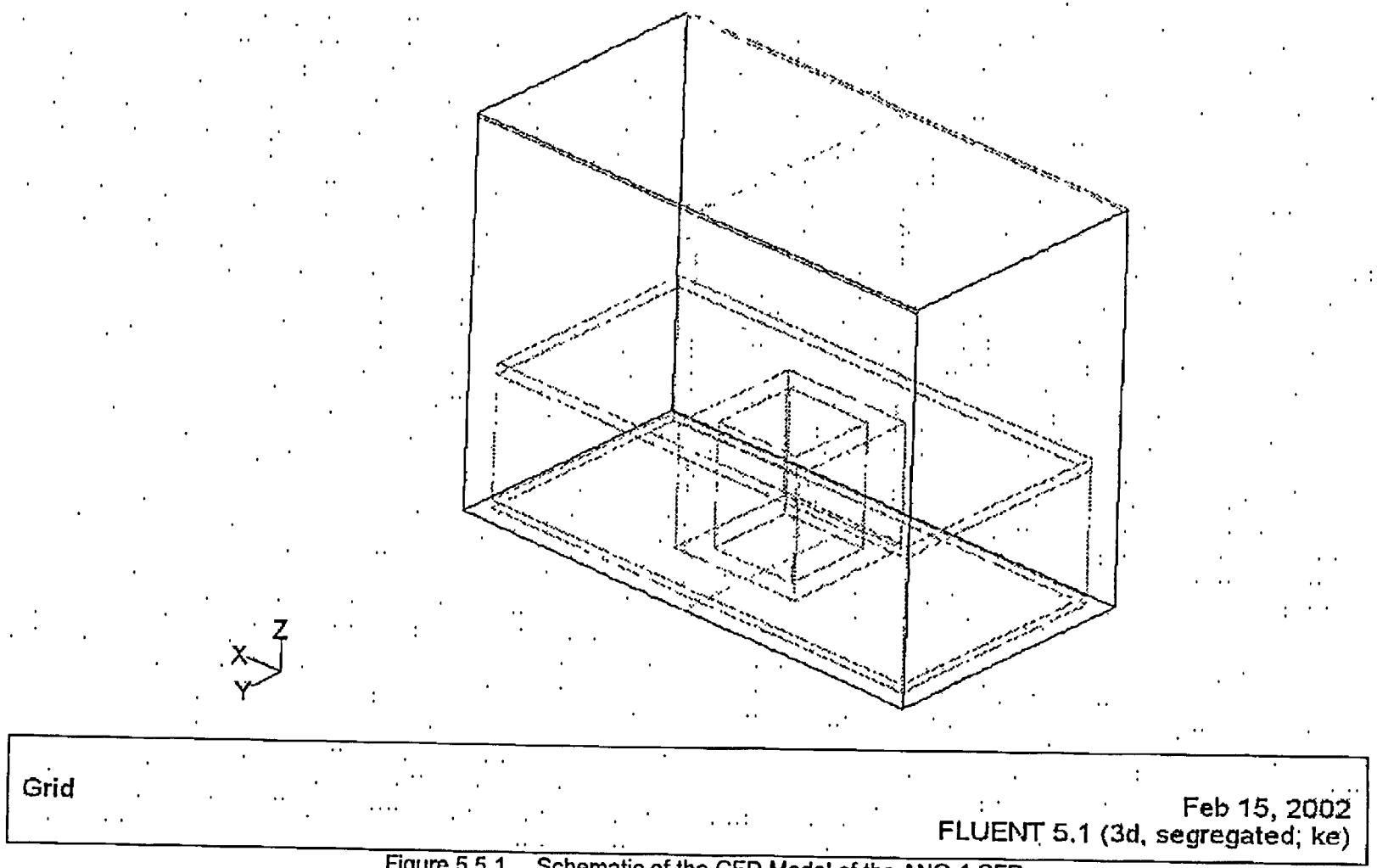

Figure 5.5.1 Schematic of the CFD Model of the ANO-1 SFP.

Figure 5.7.1 - Partial Core Offload Bounding Spent Fuel Pool Heat Load
(Including previously and recently discharged fuel and 2 SFP pumps)

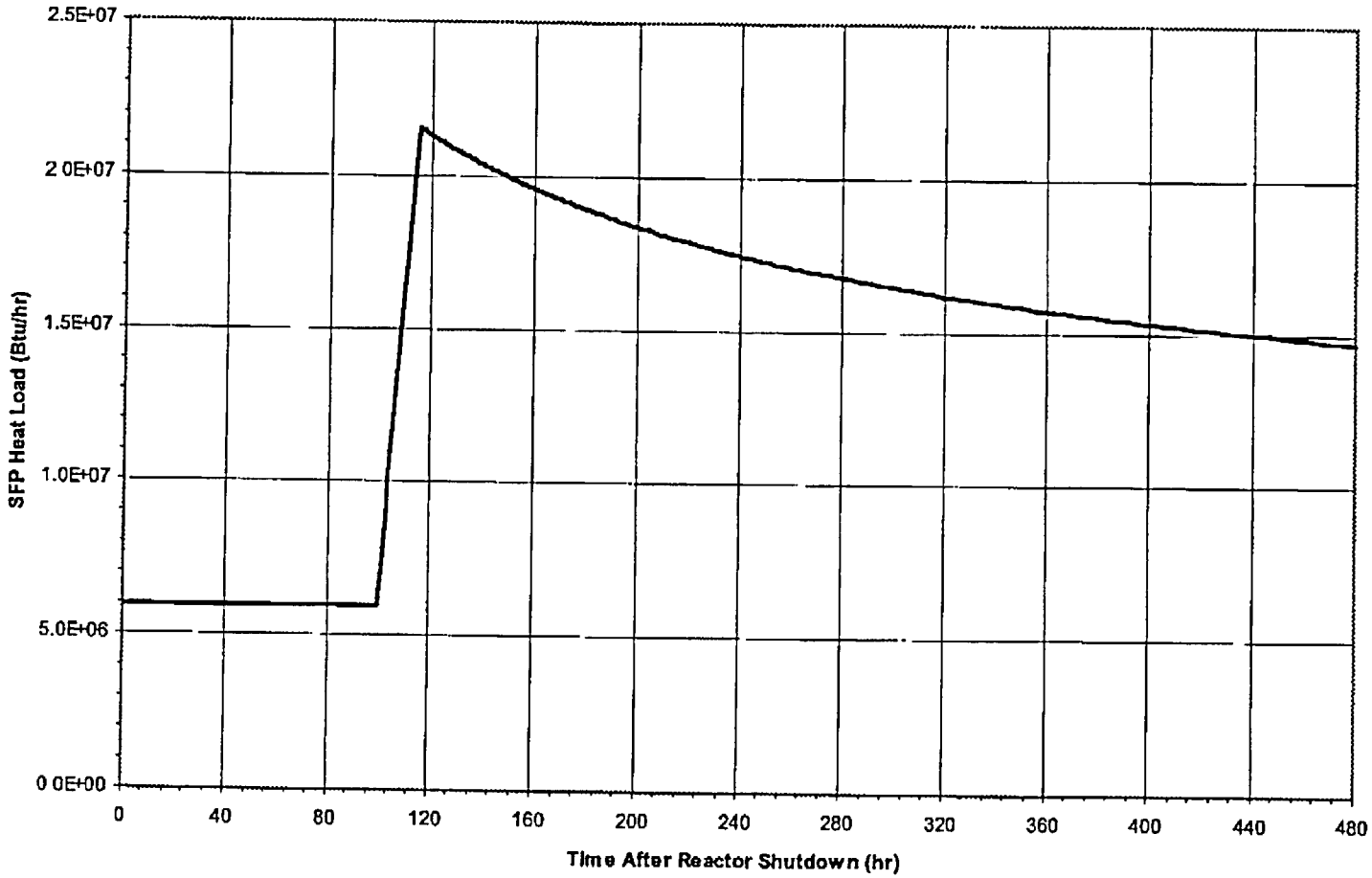

Figure 5.7.2 - Full Core Offload Bounding Spent Fuel Pool Heat Load (including previously and recently discharged fuel and 2 SFP pumps)

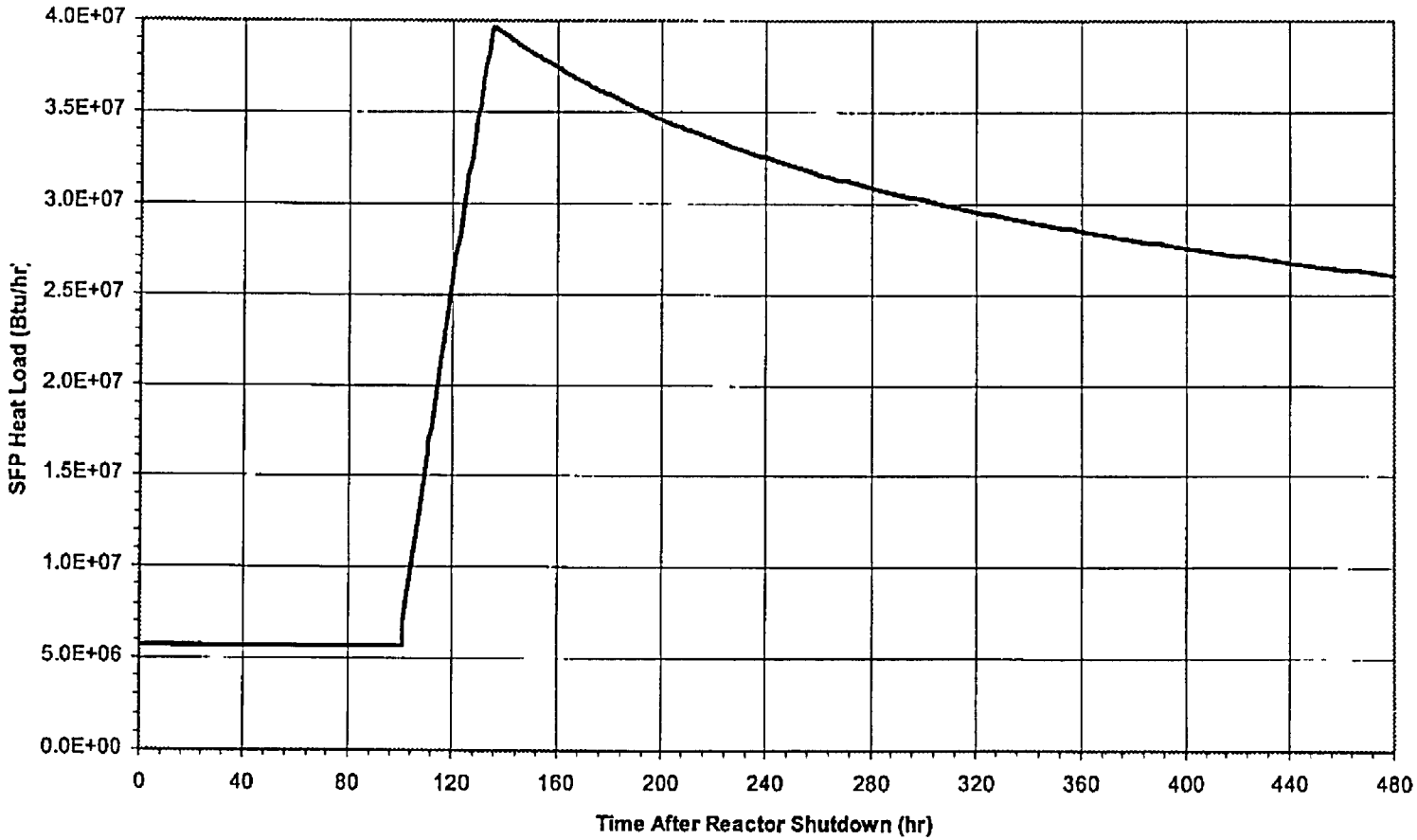

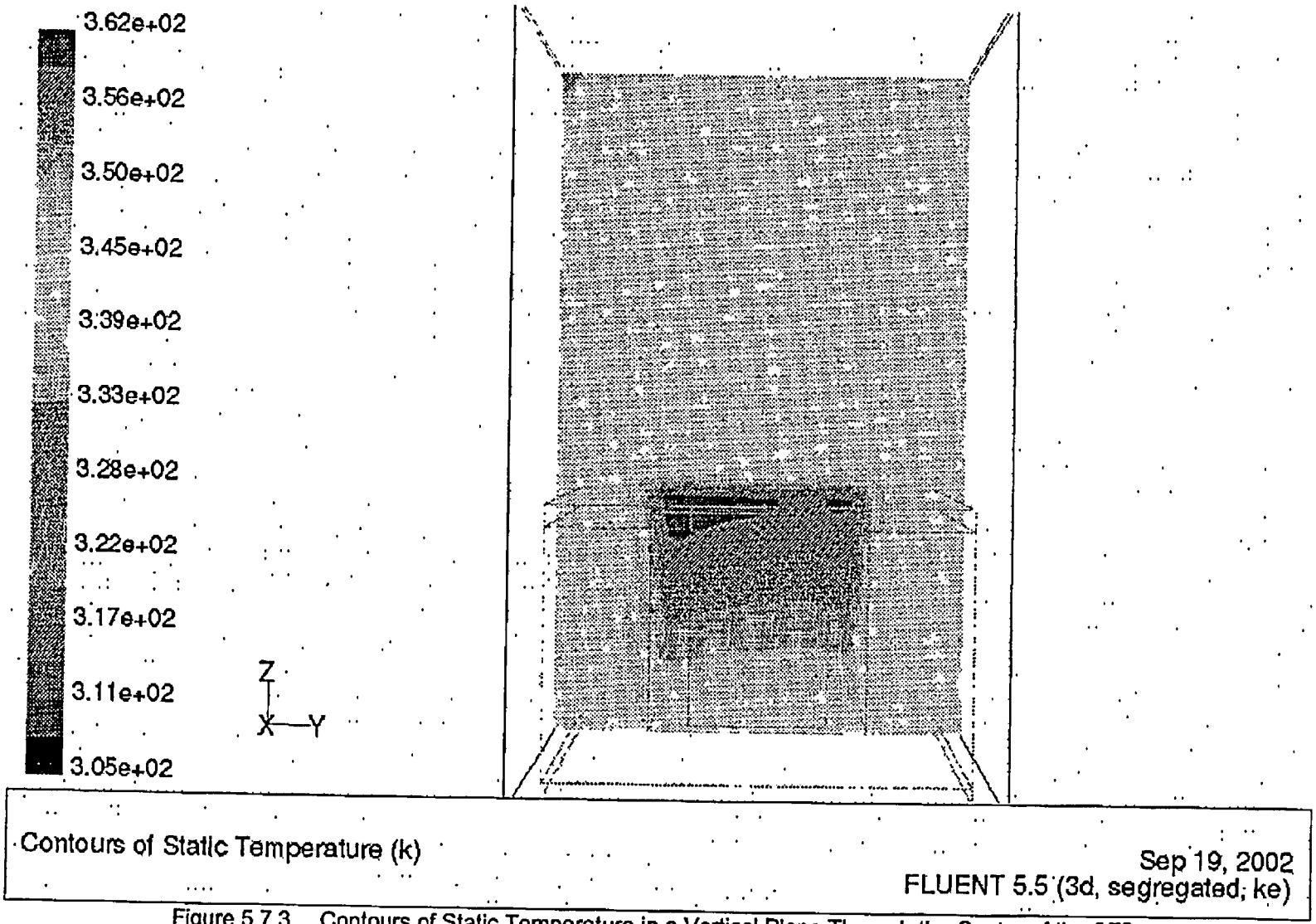

Figure 5.7.3. Contours of Static Temperature in a Vertical Plane Through the Center of the SFP.

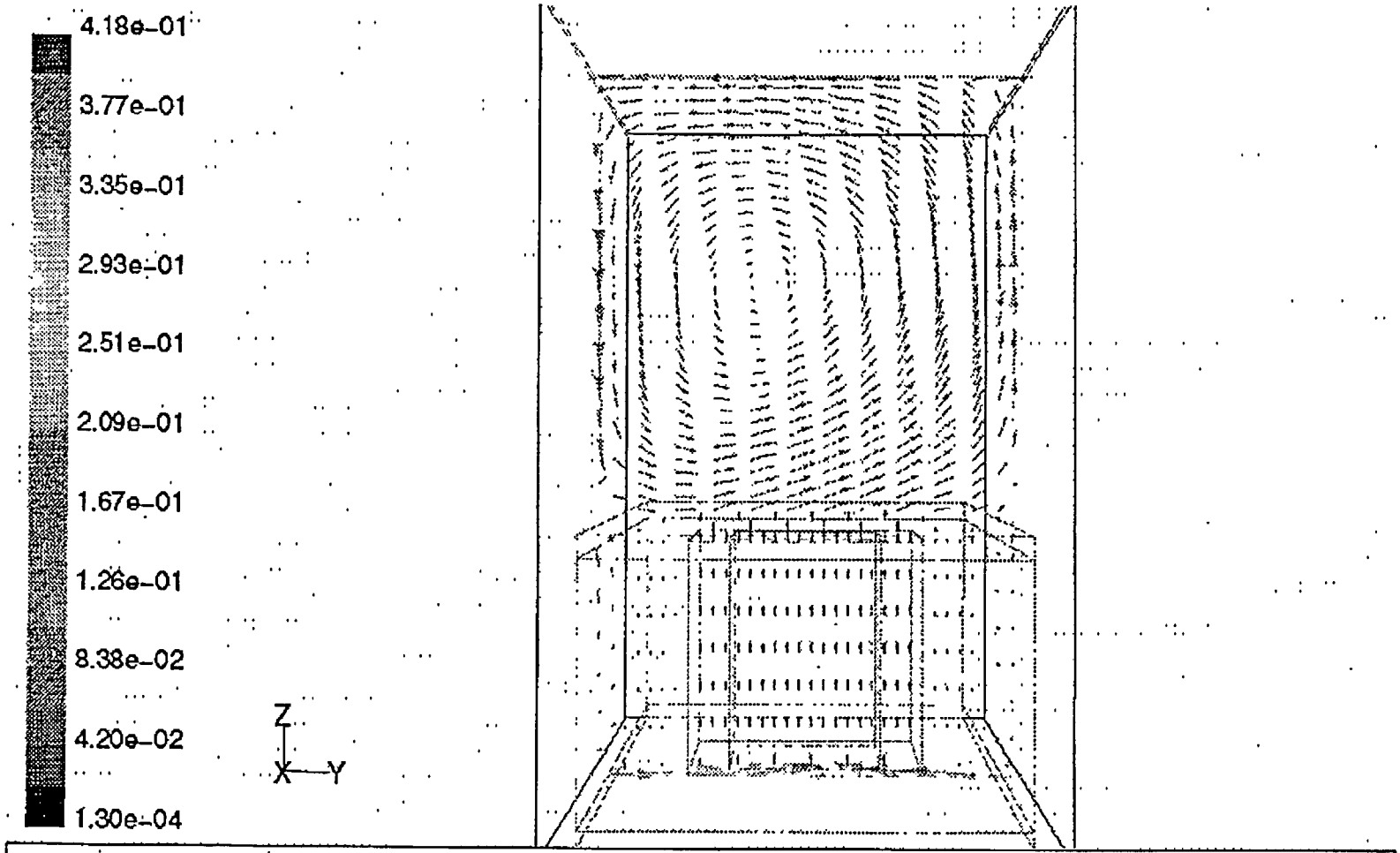

Figure 5.7.4: Velocity Vector Plot in a Vertical Plane Through the Center of the SFP.

6.0 STRUCTURAL/SEISMIC CONSIDERATIONS

6.1 INTRODUCTION

This section considers the structural adequacy of the existing spent fuel racks with new poison inserts under all loadings postulated for normal and seismic conditions at the Arkansas Nuclear One (ANO) Unit 1 reactor. The module layout is illustrated in Figure 6.1.1, along with the X and Y coordinate axes used to identify displacement orientation.

The analyses undertaken to confirm the structural integrity of the racks and the poison inserts, are performed in compliance with the OT Position Paper [6.1.2], ANO Specification No. AP&L-C-502 [6.1.3], and the ANO Unit 1 SAR [6.1.4]. An abstract of the methodology, modeling assumptions, key results, and summary of the parametric evaluation is presented. Delineation of the relevant criteria is discussed in the text associated with each analysis.

6.2 OVERVIEW OF RACK STRUCTURAL ANALYSIS METHODOLOGY

The response of a freestanding rack module to seismic inputs is highly nonlinear and involves a complex combination of motions (sliding, rocking, twisting, and turning), resulting in potential impacts and friction effects. Some of the unique attributes of the rack dynamic behavior include a large fraction of the total structural mass in a confined rattling motion, friction support of rack pedestals against lateral motion, and large fluid coupling effects due to deep submergence and independent motion of closely spaced adjacent structures.

Linear methods, such as modal analysis and response spectrum techniques, cannot accurately simulate the structural response of such a highly nonlinear structure to seismic excitation. An accurate simulation is obtained only by direct integration of the nonlinear equations of motion with the three pool slab acceleration time-histories applied as the forcing functions acting simultaneously.

Whole Pool Multi-Rack (WPMR) analysis is the vehicle utilized in this project to simulate the dynamic behavior of the complex storage rack structures. The following sections provide the basis for this selection and discussion on the development of the methodology.

6.2.1 Background of Analysis Methodology

Reliable assessment of the stress field and kinematic behavior of the rack modules calls for a conservative dynamic model incorporating all key attributes of the actual structure. This means that the model must feature the ability to execute the concurrent motion forms compatible with the freestanding installation of the modules.

The model must possess the capability to effect momentum transfers which occur due to rattling of fuel assemblies inside storage cells and the capability to simulate lift-off and subsequent impact of support pedestals with the pool liner (or bearing pad). The contribution of the water mass in the interstitial spaces around the rack modules and within the storage cells must be modeled in an accurate manner, since erring in quantification of fluid coupling on either side of the actual value is no guarantee of conservatism.

The Coulomb friction coefficient at the pedestal-to-pool liner (or bearing pad) interface may lie in a rather wide range and a conservative value of friction cannot be prescribed without analyzing this effect. In fact, a review of the results of rack dynamic analyses in numerous dockets (Table 6.2.1) indicates that an upper bound value of the coefficient of friction often maximizes the computed rack displacements as well as the equivalent elastostatic stresses.

In short, there are a large number of parameters with potential influence on the rack kinematics. The comprehensive structural evaluation must deal with all of these without sacrificing conservatism.

The three-dimensional single rack dynamic model introduced by Holtec International in the Enrico Fermi Unit 2 rack project (ca. 1980) and used in some 50 rerack projects since that time (Table 6.2.1) addresses most of the above mentioned array of parameters. The details of this methodology are also published in the permanent literature [6.2.1]. Despite the versatility of the 3-D seismic model, the accuracy of the single rack simulations has been suspect due to one key element; namely, hydrodynamic participation of water around the racks. During dynamic rack motion, hydraulic energy is either drawn from or added to the moving rack, modifying its submerged motion in a significant manner. Therefore, the dynamics of one rack affects the motion of all others in the pool.

A dynamic simulation, which treats only one rack, or a small grouping of racks, is intrinsically inadequate to predict the motion of rack modules with any quantifiable level of accuracy. Three-dimensional Whole Pool Multi-Rack analyses carried out on several previous plants demonstrate that single rack simulations may under predict rack displacement during seismic responses [6.2.2].

Briefly, the 3-D rack model dynamic simulation, involving one or more spent fuel racks, handles the array of variables as follows:

Interface Coefficient of Friction: Parametric runs are made with upper bound and lower bound values of the coefficient of friction. The limiting values are based on experimental data which has been found to be bounded by the values 0.2 and 0.8. Simulations are also performed with the array of pedestals having randomly chosen coefficients of friction in a Gaussian distribution with a mean of 0.5 and lower and upper limits of 0.2 and 0.8, respectively. In the fuel rack simulations, the Coulomb friction interface between rack support pedestal and liner is simulated by piecewise linear (friction) elements. These elements function only when the pedestal is physically in contact with the pool liner or bearing pad.

Rack Beam Behavior: Rack elasticity, relative to the rack base, is included in the model by introducing linear springs to represent the elastic bending action, twisting, and extensions.

Impact Phenomena: Compression-only gap elements are used to provide for opening and closing of interfaces such as the pedestal-to-bearing pad interface, and the fuel assembly-to-cell wall interface. These interface gaps are modeled using nonlinear spring elements. The term "nonlinear spring" is a generic term used to denote the mathematical representation of the condition where a restoring force is not linearly proportional to displacement.

Fuel Loading Scenarios: The fuel assemblies are conservatively assumed to rattle in unison which exaggerates the contribution of impact against the cell wall.

Fluid Coupling: Holtec International extended Fritz's classical two-body fluid coupling model to multiple bodies and utilized it to perform the first two-dimensional multi-rack analysis (Diablo Canyon, ca. 1987). Subsequently, laboratory experiments were conducted to validate the multi-rack fluid coupling theory. This technology was incorporated in the computer code DYNARACK [6.2.4] which handles simultaneous simulation of all racks in the pool as a Whole Pool Multi-Rack 3-D analysis. This development was first utilized in Chinshan, Oyster Creek, and Shearon Harris plants [6.2.1, 6.2.3] and, subsequently, in numerous other rerack projects. The WPMR analyses have corroborated the accuracy of the single rack 3-D solutions in predicting the maximum structural stresses, and also serve to improve predictions of rack kinematics.

For closely spaced racks, demonstration of kinematic compliance is verified by including all modules in one comprehensive simulation using a WPMR model. Additional more conservative single rack analyses are performed to confirm kinematic stability under the most adverse conditions such as fuel loading eccentricities and interim reracking configurations. In WPMR analysis, all rack modules are modeled simultaneously and the coupling effect due to this multi-body motion is included in the analysis. Due to the superiority of this technique in predicting the dynamic behavior of closely spaced submerged storage racks, the Whole Pool Multi-Rack analysis methodology is used for this project.

6.3 DESCRIPTION OF RACKS

The storage racks are analyzed as follows:

RACK WEIGHT DATA

Rack #	Array Size	# of Cells	# of Poison Inserts	Dry Weight of Rack wt% Poison Inserts (lb)	Total Weight of Rack plus Poison Inserts[††] (lb)
1	11 x 11	121	0	17,650	17,650
2	11 x 11	121	0	17,650	17,650
3	11 x 12	132	241	19,150	43,250
4	10 x 11	110	0	27,650[†]	27,650
5	11 x 11	121	0	17,650	17,650
6	11 x 11	121	0	17,650	17,650
7	11 x 12	132	241	19,150	43,250
8	10 x 11	110	0	27,650[†]	27,650

[†] Contains Boraflex.

[††] Poison inserts are conservatively assumed to weigh 100 lb each. The actual weight of a poison insert plus a lead-in device is approximately 43 lb total.

For the purpose of modeling, the racks are numbered 1 through 8 as shown in Figure 6.1.1.

The Cartesian coordinate system utilized within the rack dynamic model has the following nomenclature:

x = Horizontal axis along plant South
y = Horizontal axis along plant East
z = Vertical axis upward from the rack base

6.4 SYNTHETIC TIME-HISTORIES

The synthetic time-histories in three orthogonal directions (N-S, E-W, and vertical) are generated in accordance with the provisions of SRP [6.1.2], Section 3.7.1. In order to prepare an acceptable set of acceleration time-histories, Holtec International's proprietary code GENEQ [6.4.1] is utilized.

A preferred criterion for the synthetic time-histories in SRP 3.7.1 calls for both the response spectrum and the power spectral density corresponding to the generated acceleration time-history to envelope their target (design basis) counterparts with only finite enveloping infractions. The time-histories for the pools have been generated to satisfy this preferred criterion. The seismic files also satisfy the requirements of statistical independence mandated by SRP 3.7.1.

Figures 6.4.1 through 6.4.3 provide plots of the time-history accelerograms which were generated over a 20 second duration for the DBE event. Figures 6.4.4 through 6.4.6 provide plots of the time-history accelerograms which were generated over a 20 second duration for the OBE event. These artificial time-histories are used in all non-linear dynamic simulations of the racks.

Results of the correlation function of the three time-histories are given in Table 6.4.1. Absolute values of the correlation coefficients are shown to be less than 0.15, indicating that the desired statistical independence of the three data sets has been met.

6 5 WPMR METHODOLOGY

Recognizing that the analytical work effort must deal with both stress and displacement criteria, the sequence of model development and analysis steps that are undertaken are summarized in the following·

a Prepare 3-D dynamic models suitable for a time-history analysis of the maximum density racks. These models include the assemblage of all rack modules in each pool. Include all fluid coupling interactions and mechanical coupling appropriate to performing an accurate non-linear simulation. This 3-D simulation is referred to as a Whole Pool Multi-Rack model.

b. Perform 3-D dynamic analyses on various physical conditions (such as coefficient of friction and extent of cells containing fuel assemblies). Archive appropriate displacement and load outputs from the dynamic model for post-processing.

c. Perform stress analysis of high stress areas for the limiting case of all the rack dynamic analyses. Demonstrate compliance with ANO Specification No. AP&L-C-502 [6.1.3] and ANO Unit 1 SAR [6.1.4] limits on stress and displacement.

6.5.1 Model Details for Spent Fuel Racks

The dynamic modeling of the rack structure is prepared with special consideration of all nonlinearities and parametric variations. Particulars of modeling details and assumptions for the Whole Pool Multi-Rack analysis of racks are given in the following:

6.5.1.1 Assumptions

a. The fuel rack structure motion is captured by modeling the rack as a 12 degree-of-freedom structure. Movement of the rack cross-section at any height is described by six degrees-of-freedom of the rack base and six degrees-of-freedom at the rack top. In this manner, the response of the module, relative to the base-plate, is captured in the dynamic analyses once suitable springs are introduced to couple the rack degrees-of-freedom and simulate rack stiffness.

b. Rattling fuel assemblies within the rack are modeled by five lumped masses located at H, .75H, .5H, .25H, and at the rack base (H is the rack height measured above the base-plate). Each lumped fuel mass has two horizontal displacement degrees-of-freedom. Vertical motion of the fuel assembly mass is assumed equal to rack vertical motion at the base-plate level. The centroid of each fuel assembly mass can be located off-center, relative to the rack structure centroid at that level, to simulate a partially loaded rack.

c. Seismic motion of a fuel rack is characterized by random rattling of fuel assemblies in their individual storage locations. All fuel assemblies are assumed to move in-phase within a rack. This exaggerates computed dynamic loading on the rack structure and, therefore, yields conservative results.

d. Fluid coupling between the rack and fuel assemblies, and between the rack and wall, is simulated by appropriate inertial coupling in the system kinetic energy. Inclusion of these effects uses the methods of [6.5.2, 6.5.3] for rack/assembly coupling and for rack-to-rack coupling.

e. Sloshing is negligible 20 feet below the surface of the pool, where the racks reside, and it is, therefore, neglected in the analysis of the rack.

f. Potential impacts between the cell walls of the racks and the contained fuel assemblies are accounted for by appropriate compression-only gap elements between masses involved. The possible incidence of rack-to-wall or rack-to-rack impact is simulated by gap elements at the top and bottom of the rack in two horizontal directions. Bottom gap elements are located at the base-plate elevation. The initial gaps reflect the presence of baseplate extensions, and the rack stiffnesses are chosen to simulate local structural detail.

g. Pedestals are modeled by gap elements in the vertical direction and as "rigid links" for transferring horizontal stress. Each pedestal support is linked to the pool liner (or bearing pad) by two friction springs. The spring rate for the friction springs includes any lateral elasticity of the stub pedestals. Local pedestal vertical spring stiffness accounts for floor elasticity and for local rack elasticity just above the pedestal.

h. Rattling of fuel assemblies inside the storage locations causes the gap between fuel assemblies and cell wall to change from a maximum of twice the nominal gap to a theoretical zero gap. Fluid coupling coefficients are based on the nominal gap in order to provide a conservative measure of fluid resistance to gap closure.

i. The model for the rack is considered supported, at the base level, on four pedestals modeled as non-linear compression only gap spring elements and eight piecewise linear friction spring elements. These elements are properly located with respect to the centerline of the rack beam, and allow for arbitrary rocking and sliding motions. In reality each rack has 14 pedestals. This assumption increases the load transmitted to a single pedestal, thereby resulting in higher pedestal stresses.

j. The mass of the poison inserts, which is conservatively assumed as 100 lb per insert, is lumped with the mass of the rack. Although the model does not allow the poison insert to move inside the flux traps, the potential impact force between the poison inserts and the flux trap walls has a negligible effect on the dynamic behavior of the rack. Moreover, the potential impacts involving the poison inserts are bounded by the conservative accounting of the poison insert weight.

6.5.1.2 Element Details

Figure 6.5.1 shows a schematic of the dynamic model of a single rack The schematic depicts many of the characteristics of the model including all of the degrees-of-freedom and some of the spring restraint elements.

Table 6.5.1 provides a complete listing of each of the 22 degrees-of-freedom for a rack model. Six translational and six rotational degrees-of-freedom (three of each type on each end) describe the motion of the rack structure. Rattling fuel mass motions (shown at nodes 1^*, 2^*, 3^*, 4^*, and 5^* in Figure 6.5.1) are described by ten horizontal translational degrees-of-freedom (two at each of the five fuel masses). The vertical fuel mass motion is assumed (and modeled) to be the same as that of the rack baseplate.

Figure 6.5.2 depicts the fuel to rack impact springs (used to develop potential impact loads between the fuel assembly mass and rack cell inner walls) in a schematic isometric. Only one of the five fuel masses is shown in this figure. Four compression only springs, acting in the horizontal direction, are provided at each fuel mass.

Figure 6.5.3 provides a 2-D schematic elevation of the storage rack model, discussed in more detail in Section 6.5.3. This view shows the vertical location of the five storage masses and some of the support pedestal spring members.

Figure 6.5 4 shows the modeling technique and degrees-of-freedom associated with rack elasticity. In each bending plane a shear and bending spring simulate elastic effects [6.5.4]. Linear elastic springs coupling rack vertical and torsional degrees-of-freedom are also included in the model.

Figure 6.5.5 depicts the inter-rack impact springs (used to develop potential impact loads between racks or between rack and wall).

6.5.2 Fluid Coupling Effect

In its simplest form, the so-called "fluid coupling effect" [6.5.2, 6.5.3] can be explained by considering the proximate motion of two bodies under water. If one body (mass m_1) vibrates adjacent to a second body (mass m_2), and both bodies are submerged in frictionless fluid, then Newton's equations of motion for the two bodies are:

$(m_1 + M_{11})\, A_1 + M_{12}\, A_2 =$ applied forces on mass $m_1 + O(X_1^2)$
$M_{21}\, A_1 + (m_2 + M_{22}) A_2 =$ applied forces on mass $m_2 + O(X_2^2)$

A_1 and A_2 denote absolute accelerations of masses m_1 and m_2, respectively, and the notation $O(X^2)$ denotes nonlinear terms.

M_{11}, M_{12}, M_{21}, and M_{22} are fluid coupling coefficients which depend on body shape, relative disposition, etc. Fritz [6.5.3] gives data for M_{ij} for various body shapes and arrangements. The fluid adds mass to the body (M_{11} to mass m_1), and an inertial force proportional to acceleration of the adjacent body (mass m_2). Thus, acceleration of one body affects the force field on another. This force field is a function of inter-body gap, reaching large values for small gaps. Lateral motion of a fuel assembly inside a storage location encounters this effect. For example, fluid coupling behavior will be experienced between nodes 2 and 2* in Figure 6.5.1. The rack analysis also contains inertial fluid coupling terms, which model the effect of fluid in the gaps between adjacent racks

Terms modeling the effects of fluid flowing between adjacent racks in a single rack analysis suffer from the inaccuracies described earlier. These terms are usually computed assuming that all racks adjacent to the rack being analyzed are vibrating in-phase or 180° out of phase. The WPMR analyses do not require any assumptions with regard to phase.

Rack-to-rack gap elements have initial gaps set to 100% of the physical gap between the racks or between outermost racks and the adjacent pool walls

6.5.2.1 Multi-Body Fluid Coupling Phenomena

During the seismic event, all racks in the pool are subject to the input excitation simultaneously. The motion of each free-standing module would be autonomous and independent of others as long as they did not impact each other and no water were present in the pool. While the scenario of inter-rack impact is not a common occurrence and depends on rack spacing, the effect of water (the so-called fluid coupling effect) is a universal factor. As noted in Ref. [6.5.2, 6.5.4], the fluid forces can reach rather large values in closely spaced rack geometries. It is, therefore, essential that the contribution of the fluid forces be included in a comprehensive manner. This is possible only if all racks in the pool are allowed to execute 3-D motion in the mathematical model. For this reason, single rack or even multi-rack models involving only a portion of the racks in the pool, are inherently inaccurate. The Whole Pool Multi-Rack model removes this intrinsic limitation of the rack dynamic models by simulating the 3-D motion of all modules simultaneously. The fluid coupling effect, therefore, encompasses interaction between *every* set of racks in the pool, i.e., the motion of one rack produces fluid forces on all other racks and on the pool walls. Stated more formally, both near-field and far-field fluid coupling effects are included in the analysis.

The derivation of the fluid coupling matrix [6.5.5] relies on the classical inviscid fluid mechanics principles, namely the principle of continuity and Kelvin's recirculation theorem. While the derivation of the fluid coupling matrix is based on no artificial construct, it has been nevertheless verified by an extensive set of shake table experiments [6.5.5].

6.5.3 Stiffness Element Details

Three element types are used in the rack models. Type 1 elements are linear elastic elements used to represent the beam-like behavior of the integrated rack cell matrix. Type 2 elements are the piece-wise linear friction springs used to develop the appropriate forces between the rack pedestals and the supporting bearing pads. Type 3 elements are non-linear gap elements, which model gap closures and subsequent impact loadings i.e , between fuel assemblies and the storage cell inner walls, and rack outer periphery spaces.

If the simulation model is restricted to two dimensions (one horizontal motion plus one vertical motion, for example), for the purposes of model clarification only, then Figure 6.5.3 describes the

configuration. This simpler model is used to elaborate on the various stiffness modeling elements.

Type 3 gap elements modeling impacts between fuel assemblies and racks have local stiffness K_i in Figure 6.5.3. Support pedestal spring rates K_s are modeled by type 3 gap elements. Local compliance of the concrete floor is included in K_s The type 2 friction elements are shown in Figure 6.5.3 as K_f. The spring elements depicted in Figure 6.5.4 represent type 1 elements.

Friction at support/liner interface is modeled by the piecewise linear friction springs with suitably large stiffness K_f up to the limiting lateral load μN, where N is the current compression load at the interface between support and liner. At every time-step during transient analysis, the current value of N (either zero if the pedestal has lifted off the liner, or a compressive finite value) is computed

The gap element K_s, modeling the effective compression stiffness of the structure in the vicinity of the support, includes stiffness of the pedestal, local stiffness of the underlying pool slab, and local stiffness of the rack cellular structure above the pedestal.

The previous discussion is limited to a 2-D model solely for simplicity. Actual analyses incorporate 3-D motions.

6.5.4 Coefficients of Friction

To eliminate the last significant element of uncertainty in rack dynamic analyses, multiple simulations are performed to adjust the friction coefficient ascribed to the support pedestal/pool bearing pad interface. These friction coefficients are chosen consistent with the two bounding extremes from Rabinowicz's data [6.5.1]. Simulations are also performed by imposing friction coefficients developed by a random number generator with Gaussian normal distribution characteristics. The assigned values are then held constant during the entire simulation in order to obtain reproducible results.† Thus, in this manner, the WPMR analysis results are brought closer to the realistic structural conditions.

† It is noted that DYNARACK has the capability to change the coefficient of friction at any pedestal at each instant of contact based on a random reading of the computer clock cycle. However, exercising this option would yield results that could not be reproduced. Therefore, the random choice of coefficients is made only once per run.

The coefficient of friction (μ) between the pedestal supports and the pool floor is indeterminate. According to Rabinowicz [6.5.1], results of 199 tests performed on austenitic stainless steel plates submerged in water show a mean value of μ to be 0.503 with standard deviation of 0.125. Upper and lower bounds (based on twice standard deviation) are 0.753 and 0.253, respectively. Analyses are therefore performed for coefficient of friction values of 0.2 (lower limit) and 0.8 (upper limit), as well as for random friction values clustered about a mean of 0.5. The bounding values of μ = 0.2 and 0.8 have been found to envelope the upper limit of module response in previous rerack projects

6.5.5 Governing Equations of Motion

Using the structural model discussed in the foregoing, equations of motion corresponding to each degree-of-freedom are obtained using Lagrange's Formulation [6.5.4]. The system kinetic energy includes contnbutions from solid structures and from trapped and surrounding fluid. The final system of equations obtained have the matrix form:

$$[M]\left[\frac{d^2 q}{d t^2}\right] = [Q] + [G]$$

where:

[M] - total mass matrix (including structural and fluid mass contributions). The size of this matrix will be 22n x 22n for a WPMR analysis (n = number of racks in the model).

q - the nodal displacement vector relative to the pool slab displacement (the term with q indicates the second derivative with respect to time, i.e., acceleration)

[G] - a vector dependent on the given ground acceleration

[Q] - a vector dependent on the spring forces (linear and nonlinear) and the coupling between degrees-of-freedom

The above column vectors have length 22n. The equations can be rewritten as follows:

$$\left[\frac{d^2q}{dt^2}\right] = [M]^{-1}[Q] + [M]^{-1}[G]$$

This equation set is mass uncoupled, displacement coupled at each instant in time. The numerical solution uses a central difference scheme built into the proprietary computer program DYNARACK [6.2.4]

6.6 STRUCTURAL EVALUATION OF SPENT FUEL RACK DESIGN

6.6.1 Kinematic and Stress Acceptance Criteria

There are two sets of criteria to be satisfied by the rack modules:

a. Kinematic Criteria

According to Section 3.8.5 of Ref. [6.1.1], the minimum required safety margins against overturning under the OBE and DBE events are 1.5 and 1.1, respectively. The maximum rotations of the rack (about the two principal axes) are obtained from a post processing of the rack time history response output. The margin of safety against overturning is given by the ratio of the rotation required to produce incipient tipping in either principal plane to the actual maximum rotation in that plane predicted by the time history solution.

$$\text{Margin of Safety} = \frac{\theta \text{ required for overturning}}{\theta \text{ predicted}}$$

All ratios for the OBE and DBE events should be greater than 1.5 and 1.1, respectively, to satisfy the regulatory acceptance criteria. However, to be conservative, the OBE safety factor of 1.5 will be applied to the worst case displacements from DBE. This is conservative, since the displacement for the DBE simulations exceed those for the OBE simulation.

b. Stress Limit Criteria

Stress limits must not be exceeded under the postulated load combinations provided herein.

6.6.2 Stress Limit Evaluations

The stress limits presented below apply to the rack structure and are derived from the ASME Code, Section III, Article XVII [6.6.1]. Parameters and terminology are in accordance with the ASME Code. Material properties are obtained from the ASME Code Appendices [6.6.2], and are listed in Table 6.3.1. The yield and ultimate strengths are taken at 150 °F, which is the maximum allowable temperature for ANO Spent Fuel Pools. Per the "double contingency principle" [6.6.3], two simultaneous accident events, such as the loss of Spent Fuel Pool cooling together with an earthquake, need not be evaluated. Therefore, 150 °F is an appropriate temperature for the determination of material properties.

(i) Normal & Upset Conditions (Level A & B)

a. Allowable stress in tension on a net section is:

$F_t = 0.6\ S_y$

Where, S_y = yield stress at temperature, and F_t is equivalent to primary membrane stress.

b Allowable stress in shear on a net section is·

$F_v = .4\ S_y$

c. Allowable stress in compression on a net section is:

$$F_a = S_y\left(.47 - \frac{kl}{444\ r}\right)$$

where kl/r for the main rack body is based on the full height and cross section of

the honeycomb region and does not exceed 120 for all sections.

l = unsupported length of component

k = length coefficient which gives influence of boundary conditions. The following values are appropriate for the described end conditions:

1 (simple support both ends)

2 (cantilever beam)

½ (clamped at both ends)

r = radius of gyration of component

d. Maximum allowable bending stress at the outermost fiber of a net section, due to flexure about one plane of symmetry is:

$F_b = 0.60\ S_y$ (equivalent to primary bending)

e. Combined bending and compression on a net section satisfies:

$$\frac{f_a}{F_a} + \frac{C_{mx} f_{bx}}{D_x F_{bx}} + \frac{C_{my} f_{by}}{D_y F_{by}} < 1$$

where:

f_a = Direct compressive stress in the section

f_{bx} = Maximum bending stress along x-axis

f_{by} = Maximum bending stress along y-axis

C_{mx} = 0.85

C_{my} = 0.85

D_x = $1 - (f_a/F'_{ex})$

D_y = $1 - (f_a/F'_{ey})$

$F'_{ex,ey}$ = $(\pi^2 E)/(2.15\ (kl/r)^2_{x,y})$

E = Young's Modulus

and subscripts x,y reflect the particular bending plane.

f. Combined flexure and compression (or tension) on a net section:

$$\frac{f_a}{0.6 S_y} + \frac{f_{bx}}{F_{bx}} + \frac{f_{by}}{F_{by}} < 1.0$$

The above requirements are to be met for both direct tension and compression.

g. Welds

Allowable maximum shear stress on the net section of a weld is given by:

$$F_w = 0.3\ S_u$$

where S_u is the weld material ultimate strength at temperature. For fillet weld legs in contact with base metal, the shear stress on the gross section is limited to $0.4S_y$, where S_y is the base material yield strength at temperature

(ii) Faulted Conditions (Level D)

Per ANO Specification No. AP&L-C-502 [6.1.3], the stress limits for DBE conditions are the stress limits for Level A and B, as defined above, multiplied by 1.5.

Exceptions to the above general multiplier are the following:

a) Stresses in shear shall not exceed $0.5S_y$.

b) The maximum allowable stress in bending and tension is $0.9\ S_y$.

c) For this licensing application, AISC N-690 is conservatively used for welds and the limit on weld shear stress is set as:

Weld Allowable = $(0.3 \times S_u) \times 1.4$

6.6.3 Dimensionless Stress Factors

For convenience, the stress results are in dimensionless form. Dimensionless stress factors are defined as the ratio of the actual developed stress to the specified limiting stress value. Based on the stress limits of ASME Code Article XVII for Level A and Level D conditions, the limiting value of each stress factor is 1.0. For this evaluation, however, the stress limits defined in ANO Specification No. AP&L-C-502 [6.1.3] for Level D conditions are more restrictive than the ASME Code. As a result, the limiting values for the stress factors are less than 1.0 under DBE conditions. The following table provides the list of dimensionless stress factors along with the limiting values for OBE and DBE.

Dimensionless Stress Factors	Limiting Value	
	OBE	DBE
R_1 = Ratio of direct tensile or compressive stress on a net section to its allowable value (note pedestals only resist compression)	1.0	0.75
R_2 = Ratio of gross shear on a net section in the x-direction to its allowable value	1.0	0.694
R_3 = Ratio of maximum bending stress due to bending about the x-axis to its allowable value for the section	1.0	0.75
R_4 = Ratio of maximum bending stress due to bending about the y-axis to its allowable value for the section	1.0	0.75
R_5 = Combined flexure and compression factor (as defined in Section 3.4.1.5 above)	1.0	0.75
R_6 = Combined flexure and tension (or compression) factor (as defined in Section 3.4.1.6 above)	1.0	0.75
R_7 = Ratio of gross shear on a net section in the y-direction to its allowable value	1.0	0.694

6.6.4 Loads and Loading Combinations for Spent Fuel Racks

The applicable loads and their combinations, which are considered in the seismic analysis of rack modules, are excerpted from the OT Position [6.1.2], ANO Specification No. AP&L-C-502 [6.1.3], the Unit 1 SAR, and Section 3.8.4 of the USNRC Standard Review Plan (SRP) [6.1.1]. The SRP load combinations are not required to be met by ANO. However, for thoroughness the load equations outlined in SRP 3.8.4 are used. The load combinations considered are identified below:

Loading Combination	Service Level†	Section Reference
$D + L$ $D + L + T_o$ $D + L + T_o + E$	Level A	6.11 6.11, 6.13.2 6.8, 6.9, 6.13.2
$D + L + T_a + E$ $D + L + T_o + P_f$	Level B	6.13.2 6 14
$D + L + T_a + E'$	Level D	6.8, 6.9
$D + L + T_o + F_d$	The functional capability of the fuel racks must be demonstrated.	7.0

† The allowable stress limits for Service Levels A, B, and D are given in Section 6 6.2.

Where:

- D = Dead weight-induced loads
- L = Live Load (including stored fuel assemblies, poison inserts, and miscellaneous equipment loads)
- P_f = Upward force on the racks caused by postulated stuck fuel assembly
- F_d = Impact force from accidental drop of the heaviest load from the maximum possible height.
- E = Operating Basis Earthquake (OBE)
- E' = Design Basis Earthquake (DBE)
- T_o = Differential temperature induced loads (normal operating or shutdown condition based on the most critical transient or steady state condition)
- T_a = Differential temperature induced loads (the highest temperature associated with the postulated abnormal design conditions) T_a and T_o produce local thermal stresses. The worst thermal stress field in a fuel

rack is obtained when an isolated storage location has a fuel assembly generating heat at maximum postulated rate and surrounding storage locations contain no fuel. Heated water makes unobstructed contact with the inside of the storage walls, thereby producing maximum possible temperature difference between adjacent cells. Secondary stresses produced are limited to the body of the rack; that is, support pedestals do not experience secondary (thermal) stresses.

6.7 PARAMETRIC SIMULATIONS

The multiple rack models employ the fluid coupling effects for all racks in the pool, as discussed above, and these simulations are referred to as WPMR evaluations. In addition, single rack models are also developed for additional study of the effect of various parameters on rack displacement. The models are described as follows:

(I) Whole Pool Multi Rack Model

An array of eight racks is modeled with proper interface fluid gaps and a coefficient of friction at the support interface locations with the bearing pad generated by a Gaussian distribution random number generator with 0.5 as the mean and 0.15 standard deviation. The response to both DBE and OBE seismic excitation is determined.

(II) Single Rack Model

A single rack model is employed to study the effect of top loading the rack with miscellaneous equipment, which represents a future storage possibility. Rack number 3 is chosen for this simulation because it is one of only two racks in the pool, both of identical size, that have poison inserts. The top loaded rack simulation (Case 7) is performed using the 0.8 coefficient of friction and the DBE event since this combination generally produces the largest rack top displacements. A fictitious 2,000 lbf mass, with three translational degrees of freedom, is rigidly attached to the rack 24" above the top of the cell structure. The displacements calculated from the single rack run are used as a further check for kinematic stability.

The Whole Pool and Single Rack simulations listed in the following table have been performed to

investigate the structural integrity of the rack array, including the new poison inserts.

LIST OF WPMR AND SINGLE RACK SIMULATIONS				
Case	Model	Load Case	COF	Event
1	WPMR	All racks fully loaded	Random	OBE
2	WPMR	All racks fully loaded	0.2	OBE
3	WPMR	All racks fully loaded	0.8	OBE
4	WPMR	All racks fully loaded	Random	DBE
5	WPMR	All racks fully loaded	0.2	DBE
6	WPMR	All racks fully loaded	0.8	DBE
7	Single	Fully loaded rack w/ 2,000 lb load overhead	0.8	DBE

where Random = Gaussian distribution with a mean coeff. of friction of 0.5.
(upper and lower limits of 0.8 and 0.2, respectively)
COF = Coefficient of Friction

6.8 TIME HISTORY SIMULATION RESULTS

The results from the DYNARACK runs may be seen in the raw data output files. However, due to the huge quantity of output data, a post-processor is used to scan for worst case conditions and develop the stress factors discussed in subsection 6.6.3. Further reduction in this bulk of information is provided in this section by extracting the worst case values from the parameters of interest; namely displacements, support pedestal forces, impact loads, and stress factors. This section also summarizes additional analyses performed to develop and evaluate structural member stresses which are not determined by the post processor.

6.8.1 Rack Displacements

The maximum rack displacements are obtained from the time histories of the motion of the upper and lower four corners of each rack in each of the simulations. The maximum absolute value of displacement in the two horizontal directions, relative to the pool slab, is determined by the post-

processor for each rack, at the top and bottom corners. The maximum displacements in either direction reported from the WPMR analyses are 0.726" at the top of Rack 4 during the DBE events and 0.384" at the top of Rack 4 during the OBE events. The maximum displacement in either direction reported from the single rack analysis is 0.236", which was performed for Rack 3. It is obvious from these small displacements at the top of the racks that the safety factors for tipping are met.

6.8.2 Pedestal Vertical Forces

The maximum vertical pedestal force obtained in the WPMR simulations is 203,000 lbf for Rack 4 under DBE conditions. The maximum vertical pedestal force obtained in the OBE simulation is 138,000 lbf for Rack 8.

6.8.3 Pedestal Friction Forces

The maximum interface shear force value in any direction bounding all pedestals in the WPMR simulations is 89,700 lbf for Rack 3 in Case 6.

6.8.4 Rack Impact Loads

A freestanding rack, by definition, is a structure subject to potential impacts during a seismic event. Impacts arise from rattling of the fuel assemblies in the storage rack locations and, in some instances, from localized impacts between the racks, or between a peripheral rack and the pool wall. The following sections discuss the bounding values of these impact loads.

6.8 4.1 Rack to Rack Impacts

Gap elements track the potential for impacts between adjacent racks. The results for each simulation have been scanned for non-zero impact forces. The simulation results show that no gap element between any two racks closes. Thus, there are no rack-to-rack impacts

6.8.4.2 Rack to Wall Impacts

The storage racks do not impact the pool walls under any simulation.

6.8.4.3 Fuel to Cell Wall Impact Loads

A review of all simulations performed allows determination of the maximum instantaneous impact load between fuel assembly and fuel cell wall at any modeled impact site. The maximum fuel/cell wall impact loads are 1263 lbf in Rack 4 in the DBE case of the WPMR analyses and 853 lbf for the OBE case in Rack 4. The cell wall integrity under this instantaneous impact load has been evaluated and shown to remain intact with no permanent damage.

The permissible lateral load on an irradiated spent fuel assembly has been studied by the Lawrence Livermore National Laboratory. The LLNL report [6.8.1] states that "...for the most vulnerable fuel assembly, axial buckling varies from 82g's at initial storage to 95g's after 20 years' storage. In a side drop, no yielding is expected below 63g's at initial storage to 74g's after 20 years' [dry] storage." The most significant load on the fuel assembly arises from rattling during the seismic event. For the five lumped mass model, the limiting lateral load, therefore, is equal to F_e, where

$$F_e = (w \times a)/4$$

where:

w = weight of one fuel assembly (upper bound value = 1700 lbs)

a = permissible lateral acceleration in g's (a = 63)

Therefore, F_e = 26,775 lbs

The maximum fuel-to-storage cell rattling force from the WPMR runs is 1263 lbs. Therefore, the nominal factor of safety against fuel failure is roughly equal to 21.

6.9 RACK STRUCTURAL EVALUATION

6.9.1 Rack Stress Factors

The time history results from the DYNARACK solver provide the pedestal normal and lateral interface forces, which may be converted to the limiting bending moment and shear force at the bottom baseplate-pedestal interface. In particular, maximum values for the previously defined stress factors are determined for every pedestal in the array of racks. With this information available, the structural integrity of the pedestal can be assessed and reported. The net section maximum (in time) bending moments and shear forces can also be determined at the bottom baseplate-rack cellular structure interface for each spent fuel rack in the pool. Using these forces and moments, the maximum stress in the limiting rack cell (box) can be evaluated.

The stress factor results for male and female pedestals, and for the entire spent fuel rack cellular cross section just above the baseplate have been determined. These factors are reported for every rack in each simulation, and for each pedestal in every rack. These locations are the most heavily loaded net sections in the structure so that satisfaction of the stress factor criteria at these locations ensures that the overall structural criteria set forth in Section 6.6 are met.

The maximum pedestal stress factor for OBE is 0.221, which occurs in Rack 7 during Case 3, and for DBE is 0.216, which occurs in Rack 4 during Case 6. The maximum cell wall stress factor is computed to be 0.344 for OBE in Rack 7 during Case 3 and 0.245 for DBE in Rack 2 during Case 6. An evaluation of the stress factors, for all of the simulations performed, leads to the conclusion that all stress factors are less than the limits specified in Section 6.6.3. Therefore, the requirements of Section 6.6.2 are indeed satisfied for the load levels considered for every limiting location in the rack.

6.9.2 Pedestal Thread Shear Stress

From the WPMR simulations, the maximum thread engagement stresses under seismic conditions for every pedestal for every rack in the pool are 12,843 psi under DBE conditions and 8,730 psi under OBE conditions. The yield stress for the pedestal material is 27,500 psi. The allowable shear stress for Level B conditions is 0.4 times the yield stress, which gives 11,000 psi. Since 8,730 psi (occurs during OBE run) is less than the OBE allowable of 11,000 psi, the

female pedestal threads are shown to be acceptable. The maximum shear stress in the pedestal thread under DBE condition is 12,843 psi, which is less than $0.5S_y$ (or 13,750 psi).

6.9.3 Local Stresses Due to Impacts

Impact loads at the pedestal base (discussed in subsection 6.8.4.1) produce stresses in the pedestal for which explicit stress limits are prescribed in the Code. However, impact loads on the cellular region of the racks, as discussed in subsection 6.8.4.3 above, produce stresses which attenuate rapidly away from the loaded region. This behavior is characteristic of secondary stresses.

Even though limits on secondary stresses are not prescribed in the Code for class 3 NF structures, evaluations are made to ensure that the localized impacts do not lead to plastic deformations in the storage cells which affect the sub-criticality of the stored fuel array.

a. Impact Loading Between Fuel Assembly and Cell Wall

Local cell wall integrity is conservatively estimated from peak impact loads. Plastic analysis is used to obtain the limiting impact load which would lead to gross permanent deformation The limiting impact load of 2,436 lbf (including a safety factor of 2.0) is much greater than the highest calculated impact load value of 1263 lbf (see subsection 6.8.4.3) obtained from any of the rack analyses. Therefore, fuel impacts do not represent a significant concern with respect to fuel rack cell deformation.

b. Impacts Between Adjacent Racks

As may be seen from subsection 6.8.4.1, no impacts are predicted between adjacent racks.

6.9.4 Weld Stresses

Weld locations subjected to significant seismic loading are at the bottom of the rack at the baseplate-to-cell connection, at the top of the pedestal support at the baseplate connection, and at cell-to-cell connections. Bounding values of resultant loads are used to qualify the connections.

a. Baseplate-to-Rack Cell Welds

For Level A or B conditions, Ref. [6.6.1] permits an allowable weld stress of $\tau = .3\ S_u$ = 21900 psi. As stated in subsection 6.6.2, the allowable may be increased for Level D by an amplification factor which is equal to 1.4.

Weld dimensionless stress factors are produced through the use of a simple conversion (ratio) factor applied to the corresponding stress factor in the adjacent rack material. The ratio 0.819 is developed from the differences in material thickness and length versus weld throat dimension and length:

RATIO = (Cell wall thickness * Avg. Cell Wall Length)/(Effective Weld Size * Weld Length)
= (0.062 * 8.97) / (0.12 * 0.7071 * 8.0)

The highest predicted cell to baseplate weld stress is calculated based on the highest R6 value for the rack cell region tension stress factor and R2 and R7 values for the rack cell region shear stress factors. Refer to subsection 6.6.3 for definition of these factors. These cell wall stress factors may be converted into weld stress values as follows:

$[R6 * (1.2) + R2 * (0.72) + R7 * (0.72)] * S_y * \text{Ratio} =$
$[0.245 * (1.2) + 0.027 * (0.72) + 0.029 * (0.72)] * 27{,}500 * 0.819 = 7{,}530$ psi

This calculation is conservative for the following reasons:

1) The directional stresses associated with the normal stress τ_y and the two shear stresses τ_x and τ_y should be combined using SRSS instead of direct summation.

2) The maximum stress factors used above do not all occur at the same time instant, in the same storage rack, or during the same simulation.

The DBE condition governs since the ratio of the DBE weld stress to the OBE weld stress

is greater than 1.4 (see paragraph 6.6.2(ii)(c)). The maximum weld stress is less than the DBE allowable for base metal shear stress, which is 13,750 psi. Therefore, the welds are acceptable, with a safety factor of (13,750/7,530) = 1.83

b. Baseplate-to-Pedestal Welds

The weld between baseplate and support pedestal is checked using finite element analysis to determine the maximum weld stresses. The maximum weld stresses under OBE and DBE conditions are 12,150 and 26,920 psi, respectively. These calculated stress values are below the corresponding OBE and DBE weld allowables of 21,900 psi and 30,660 psi, respectively. Therefore, these welds have been determined to be acceptable

The maximum shear stresses in the metal adjacent to the weld are 1,736 psi and 856 psi, respectively, under DBE and OBE conditions. Both of these calculated stress values are well below OBE metal allowable of 11,000 psi.

c Cell-to-Cell Welds

Cell-to-cell connections are by a series of connecting welds along the cell height. Stresses in storage cell to cell welds develop due to fuel assembly impacts with the cell wall. These weld stresses are conservatively calculated by assuming that fuel assemblies in adjacent cells are moving out of phase with one another so that impact loads in two adjacent cells are in opposite directions; this tends to separate the two cells from each other at the weld.

Table 6.9.1 gives the computed results for the maximum allowable load that can be transferred by these welds based on the available weld area. The upper bound on the applied load transferred is also given in Table 6.9.1. This upper bound value is very conservatively obtained by applying the bounding rack-to-fuel impact load from any simulation in two orthogonal directions simultaneously, and multiplying the result by 2 to account for the simultaneous impact of two assemblies in adjacent cells moving in opposing directions. An equilibrium analysis at the connection then yields the upper bound load to be transferred. As shown in Table 6.9.1, the calculated shear stress in the base metal adjacent to the weld is 7,363 psi under DBE condition and 4,997 psi under

OBE conditions. These values are less than the allowable OBE and DBE stress limits of 11,000 psi and 13,750 psi, respectively.

6.10 POISON INSERT STRUCTURAL EVALUATION

A structural evaluation will be performed to demonstrate that the stresses in the poison insert, under normal and accident conditions, meet the appropriate stress limits from ANO Specification No. AP&L-C-502 [6.1.3] and the ANO Unit 1 SAR [6.1.3]. The design details of the poison insert are provided in Section 2.5. The minimum calculated safety factor for the poison insert for all loading conditions will be greater than 1 0.

6.11 LEVEL A EVALUATION

The stress allowables are the same for Level A and Level B conditions. The Upset (OBE) condition controls over normal (Gravity) condition. Therefore, no further evaluation is required for these load cases.

6.12 HYDRODYNAMIC LOADS ON POOL WALLS

The hydrodynamic pressures that develop between adjacent racks and the pool walls can be developed from the archived results produced by the WPMR analysis. Of the racks next to the SFP walls, the one that resulted in the maximum displacement generates the maximum hydrodynamic load on its adjacent wall. The maximum hydrodynamic pressure is considered as an individual load in the structure qualification of the spent fuel pool. The pressure plots on the four walls of the SFP at the time of maximum (in absolute value) instantaneous hydrodynamic pressure for the OBE and DBE events are shown in Figure 6.11.1.

6.13 LOCAL STRESS CONSIDERATIONS

This section presents the results of evaluations for the possibility of cell wall buckling and the secondary stresses produced by temperature effects.

6.13.1 Cell Wall Buckling

The allowable local buckling stresses in the fuel cell walls are obtained by using classical plate buckling analysis. The evaluation for cell wall buckling is based on the applied stress being uniform along the entire length of the cell wall In the actual fuel rack, the compressive stress comes from consideration of overall bending of the rack structures during a seismic event, and as such is negligible at the rack top, and maximum at the rack bottom.

The critical buckling stress is determined to be 4,663 psi. The average compressive stress in the cell wall, based on the R6 stress factor, is 2,838 psi. Therefore, there is a 64.3% margin of safety against local cell wall buckling.

6.13.2 Thermal Loads

The rack is freestanding; thus, there is minimal or no restraint against free thermal expansion of the rack. The high thermal conductivity of the stainless steel material, the buoyancy driven flow of the SFP water, and the thin sheet metal construction tend to diminish the thermal gradients in the spent fuel racks. Thermal loads applied to the rack are, therefore, not included in the stress combinations.

6.14 EVALUATION OF POSTULATED STUCK FUEL ASSEMBLY

The ability of the spent fuel racks to withstand the uplift forces due to a postulated stuck fuel assembly is also evaluated. Strength of materials formulas are used to determine the effects of a 5,000 lb force, which bounds the fuel handling crane's cut-off limit, applied at various locations on the storage cell. For a load applied vertically anywhere along a cell wall, the tensile stress is 8,991 psi, which is below the yield stress of the material. When the load is applied at a 45 degree angle to the top of a cell wall, the damaged region extends downward, from the top of the rack, no more than 2.59 inches, which is well short of the poison insert.

6.15 CONCLUSION

Seven discrete freestanding dynamic simulations of maximum density spent fuel storage racks have been performed to establish the structural margins of safety. Of the seven parametric

analyses, six simulations consisted of modeling all 8 fuel racks in the pool in one comprehensive Whole Pool Multi Rack (WPMR) model The remaining run was carried out with the classical single rack 3-D model. The parameters varied in the different runs consisted of the rack/pool liner interface coefficient of friction and the type of seismic input (DBE or OBE). Maximum (maximum in time and space) values of pedestal vertical, shear forces, displacements and stress factors have been post-processed from the array of runs and summarized in tables in this chapter. The results show that:

(i) All stresses are well below the specified allowable limits.

(ii) There is no rack-to-rack or rack-to-wall impact anywhere in the cellular region of the rack modules

(iii) The factor of safety against overturning of a rack is in excess of 60.

In conclusion, all evaluations of structural safety, mandated by the OT Position Paper [6.1.2] and the contemporary fuel rack structural analysis practice have been carried out. They demonstrate consistently large margins of safety in all storage modules

6.16 REFERENCES

[6.1.1] USNRC NUREG-0800, Standard Review Plan, June 1987.

[6.1.2] (USNRC Office of Technology) "OT Position for Review and Acceptance of Spent Fuel Storage and Handling Applications", dated April 14, 1978, and January 18, 1979 amendment thereto.

[6.1.3] Technical Specification for Earthquake Resistance Design of Structures and/or Components Located in the Auxiliary Building for the Arkansas Nuclear One Unit 1 Power Plant, Arkansas Power and Light Company, Little Rock, Arkansas, Specification Number AP&L-C-502, Revision 2.

[6 1.4] Arkansas Nuclear One Unit 1 Safety Analysis Report (SAR).

[6.2.1] Soler, A. I. and Singh, K. P., "Seismic Responses of Free Standing Fuel Rack Constructions to 3-D Motions", Nuclear Engineering and Design, Vol. 80, pp. 315-329 (1984).

[6.2.2] Soler, A. I. and Singh, K. P., "Some Results from Simultaneous Seismic Simulations of All Racks in a Fuel Pool", INNM Spent Fuel Management Seminar X, January, 1993.

[6.2.3] Singh, K. P. and Soler, A. I., "Seismic Qualification of Free Standing Nuclear Fuel Storage Racks - the Chin Shan Experience, Nuclear Engineering International, UK (March 1991).

[6.2.4] Holtec Proprietary Report HI-961465 - WPMR Analysis User Manual for Pre & Post Processors & Solver, August, 1997.

[6.4.1] Holtec Proprietary Report HI-89364 - Verification and User's Manual for Computer Code GENEQ, January, 1990.

[6.5.1] Rabinowicz, E., "Friction Coefficients of Water Lubricated Stainless Steels for a Spent Fuel Rack Facility," MIT, a report for Boston Edison Company, 1976.

[6.5 2] Singh, K P. and Soler, A. I., "Dynamic Coupling in a Closely Spaced Two-Body System Vibrating in Liquid Medium· The Case of Fuel Racks," 3rd International Conference on Nuclear Power Safety, Keswick, England, May 1982.

[6.5.3] Fritz, R. J., "The Effects of Liquids on the Dynamic Motions of Immersed Solids," Journal of Engineering for Industry, Trans. of the ASME, February 1972, pp 167-172.

[6.5.4] Levy, S. and Wilkinson, J. P. D., "The Component Element Method in Dynamics with Application to Earthquake and Vehicle Engineering," McGraw Hill, 1976.

[6.5.5] Paul, B., "Fluid Coupling in Fuel Racks: Correlation of Theory and Experiment", (Proprietary), NUSCO/Holtec Report HI-88243

[6.6.1] ASME Boiler & Pressure Vessel Code, Section III, Article XVII, 1980 Edition with Winter 1981 Addenda.

[6.6.2] ASME Boiler & Pressure Vessel Code, Section III, Appendix I, Table I-3, 1980 Edition with Winter 1981 Addenda.

[6.6.3] Kopp, L., "Guidance on the Regulatory Requirements for Criticality Analysis of Fuel Storage at Light Water Reactor Power Plants," USNRC Internal Memorandum, 1998.

[6.8.1] Chun, R., Witte, M. and Schwartz, M., "Dynamic Impact Effects on Spent Fuel Assemblies," UCID-21246, Lawrence Livermore National Laboratory, October 1987.

[6.9.1] ACI 349-85, Code Requirements for Nuclear Safety Related Concrete Structures, American Concrete Institute, Detroit, Michigan, 1985.

[6.9.2] ACI 318-95, Building Code requirements for Structural Concrete," American Concrete Institute, Detroit, Michigan, 1995.

[6.9.3] Holtec report HI-89330, Rev. 1, "Seismic Analysis of High Density Fuel Racks; Part III: Structural Design Calculations - Theory."

[6.10.1] ASME Boiler & Pressure Vessel Code, Section III, Subsection NF, 1998 Edition.

Table 6.2.1

Partial Listing of Fuel Rack Applications Using Dynarack

PLANT	DOCKET NUMBER(s)	YEAR
Enrico Fermi Unit 2	USNRC 50-341	1980
Quad Cities 1 & 2	USNRC 50-254, 50-265	1981
Rancho Seco	USNRC 50-312	1982
Grand Gulf Unit 1	USNRC 50-416	1984
Oyster Creek	USNRC 50-219	1984
Pilgrim	USNRC 50-293	1985
V.C. Summer	USNRC 50-395	1984
Diablo Canyon Units 1 & 2	USNRC 50-275, 50-323	1986
Byron Units 1 & 2	USNRC 50-454, 50-455	1987
Braidwood Units 1 & 2	USNRC 50-456, 50-457	1987
Vogtle Unit 2	USNRC 50-425	1988
St. Lucie Unit 1	USNRC 50-335	1987
Millstone Point Unit 1	USNRC 50-245	1989
Chinshan	Taiwan Power	1988
D.C Cook Units 1 & 2	USNRC 50-315, 50-316	1992
Indian Point Unit 2	USNRC 50-247	1990
Three Mile Island Unit 1	USNRC 50-289	1991
James A FitzPatrick	USNRC 50-333	1990
Shearon Harris Unit 2	USNRC 50-401	1991
Hope Creek	USNRC 50-354	1990
Kuosheng Units 1 & 2	Taiwan Power Company	1990
Ulchin Unit 2	Korea Electric Power Co.	1990
Laguna Verde Units 1 & 2	Comision Federal de Electricidad	1991

Table 6.2.1

Partial Listing of Fuel Rack Applications Using Dynarack

PLANT	DOCKET NUMBER(s)	YEAR
Zion Station Units 1 & 2	USNRC 50-295, 50-304	1992
Sequoyah	USNRC 50-327, 50-328	1992
LaSalle Unit 1	USNRC 50-373	1992
Duane Arnold Energy Center	USNRC 50-331	1992
Fort Calhoun	USNRC 50-285	1992
Nine Mile Point Unit 1	USNRC 50-220	1993
Beaver Valley Unit 1	USNRC 50-334	1992
Salem Units 1 & 2	USNRC 50-272, 50-311	1993
Limerick	USNRC 50-352, 50-353	1994
Ulchin Unit 1	KINS	1995
Yonggwang Units 1 & 2	KINS	1996
Kori-4	KINS	1996
Connecticut Yankee	USNRC 50-213	1996
Angra Unit 1	Brazil	1996
Sizewell B	United Kingdom	1996
Waterford 3	USNRC 50-382	1997
J.A. Fitzpatrick	USNRC 50-333	1998
Callaway	USNRC 50-483	1998
Nine Mile Unit 1	USNRC 50-220	1998
Chin Shan	Taiwan Power Company	1998
Vermont Yankee	USNRC 50-271	1998
Millstone 3	USNRC 50-423	1998
Byron/Braidwood	USNRC 50-454, 50-455, 50-567, 50-457	1999

Table 6.2.1

Partial Listing of Fuel Rack Applications Using Dynarack

PLANT	DOCKET NUMBER(s)	YEAR
Wolf Creek	USNRC 50-482	1999
Plant Hatch Units 1 & 2	USNRC 50-321, 50-366	1999
Harris Pools C and D	USNRC 50-401	1999
Davis-Besse	USNRC 50-346	1999
Enrico Fermi Unit 2	USNRC 50-341	2000
Kewaunee	USNRC 50-305	2001

Table 6.3.1 Rack Material Data (150 °F) (ASME - Section II, Part D)			
Stainless Steel Material	Young's Modulus E (psi)	Yield Strength S_y (psi)	Ultimate Strength S_u (psi)
SA240, Type 304 (cell boxes)	27.9×10^6	27,500	73,000
Support Material Data (150 °F)			
SA240, Type 304 (upper part of support feet)	27.9×10^6	27,500	73,000
SA479, Type 304 (lower part of support feet)	27.9×10^6	27,500	73,000

Table 6.4.1 Time-History Statistical Correlation Results	
OBE	
Data1 to Data2	0.025
Data1 to Data3	0.100
Data2 to Data3	0.032
DBE	
Data1 to Data2	0.020
Data1 to Data3	0.103
Data2 to Data3	0.034

Data1 corresponds to the time-history acceleration values along the X axis (South)

Data2 corresponds to the time-history acceleration values along the Y axis (East)

Data3 corresponds to the time-history acceleration values along the Z axis (Vertical)

Table 6.5.1
Degrees-of-freedom

LOCATION (Node)	DISPLACEMENT			ROTATION		
	U_x	U_y	U_z	θ_x	θ_y	θ_z
1	p_1	p_2	p_3	q_4	q_5	q_6
2	p_{17}	p_{18}	p_{19}	q_{20}	q_{21}	q_{22}

Node 1 is assumed to be attached to the rack at the bottom most point.
Node 2 is assumed to be attached to the rack at the top most point.
Refer to Figure 6.5.1 for node identification.

2*	p_7	p_8
3*	p_9	p_{10}
4*	p_{11}	p_{12}
5*	p_{13}	p_{14}
1*	p_{15}	p_{16}

where the relative displacement variables p_i are defined as:

$p_i = q_i(t) + U_x(t)$ $\quad i = 1,7,9,11,13,15,17$
$= q_i(t) + U_y(t)$ $\quad i = 2,8,10,12,14,16,18$
$= q_i(t) + U_z(t)$ $\quad i = 3,19$
$= q_i(t)$ $\quad i = 4,5,6,20,21,22$

p_i denotes absolute displacement with respect to inertial space
q_i denotes relative rotation with respect to the floor slab
$U(t)$ are the three known earthquake displacements

* denotes fuel mass nodes

Table 6.9.1
Comparison of Bounding Calculated Stresses vs. Code Allowables at Impact Locations and at Welds

	DBE[†]	
Item/Location	Calculated	Allowable
Rack/baseplate weld, psi	7,530	13,750
Female pedestal/baseplate weld, psi	26,920	30,660
Cell/cell welds, psi [††]	7,363	13,750

[†] DBE controls over OBE.

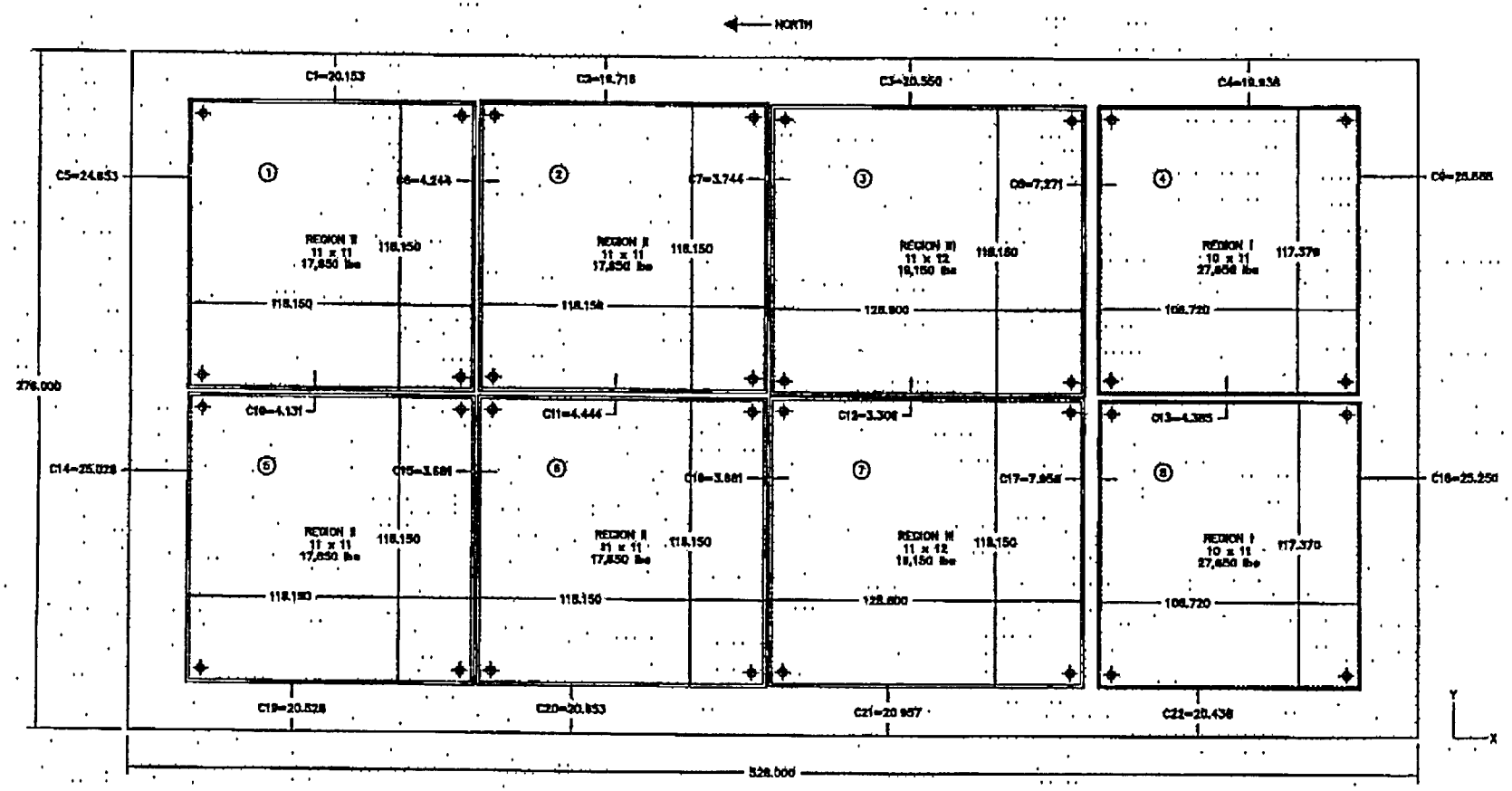

Figure 6.1.1 – ANO-1 Spent Fuel Pool Layout

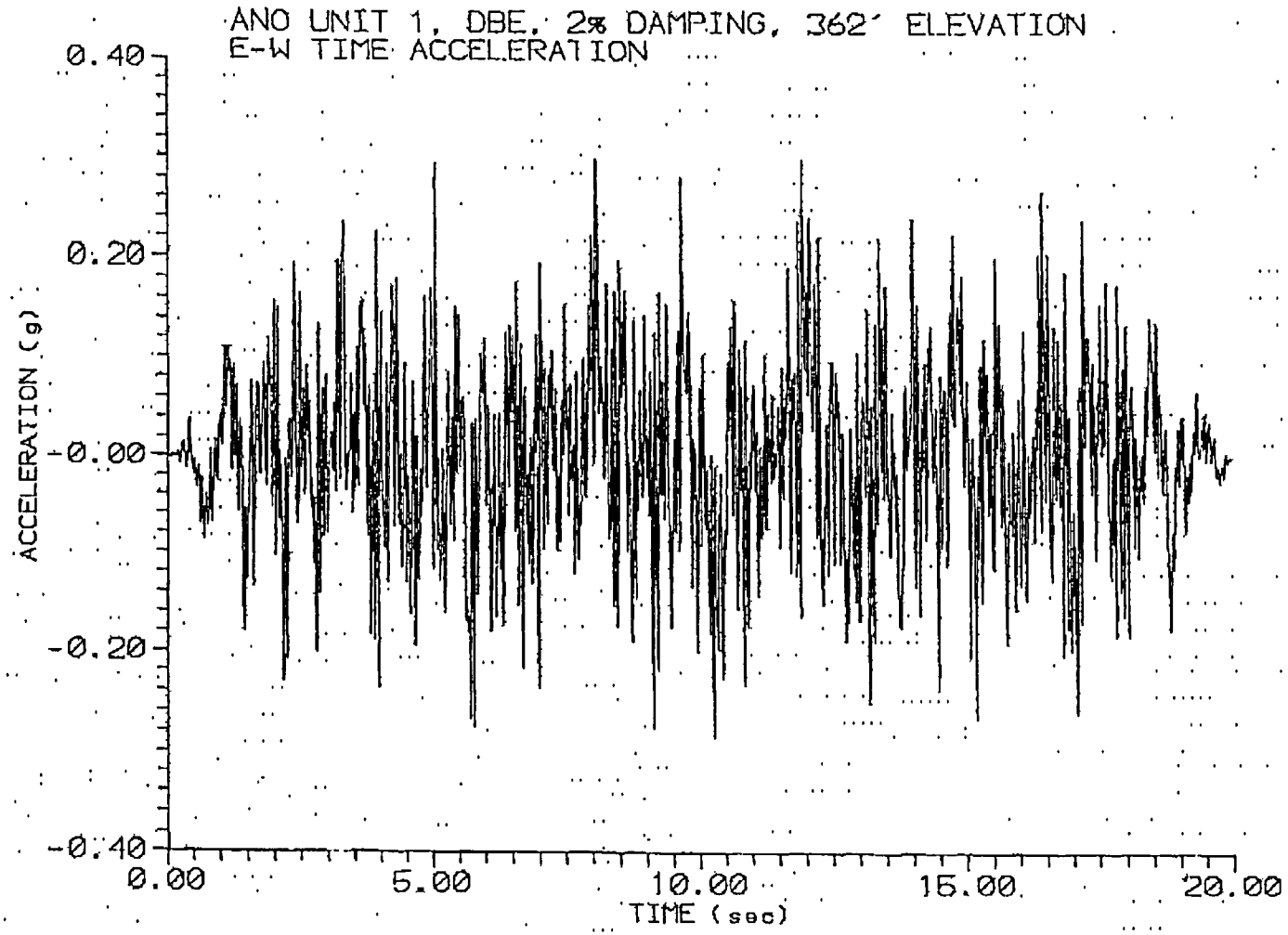
ANO UNIT 1, DBE, 2% DAMPING, 362' ELEVATION
E-W TIME ACCELERATION
0.40
0.20
-0.00
-0.20
-0.40
ACCELERATION (g)
0.00
5.00
10.00
15.00
20.00
TIME (sec)

Figure 6.4.1

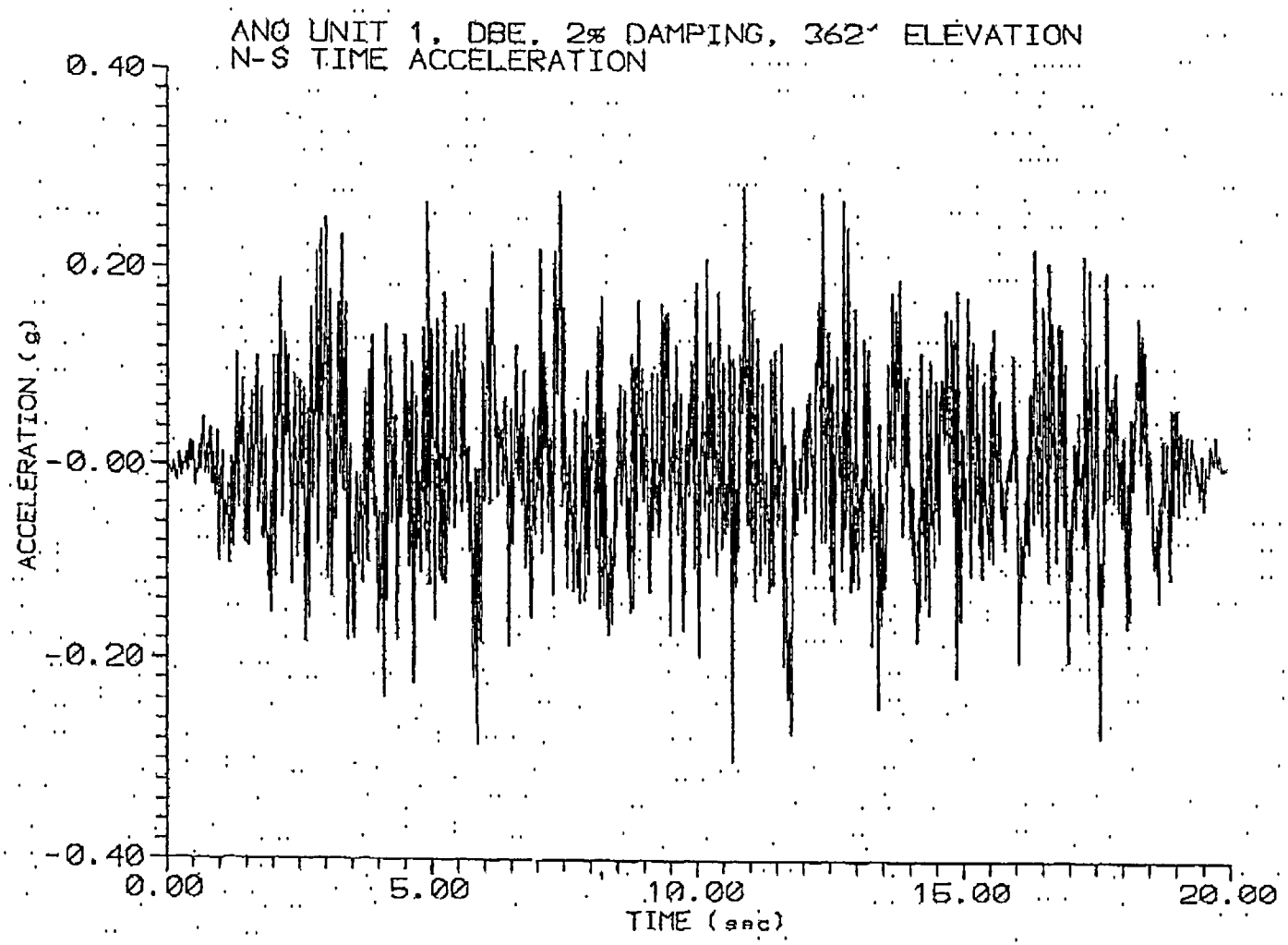
ANO UNIT 1, DBE, 2% DAMPING, 362' ELEVATION
N-S TIME ACCELERATION
0.40
0.20
-0.00
-0.20
-0.40
ACCELERATION (g)
0.00
5.00
10.00
15.00
20.00
TIME (sec)

Figure 6.4.2

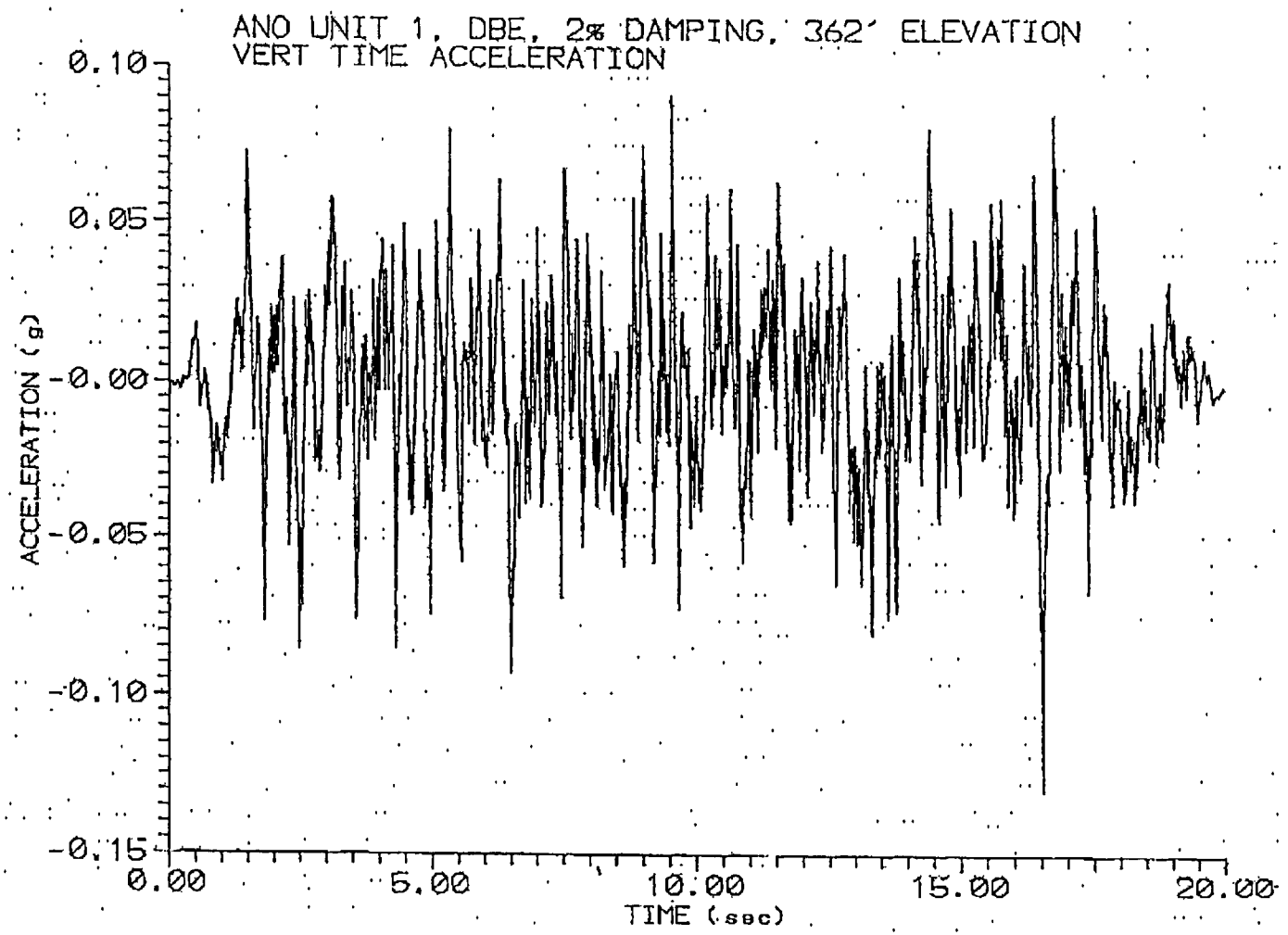
ANO UNIT 1, DBE, 2% DAMPING, 362' ELEVATION
VERT TIME ACCELERATION
ACCELERATION (g)
0.10
0.05
-0.00
-0.05
-0.10
-0.15
0.00
5.00
10.00
15.00
20.00
TIME (sec)

Figure 6.4.3

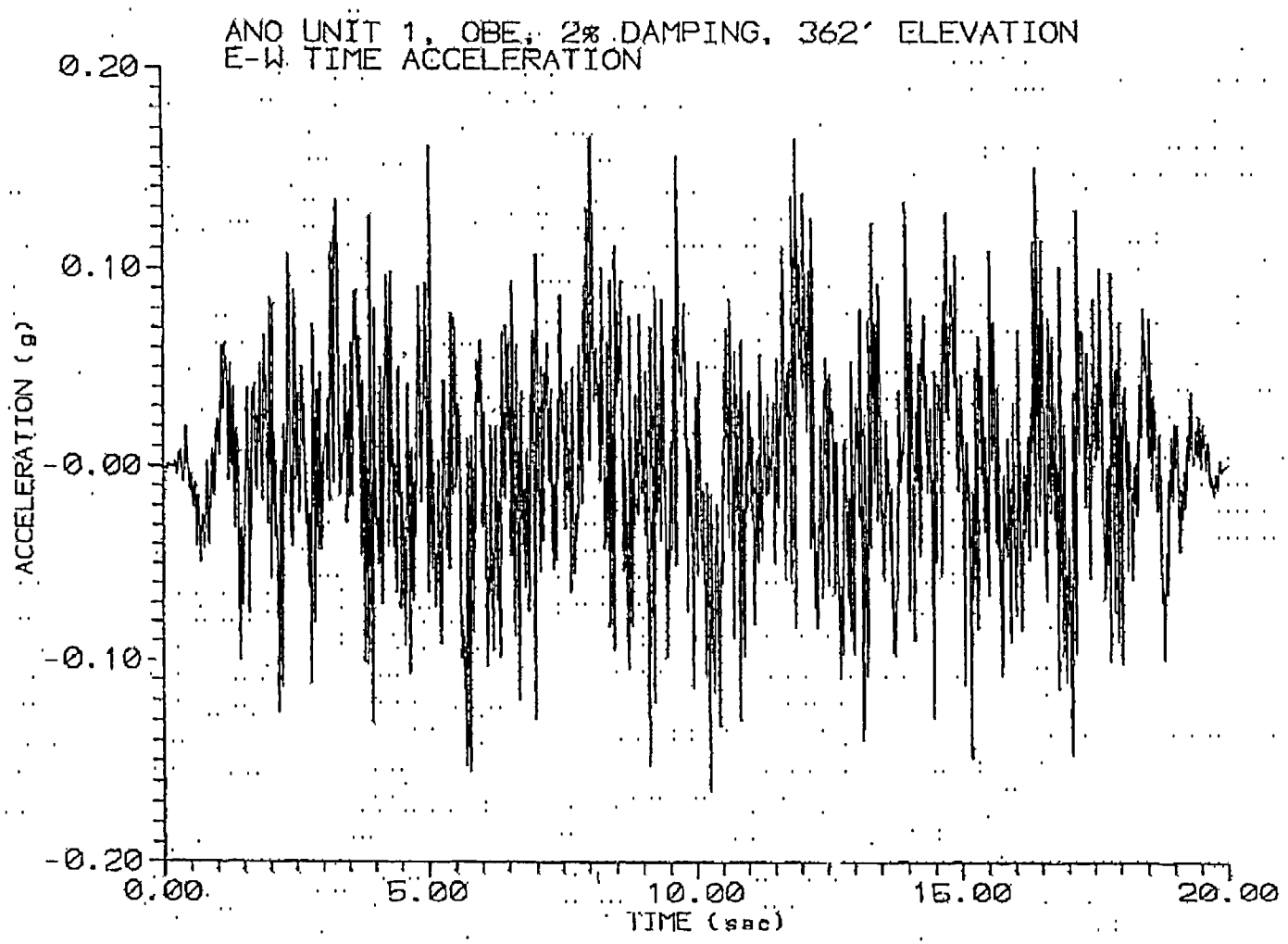
ANO UNIT 1, OBE, 2% DAMPING, 362' ELEVATION
E-W TIME ACCELERATION
ACCELERATION (g)
0.20
0.10
-0.00
-0.10
-0.20
0.00
5.00
10.00
15.00
20.00
TIME (sec)

Figure 6.4.4

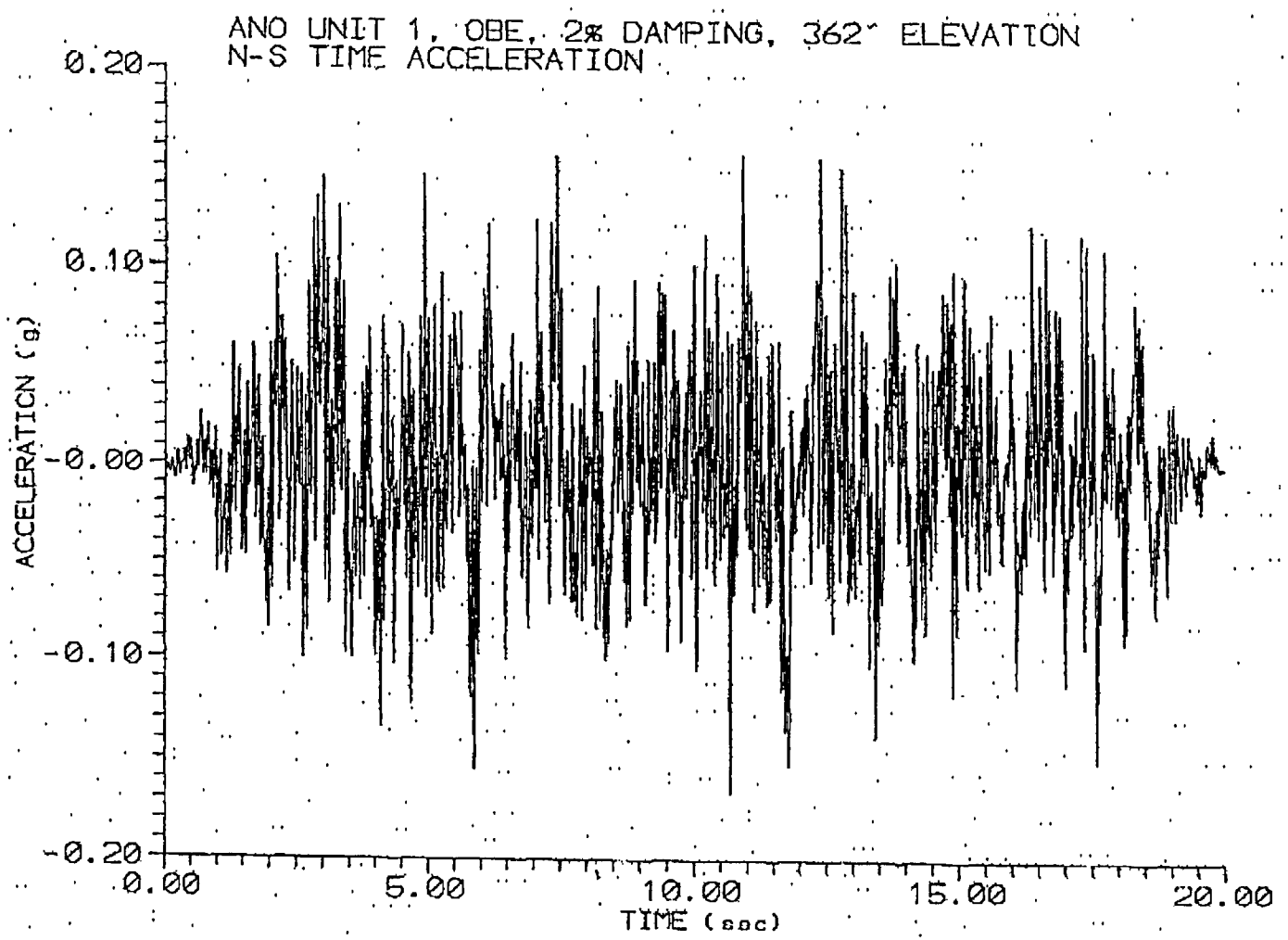
ANO UNIT 1, OBE, 2% DAMPING, 362' ELEVATION
N-S TIME ACCELERATION
0.20
0.10
-0.00
-0.10
-0.20
ACCELERATION (g)
0.00
5.00
10.00
15.00
20.00
TIME (sec)

Figure 6.4.5

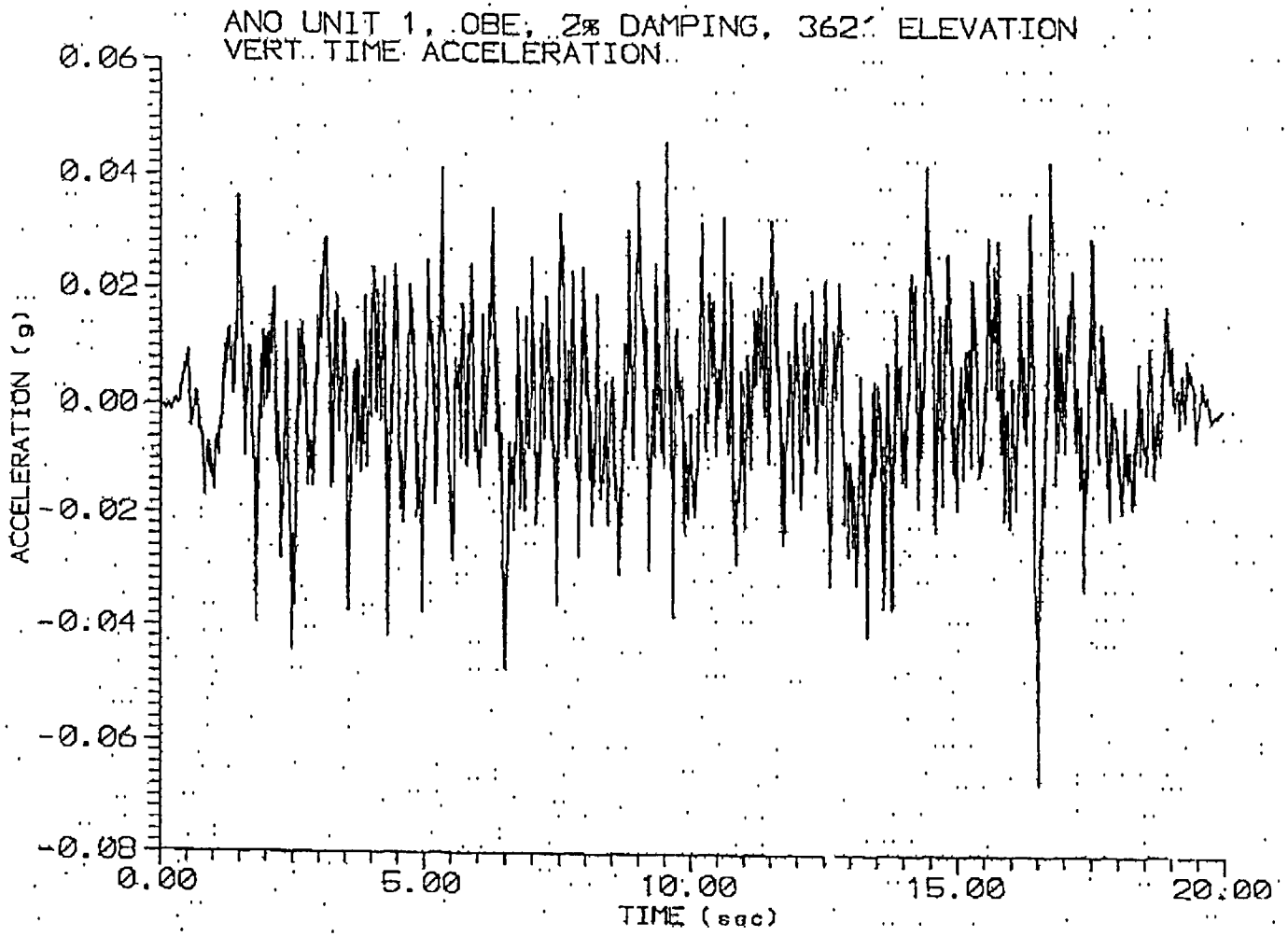
ANO UNIT 1, OBE, 2% DAMPING, 362' ELEVATION
VERT. TIME ACCELERATION
ACCELERATION (g)
0.06
0.04
0.02
0.00
-0.02
-0.04
-0.06
-0.08
0.00
5.00
10.00
15.00
20.00
TIME (sec)

Figure 6.4.6

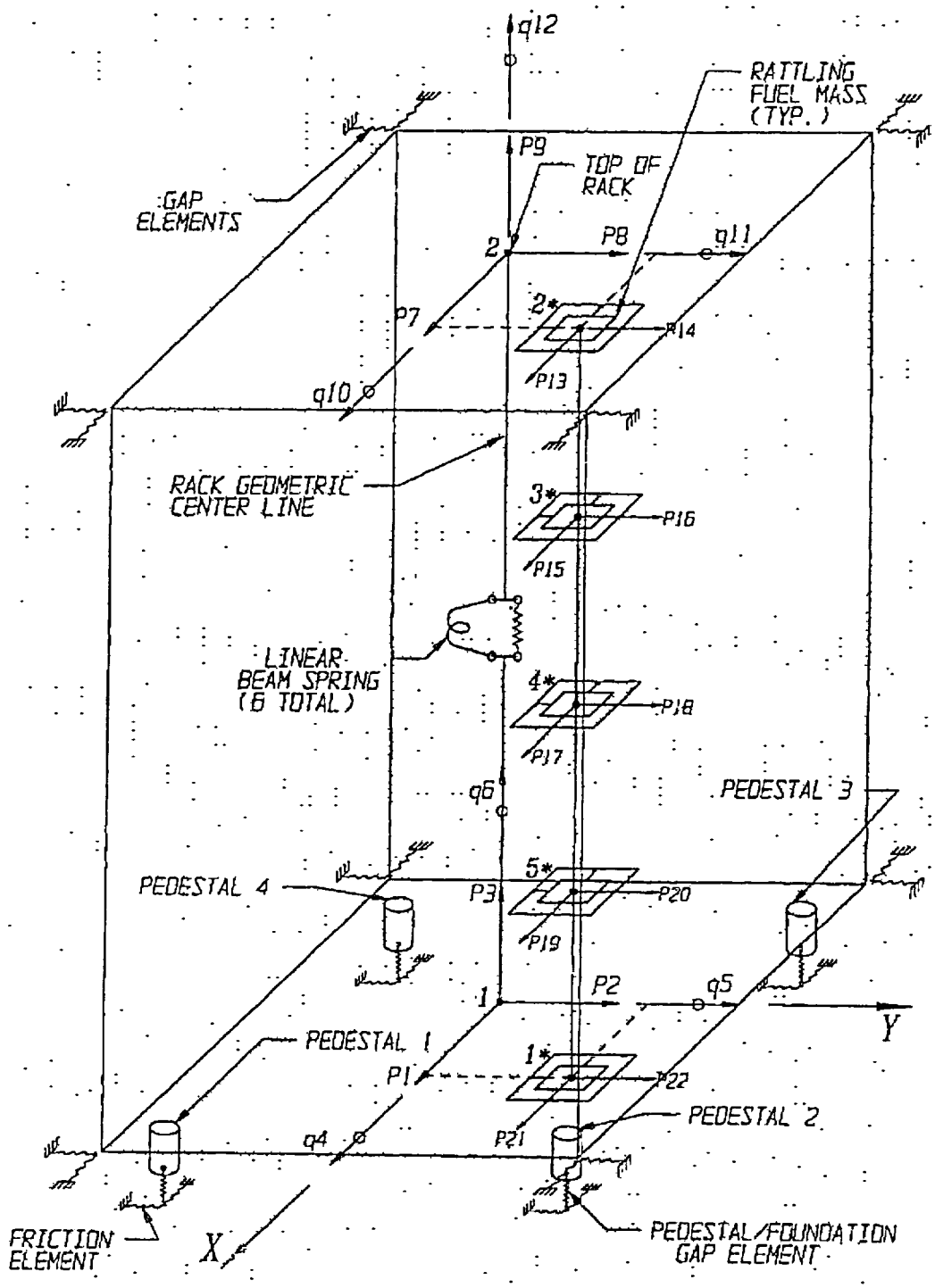

Figure 6.5.1 – Schematic of Single Rack Dynamic Model Used in Dynarack

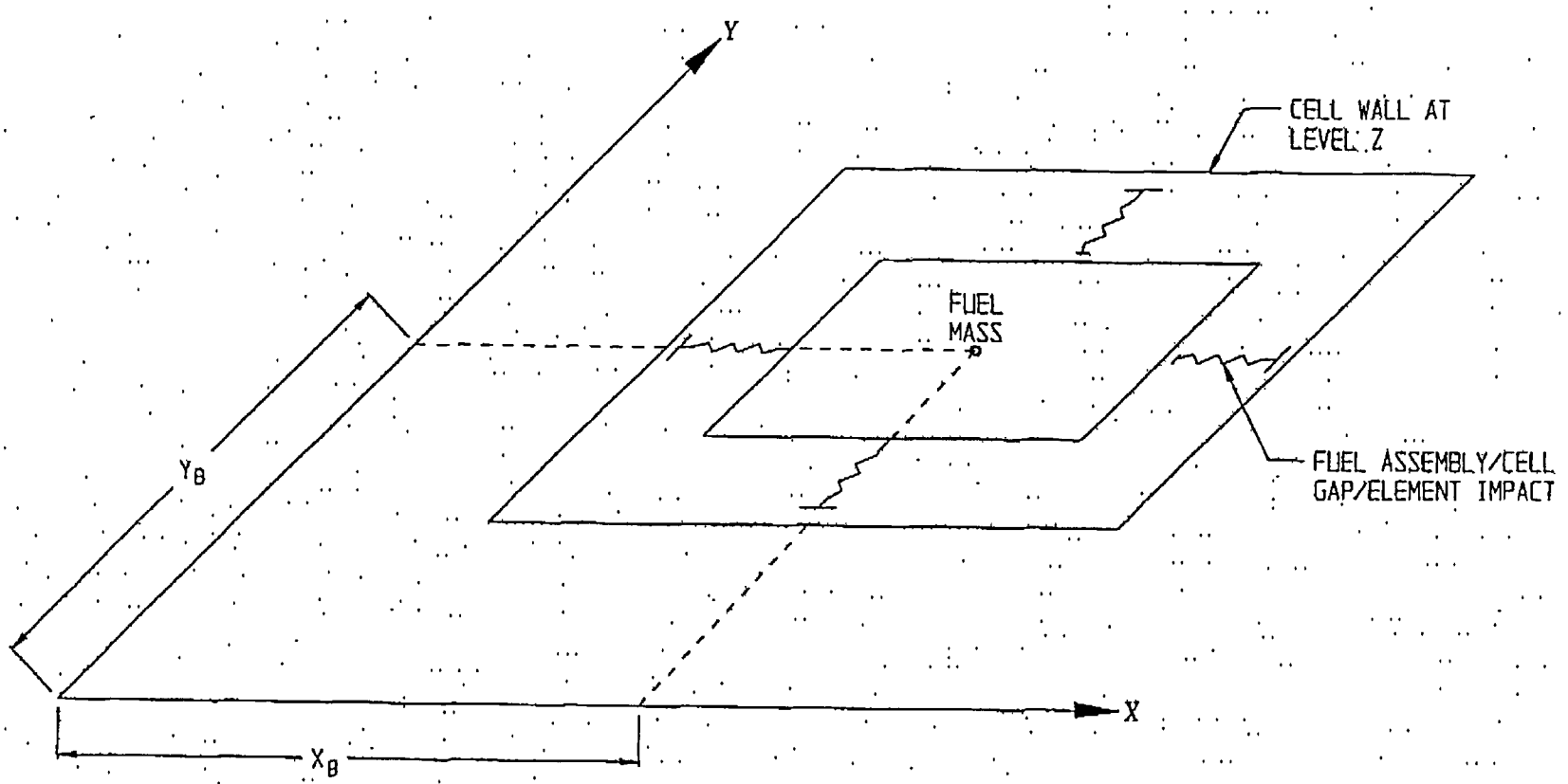

Figure 6.5.2 – Fuel-to-Rack Gap/Impact Elements at Level of Rattling Mass

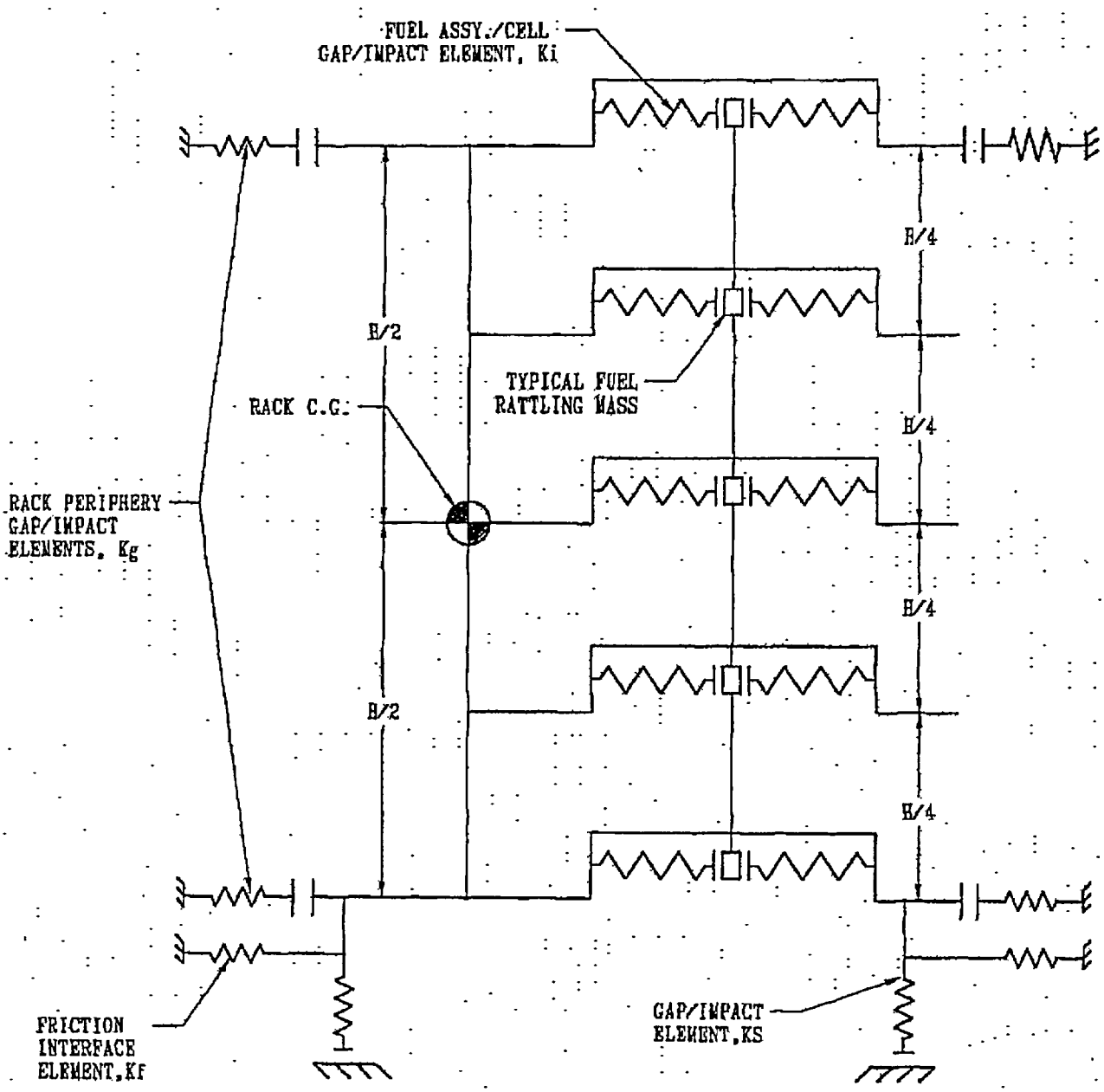

Figure 6.5.3 – Two Dimensional View of Spring-Mass Simulation

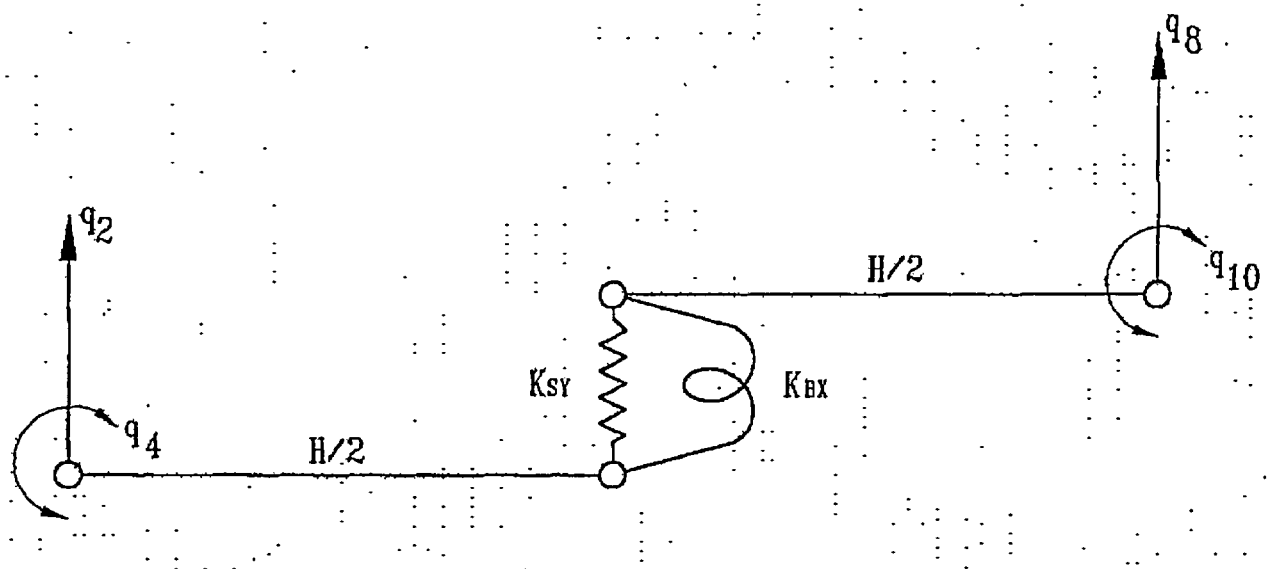

RACK DEGREES-OF-FREEDOM FOR Y-Z PLANE BENDING WITH SHEAR AND BENDING SPRING

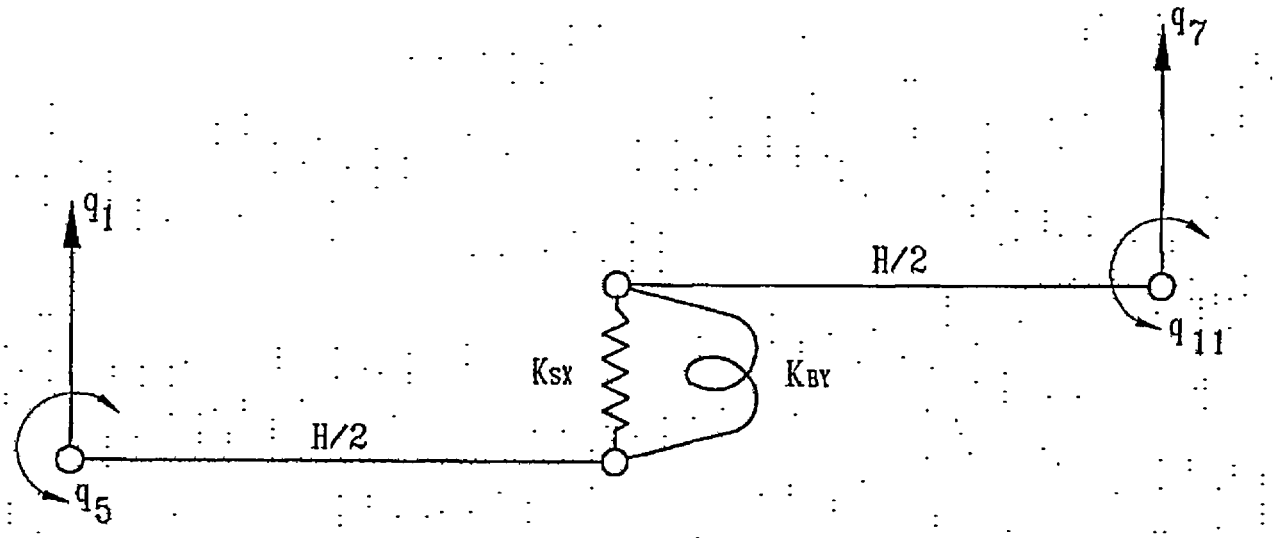

RACK DEGREES-OF-FREEDOM FOR X-Z PLANE BENDING WITH SHEAR AND BENDING SPRING

Figure 6.5.4 – Shear and Bending Springs Representing Rack Elasticity in X-Z and Y-Z Planes

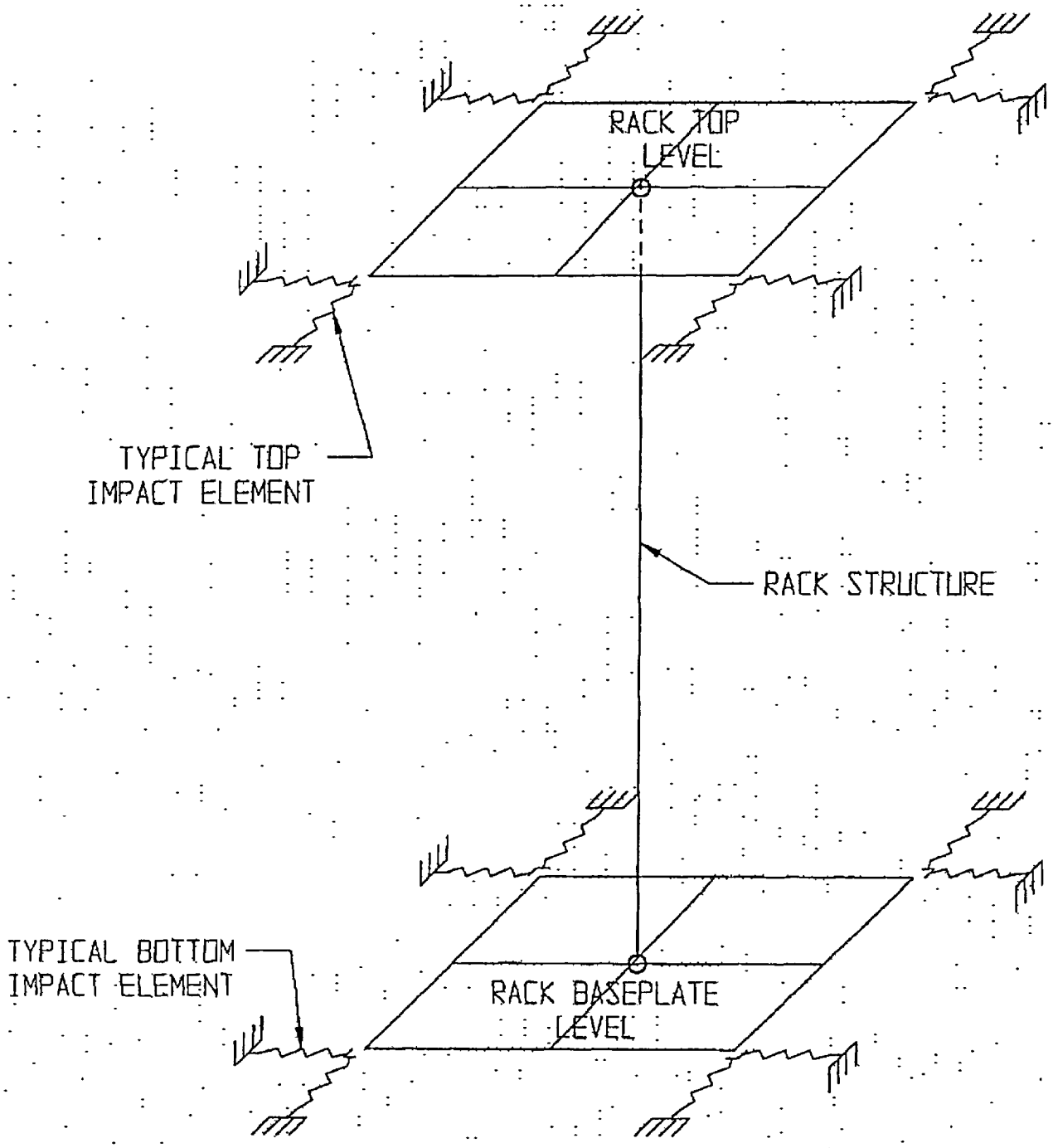

Figure 6.5.5 – Rack Periphery Gap/Impact Elements

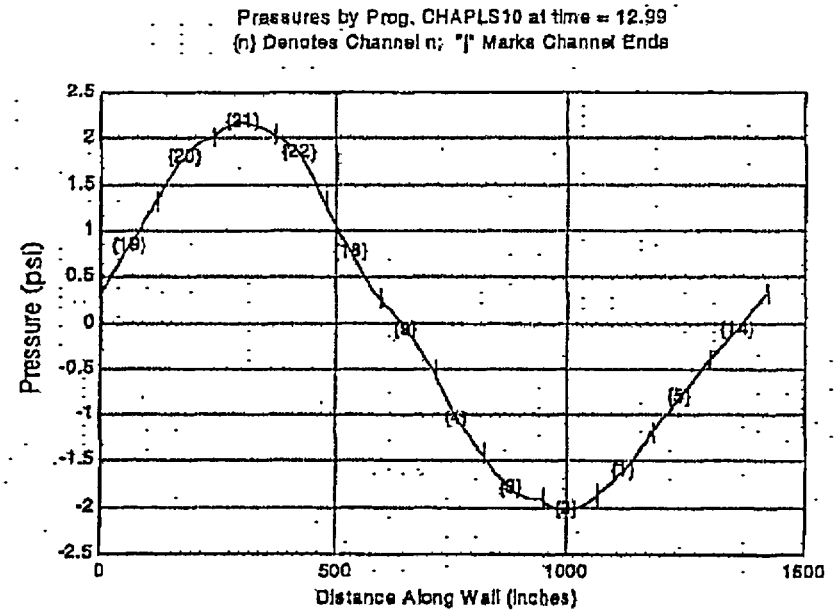

DBE, 0.2 Coefficient of Friction

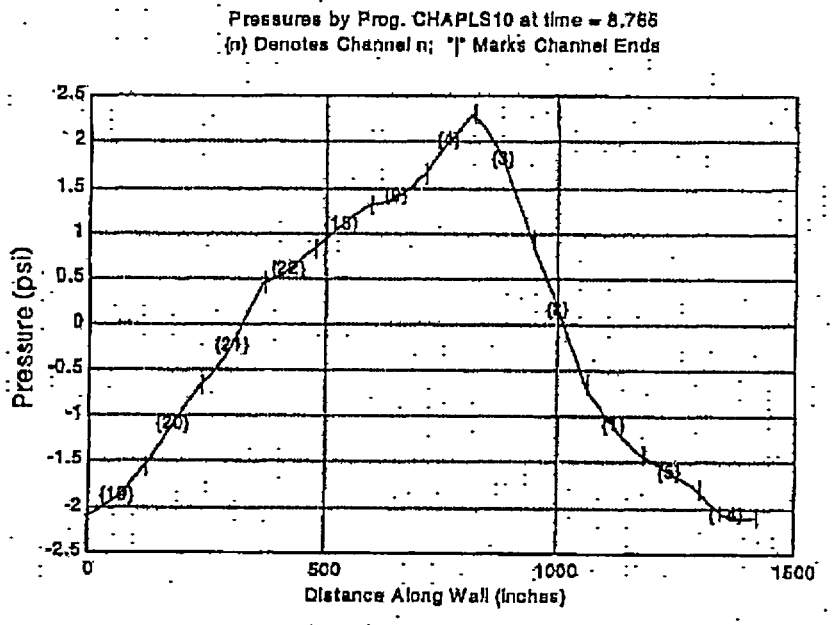

DBE, 0.8 Coefficient of Friction

Figure 6.11.1 – Maximum Instantaneous Hydrodynamic Pressures

7.0 MECHANICAL ACCIDENTS

7.1 INTRODUCTION

The USNRC OT position paper [7.1.1] specifies that the design of the rack must ensure the functional integrity of the spent fuel racks under all credible drop events.

The postulated fuel drop events on the ANO-1 spent fuel pool Region 3 racks, which will be inserted with Metamic® material in the rack flux traps with lead-ins installed on the top of flux traps, are evaluated.

The proposed change to the rack does not impact conclusions in the current licensing basis on the potential fuel damage due to mechanical accidents.

7.2 DESCRIPTION OF MECHANICAL ACCIDENTS

The postulated drop accidents assume that a fuel assembly, along with the portion of handling tool will drop vertically and hit the top of the rack at one of two enveloping locations: the cell wall edge, or the cell wall corner intersection. The weight and drop height in the postulated fuel drop accident are at most 2,580 lbs and 29.25 inches, respectively.

7.3 EVALUATION OF MECHANICAL ACCIDENTS

To obtain conservative results, the postulated mechanical drop accidents were evaluated based on the maximum impact energy, a thinner rack wall thickness, weakest weld size and configuration, and worst case fabrication tolerance for the ANO-1 Region 3 racks. The evaluation of the postulated drop events demonstrated that, with the previously described conservative considerations, the postulated mechanical drop accidents would result in significant damage to the impacted cell wall down into the active fuel region of the racks, leading to the failure of Metamic® inserts inside the flux trap.

7.4 CONCLUSION

The fuel assembly drop events postulated for the ANO-1 spent fuel pool Region 3 racks were conservatively evaluated and found that the poison inserts, as well as the cell wall, of the impacted rack cell could be significantly damaged under the postulated accidental events. To ensure the functional integrity of the rack, the criticality safety evaluation (reported in Section 4.0) conservatively analyzed the Region 3 racks under the postulated assumption that all poison inserts in the impacted cell are damaged. The racks were determined to remain subcritical even under this extremely conservative postulate, when credit was taken for the technical specification limit of 1600 ppm soluble boron in the pool.

7.5 REFERENCES

[7.1.1] "OT Position for Review and Acceptance of Spent Fuel Storage and Handling Applications," dated April 14, 1978, and addendum dated 1979.

Attachment 5

1CAN040302

Evaluation of Spent Fuel Pool Structural Integrity
for
Increased Loads from Spent Fuel Racks

The ANO-1 spent fuel pool consists of 6'-0" thick reinforced concrete walls and a 5'-6" thick floor slab. The pool is supported below by thick foundation walls. Concrete compressive strength for the ANO-1 spent fuel pool is 5000 psi and reinforcement used was Grade 40.

The spent fuel pool was originally designed by Bechtel Corp. in accordance with the ACI 318-63 reinforced concrete building code, for loadings including deadweight of the structure, water, and spent fuel racks, hydrodynamic pressure from the water, operating thermal, accident thermal, seismic, tornado and flood loads. Rack loads were treated as a uniform load spread across the pool floor slab.

In 1981-1982, a reanalysis of the spent fuel pool structure including the foundation walls, refueling canal, and cask storage area was performed by Structural Dynamics Inc. in support of the re-rack project for ANO-1. Finite element methodology was used for this analysis. The same loads as described above in the Bechtel design were included in the analysis. The loads from the spent fuel racks included their deadweight (treated as live load on the pool floor slab) and vertical and horizontal seismic load effects. Rack loads were provided by Westinghouse Corp. This analysis, again used the acceptance criteria in the ACI 318-63 code, but supplemented the strength design methodology using provisions from the ACI 349-80 Nuclear Structure Reinforced Concrete Code. The load combinations used were in accordance with Standard Review Plan, Section 3.8.

The dominant load effects were due to thermal expansion from the accident thermal loading for both analyses of the ANO-1 Spent Fuel Pool.

The recent evaluation of the spent fuel racks by Holtec International was performed to evaluate the effects on two of the racks for the additional weight of proposed poison inserts to two of the racks. This evaluation included analyses of the racks as described in Sections 3 through 6 of Attachment 4, and resulted in revised loads imparted from the racks to the pool floor slab. ANO engineering also conservatively redefined the total deadweight of all the racks, and included 5000 lb contingency loads between each rack and the pool walls around the periphery of the pool, (60,000 lb total), to account for miscellaneous items stored in this area of the pool.

Additionally, Holtec specified a conservative hydrodynamic pressure resulting from the seismic displacement of the racks, which loads the pool walls for the height of the racks.

A review of the pool structure was performed using the 1981-1982 analysis by Structural Dynamics with the applied loads including the rack load effects. These effects were amplified using conservatively determined factors to account for the increased loads from the racks. Specifically, the deadweight loading of the racks was factored up by the ratio of the maximum increase for any of the racks. The seismic load contribution (which consisted of combined seismic effects for the pool structure, the water, plus the rack seismic loads) was factored in their entirety, by the maximum ratio calculated for the worst case rack in either the horizontal or vertical directions. This also conservatively accounted for the added hydrodynamic pressure on the pool walls.

The 1981-1982 analysis checked 21 points for section moment, transverse shear, and in-plane shear. These 21 points were the highest stressed points for the various elements of the pool structure (e.g. the highest stressed points for each direction for the pool floor slab, the highest stressed point in each of the pool walls, etc.). Of these locations, two were for the pool floor slab and three were for the pool foundation walls. The spent fuel racks are supported only by the pool floor slab, which transmits load effects from the racks to the foundation walls, to the ground. Above the pool slab level, the rack loads have little impact on the pool structural elements.

Hence, the five critical locations for the pool floor slab and foundation walls were reviewed in detail, with the rack deadweight (live load case) and the seismic loading combinations factored as described above. The following table summarizes the results of the review of these five locations.

Summary of Section Strength Review of Selected Locations

Location	Section Strength Parameter	Previous Analysis Ratio to Code Allowable	Conservative Estimate of Ratio to Code Allowable for Increased Rack Loads
Pool Floor Slab East-West Section	Moment	0.76	0.76
	Transverse Shear	0.24	0.213
	In-Plane Shear	0.16	0.177
Pool Floor Slab North-South Section	Moment	0.59	0.636
	Transverse Shear	0.29	0.265
	In-Plane Shear	0.42	0.477
Pool Foundation South Wall	Moment	0.39	0.402
	Transverse Shear	0.40	0.443
	In-Plane Shear	0.55	0.821
Pool Foundation East Wall	Moment	0.42	0.456
	Transverse Shear	0.48	0.431
	In-Plane Shear	0.96	0.982
Pool Foundation West Wall	Moment	0.49	0.496
	Transverse Shear	0.58	0.588
	In-Plane Shear	0.80	0.906

The greatest increase for any location reviewed was for the South Pool Foundation Wall, for in-plane shear. The previous ratio for indicated shear to the allowable was 0.55. The conservatively estimated increased ratio is 0.82 or about a 49% increase. The highest stressed point was for the East Pool Foundation Wall, with a previous ratio of indicated in-plane shear to allowable of 0.96. The increased ratio is 0.982, which is about a 2% increase. The allowable of 1.0 is not exceeded.

It should be noted that the added poison inserts increase the deadweight for only two of the racks by a total of about 16870 pounds, which is about a 3.5% increase in deadweight for these two racks. For the review performed however, the weights for all racks were effectively increased about 29.5%. Additionally, the factored seismic loads included factoring the pool

structural seismic loads as well, which have not changed. Hence in general, it can be seen that the increased load effects as applied for this review resulted in only slight increases, and if only the added poison inserts were considered, the changes would be very small.

The results of this review demonstrate that the indicated increased loads from the racks have minimal effects on the pool structural elements, and that the structural integrity of the pool structure is maintained.

Attachment 6

1CAN040302

List of Regulatory Commitments

List of Regulatory Commitments

The following table identifies those actions committed to by Entergy in this document. Any other statements in this submittal are provided for information purposes and are not considered to be regulatory commitments.

COMMITMENT	TYPE (Check one)		SCHEDULED COMPLETION DATE (If Required)
	ONE-TIME ACTION	CONTINUING COMPLIANCE	
Loading pattern restrictions including the vacant space required by checkerboard storage configurations will be procedurally controlled		x	
Entergy will establish a coupon sampling program to ensure that the physical and chemical properties of Metamic® behave in a similar manner to that found at the test facilities.		x	Within 90 days of TS approval
Entergy will complete the analysis of the structural integrity of the poison panel inserts for normal and seismic conditions considering the finalized design modification to ensure all safety factors are greater than 1.0.	x		Within 90 days of TS approval
A SAR change will be submitted to Licensing reflecting the changes made by this amendment	x		Within 90 days of TS approval